Table 1
The operating condition of each heating process

Processing method	Raw materials	IMC (% d.b.)	Temperature[a] (°C)
Twin-screw extruder (laboratory)	Milled soya flour	18, 24, 27	100, 110, 120, 130, 140
Spouted bed (TDSB) (laboratory)	Full-fat soybean	14, 22, 28	120, 130, 140, 150
Single layer infrared dryer (laboratory)	Full-fat soybean	18, 24, 27	100, 120, 140, 160
Single-screw extruder (commercial-scale)	Milled soya flour	13	104–115
FBD (commercial-scale)	Full-fat soybean	12	160–170
Micronizer (commercial-scale)	Full-fat soybean	11.4	180–220

Note: FBD: Fluidized bed dryer; TDSB: Two-dimensional spouted bed; IMC: Initial moisture content.
[a] Accuracy of temperature controller ±1 °C.

activity. The pH difference value was measured by the Mettler pH meter (Model No. DELTA 340) and was then converted to the percentage of urease inactivation by the equation proposed by Savage, Wei, Sutherland, and Schmidt (1995). The acceptable level of pH difference should be in the range lower than 0.3, corresponding to the urease inactivation of 97%.

According to AOCS method Aa 5-38 (AOCS, 1984), the percentage of crude protein can be calculated by percentage of nitrogen multiplied by a nitrogen-to-protein factor (6.25) and the percentage of nitrogen in the soybean was estimated by the Kjeldahl method, using a TKN analyzer (Model No. Antek 9000N). Protein solubility indicates the level of protein dispersion in a 0.2% KOH solution. According to Cheong (1997), protein solubility should be in a normal range between 70% and 85%. If its value is lower than 70%, it means the soybean is overcooked, but if higher than 85%, soybean is insufficiently cooked. Protein solubility is calculated by

$$\text{Protein solubility} = \frac{\text{nitrogen of the supernatant in 0.2\%KOH solution}}{\text{crude protein}} \times 100 \quad (3)$$

In addition, the lysine in soy protein was also analyzed by the AccQ-Tag method. Soybean sample was hydrolyzed at 110 °C for 22 h with AccQ-Flour reagent. Finally, it was analyzed by high performance liquid chromatography (Model No. Waters Lambda-Max 481).

The experimental conditions for treating soybeans in each process are shown in Table 1.

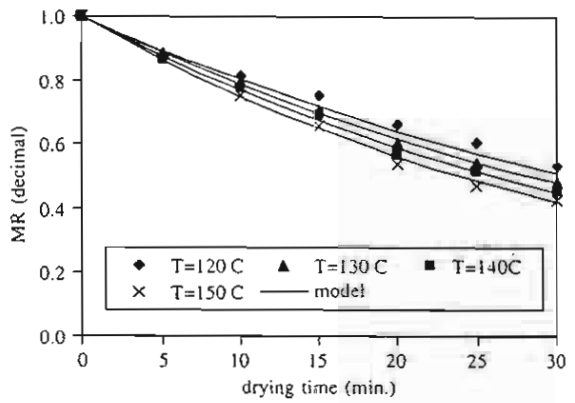

Fig. 7. Comparison of moisture ratio between experiment (dots) and prediction (lines) at different temperature and initial moisture content of 28% dry basis using two-dimensional spouted bed (lab-scale).

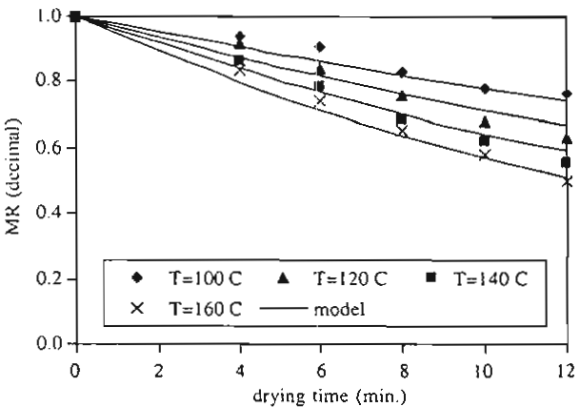

Fig. 8. Comparison of moisture ratio between experiment (dots) and prediction (lines) at different temperature and initial moisture content of 24% dry basis using single layer infrared dryer (lab-scale).

3. Results and discussions

3.1. Reduction of moisture content

The drying rates of the soybeans in the spouted bed and single layer infrared dryer at different inlet air temperatures are shown in Figs. 7 and 8 respectively. The characteristics of the drying curves from such heating methods are very similar, the moisture exhibiting a typically decrease with drying time, but the rate of moisture removal by spouted bed is noticeably lower, as indicated by the slope of the drying curve. The lower drying rate is due to the fact that the energy from the hot air is conducted to the water inside the kernel via the complex physical structure of the food material and this structure resists the heat transport. In addition, the

inherent characteristics of the spouted bed that consists of spout and downcomer regions result in slow water transport inside the kernels since the kernels stay in the downcomer, where the rates of heat and mass transfer are very poor, for a relatively longer time than that spent in the spout region. The influence of temperature on the drying rate can also be observed in these figures: the higher the temperature the faster the moisture decrease, as expected. This factor has a profound effect whilst the initial moisture content has a lesser contribution. The data of moisture effect was not shown here.

Knowing the experimental value of moisture content at various times and conditions, the drying constant was determined using a non-linear regression approach. To obtain this parameter, the drying constant formulation was correlated with temperature and initial moisture content in the following form:

$$k = AM_{in}^{B}\exp(-E/T_{abs}) \tag{4}$$

where T_{abs} is the absolute temperature (K) and A, B and E are the constant parameters, all of which depend on the heating technique. Substituting Eq. (2) into Eq. (1), it was then fitted to the experimental data by a single-step regression. The results of regression analysis using the original data are shown in Table 2, with the values of R^2 and MSE, demonstrating the adequacy of the proposed model. The mean sum squares of error (MSE) is defined as (López, Piqué, Romero, & Aletá, 1998)

$$\mathrm{MSE} = \frac{\sum_{i=1}^{n}(MR_{obs} - MR_{pre})^2}{n - z} \tag{5}$$

where MR_{obs} is the experimental moisture ratio, MR_{pre} is the predicted moisture ratio, n is the number of data points and z is the number of unknown parameters. As seen in Figs. 7 and 8, the thin layer drying reasonably predicted the data over the drying conditions.

The result of the calculated drying constants at various temperatures for the spouted bed and infrared heating is shown in Fig. 9, indicating a significantly higher value of the drying constant for the infrared heating compared to that for the spouted bed. Moreover, the drying constant for the infrared heating was strongly affected by temperature whilst it was only slightly changed for the spouted bed. These results emphasize that the infrared technique shows a higher potential capability for removing water and its capability is more effective when operated at higher temperature, as indicated by the positive slope in Fig. 9. The experimental results for the other initial moisture contents show the same trend as found in Fig. 9.

Table 2
Drying constants of spouted bed and single infrared dryer (lab-scale)

Processing method	A	B	E	R^2	MSE
Spouted bed dryer	0.7652	0.0559	−1467.12	0.98	0.0004
Single layer infrared dryer	6.72705	−0.22633	−2212.67	0.97	0.0005

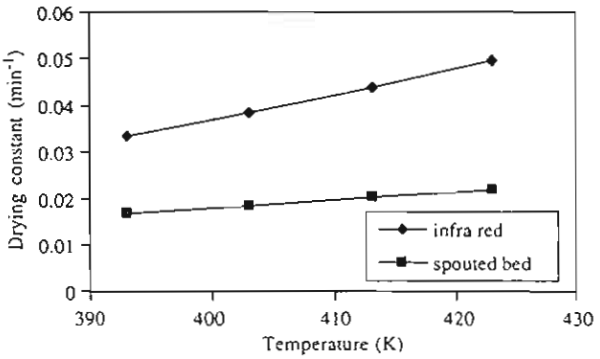

Fig. 9. Relationship between drying constant and inlet air temperature when using two-dimensional spouted bed and single layer infrared dryer (M_{in} = 18% d.b.).

3.2. Urease activity and urease inactivation

Figs. 10 and 11 show the urease activity, measured as pH difference, and the percentage of urease inactivation in the soybeans treated by the respective spouted bed and single layer infrared techniques. The urease activity of raw soybeans is approximately 2.2–2.5 at the beginning and reduced with drying time. In some cases, insufficient inactivation occurs, in particular when raw soybeans with a low initial moisture content are treated at a low temperature for a certain period. This can be observed from the soybeans at initial moisture contents below 24% d.b. which were treated by the spouted bed at a lower temperature of 130 °C and infrared radiation at a lower temperature of 120 °C. The percentage of urease inactivation at the end is between 60% and 80% for times of 30 min in the spouted bed and 12 min in the infrared. Since the treated soybeans became brown in colour, we were not interested in examining them at longer treating times although it was expected that the pH difference would decrease to acceptable limit.

Adequate inactivation, implying a pH difference lower than 0.3, can be accomplished in the raw soybeans at 22–24% d.b. using a temperature of 140 °C for 30 min in the spouted bed and 12 min in the infrared. Under such heating conditions, the moisture content at the end was about 14% or 15% d.b. at which it is safe for long-term storage. When the initial moisture content increased beyond 24% d.b., the treating temperature or the treating time for sufficient inactivation can be reduced. It needs 30 min at 120 °C and 25 min at 130–140 °C for the spouted bed as well as 10 min at 140–160 °C for the infrared technique. The reduction in such operating parameters is due to the fact that high initial moisture favours rapid cooking (Wright, 1981).

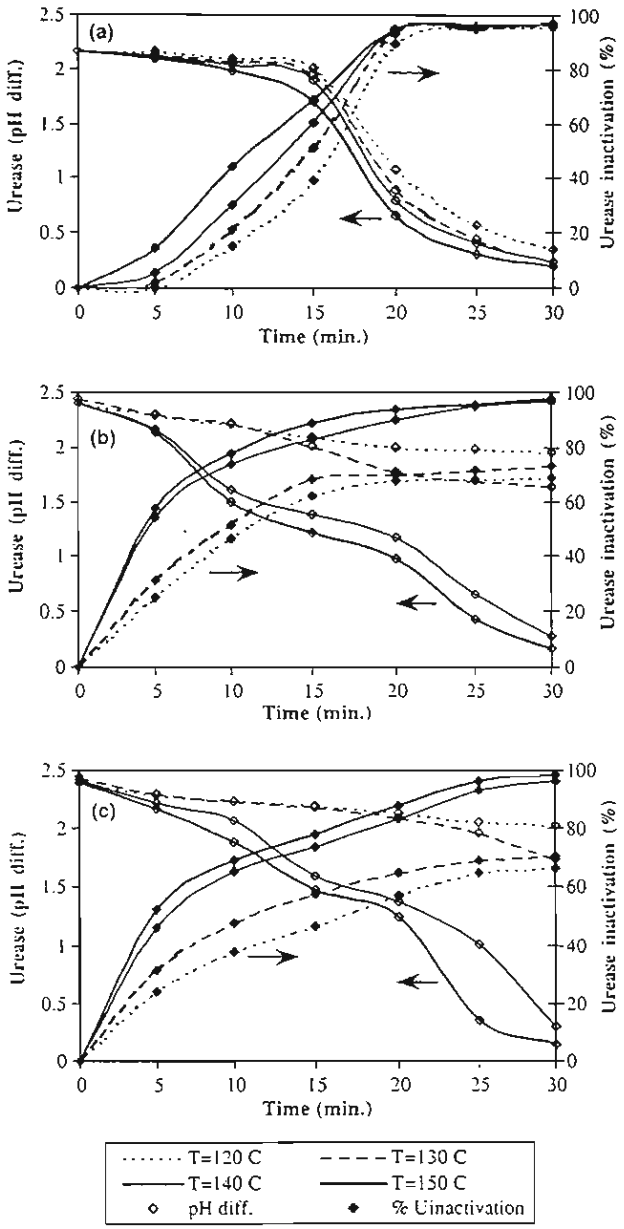

Fig. 10. Effect of moisture on the urease activity and percentage of urease inactivation for two-dimensional spouted bed dryer (a) 28%, (b) 22% and (c) 14% d.b.

In addition to the lab-scale test, we also examined the dry soybean quality after treating in large-scale equipment at commercial sites. The result from the industrial-scale micronizer is shown in Table 5 and reveals that an environmental temperature between 180 and 220 °C, corresponding to a grain temperature of 119–122 °C, yields a pH difference of 0.1–0.16 at treating times of less than 5 min. For the continuous fluidized bed dryer, in which the kernels are rigorously mixed, the colour of the treated soybeans was rather brown and their pH difference fell into the acceptable range, being between 0.21

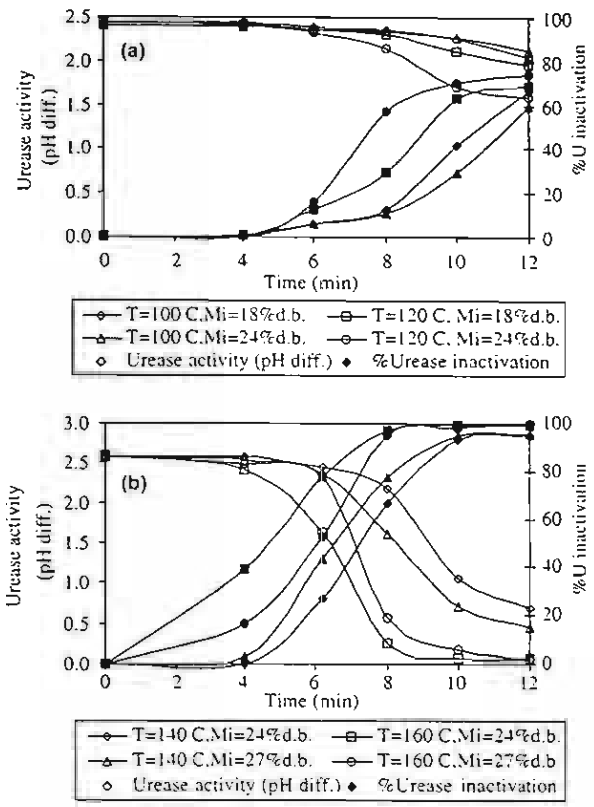

Fig. 11. Urease activity (pH difference) and urease inactivity using single layer infrared dryer (lab-scale). (a) Operating at dryer room temperature of 100 and 120 °C and initial moisture content of 18% and 24% d.b. (b) Operating at dryer room temperature of 140 and 160 °C and initial moisture content of 24% and 27% d.b.

and 0.27 for treatment time of 10 min using inlet air temperatures of 164.5 °C as shown in Table 6. These data also indicate that the extent of urease inactivation at the exit from the dryer is almost uniform although there is a certain degree of mixing of solid particles while being moved in the dryer. To avoid the undesirable colour, temperatures below 160 °C can be employed, but for inactivating urease, times should be longer than 10 min (Osella et al., 1997). This suggestion is for dry soybean. For moist soybeans, it requires treatment times shorter than 10 min.

These findings demonstrate that intensive heating techniques i.e. fluidized bed and infrared require a relatively short treatment time for the inactivation whilst mild heating techniques like a spouted bed takes longer. The time required was approximately 25 min at 150 °C and 30 min at 140 °C. The longer time for the spouted bed is caused by the particles remaining in the downcomer due to the low airflow rate in this region.

Extrusion technique is distinctly different to the above-mentioned techniques in that the raw soybean kernels must be ground before passing through the extruder. The operating conditions for the twin-screw

extruder and analytical results after passing the extruder are presented in Table 3. The retention time varied between 2.2 and 4.8 min, depending on the screw speed, and the heating temperature was in the range of 100–140 °C corresponding to product temperatures of 91–130 °C, respectively. The results of final moisture content and urease activity of the extruded soybeans are within the range recommended by the American Soybean Association (1990), except for run nos. 1 and 8, both of which had pH differences that were nearly as high as raw soybeans. This implies that the urease is not inactivated at product temperatures below 100 °C even though the retention time or initial moisture content increased. When the product temperature is 100 °C, corresponding to a heating temperature of 110 °C or higher, the pH difference of the treated samples lies in the standard range.

In addition to the temperature, the initial moisture content also had some effects. The degree of urease inactivation for the extruded soybeans trends to contradict those results from the spouted bed and infrared systems: using soy flour with initial moisture content higher than 24% d.b. inhibits the urease inactivation as shown in Table 3. The corresponding values of pH difference become higher but still fall into the desirable range for feed meal products, except for run no. 17. These results clearly indicated that the addition of water into the soybean flour is unnecessary since an excessive quantity of water in soy flour causes a dense agglomeration of flour between the gap of the screws. The subsequent dispersion of soy flour within the barrel is not mixed well, so that the product unevenly absorbs the heat generated in the barrel. High moisture content also caused unstable operation. The extruder was automatically shut off, as is obvious from the experiment at a moisture content of 26% d.b. for run no. 24. Similar results for the urease inactivation were also found with the single-screw extruder as presented in Table 4, the pH difference being between 0.01 and 0.04.

3.3. Protein solubility

In addition to the urease activity, protein solubility is also an important parameter that characterizes the protein quality of soybean. During heating, in order to inactivate the anti-nutritional factors, proteins are denatured and protein aggregates are formed. The protein solubility of raw soybean in the present study was approximately 92.8% and it was reduced after heat treatment. The magnitude of its reduction depended on

Table 3
The operating condition and analytical results after passing extruder (lab-scale)

Run no.	Screw speed (rpm)	Residence time (min)	Temperature (°C)		Moisture (% d.b.)		Urease activity (pH diff.)	Protein solubility (%)
			Heating temperature	Product temperature	Inlet	Outlet		
1	100	3.4	100	91	18.1	15.8	2.27	83.0
2	100	3.4	120	112	18.1	14.8	0.03	78.8
3	100	3.4	140	129	18.1	10.1	0.01	72.8
4	120	2.2	110	100	23.8	19.9	0.19	84.3
5	120	2.2	120	109	23.8	18.1	0.06	81.4
6	120	2.2	130	118	23.8	17.1	0.07	79.8
7	120	2.2	140	130	23.8	11.4	0.09	71.7
8	100	3.4	100	92	24.4	20.8	2.29	NA
9	100	3.4	110	103	24.4	20.0	0.01	NA
10	100	3.4	120	111	24.4	18.7	0.02	NA
11	100	3.4	130	121	24.4	17.6	0.02	NA
12	100	3.4	140	130	24.4	11.5	0.01	NA
13	80	4.8	110	100	24.4	18.8	0.05	NA
14	80	4.8	120	111	24.4	17.2	0.03	NA
15	80	4.8	130	120	24.4	15.3	0.03	NA
16	80	4.8	140	131	24.4	11.1	0.02	NA
17	120	2.2	110	100	26.9	21.8	0.36	81.4
18	120	2.2	120	113	26.9	18.3	0.24	78.6
19	120	2.2	130	119	26.9	16.3	0.26	75.9
20	120	2.2	140	128	26.9	12.0	0.14	73.3
21	100	3.4	110	100	26.9	20.7	0.15	NA
22	100	3.4	120	112	26.9	17.3	0.15	NA
23	100	3.4	130	118	26.9	15.8	0.21	NA
24	100	–	140	–	26.9	–	–	–

Note: Urease activity (pH difference) of raw soybean = 2.33–2.46.

Table 4
Full-fat soy flour analysis after passing single screw extruder (commercial-scale)

Time (min)	Temperature (°C)		Moisture content (% d.b.)		Urease activity (pH change)	Protein solubility (%)
	Pre-conditioner	Product	Inlet	Outlet		
15	89	105	12.9	11.4		
30	88	104	13.0	11.6	0.04	79.3
45	91	108	13.4	12.1		
60	92	111	14.1	12.5	0.04	76.4
75	92	110	12.9	11.3		
90	92	111	12.7	11.1	0.03	75.0
105	94	113	12.9	11.6		
120	93	115	13.5	11.3	0.03	72.8
135	93	114	13.3	11.8		
150	92	112	12.9	11.4	0.01	75.6
165	92	113	12.9	11.2		
180	92	112	12.8	11.7	0.01	76.2

the heating process and operating conditions, i.e. temperature and time.

The results of protein solubility for the soybeans treated by different types of laboratory-scale heating processes are shown in Fig. 12. The data presented were measured at the ends of the experiment, namely, after 30 min in the spouted bed, 3.4 min in the extruder and 12 min in the infrared. It is evident that the protein solubility for the soybeans treated by various thermal processes declines to the recommended range, except that of soybeans processed with the spouted bed and infrared at 120 °C which was above 85%. However, this temperature is not high enough to inactivate the urease to the level lower than 0.3 pH difference within a given time. To maintain the product in the range of 70–85% together with the acceptable pH difference, soybeans should therefore be treated at a temperature higher than 140 °C.

As noticed, the quality from each technique is rather different; the higher protein solubility is obtained with the single layer infrared and spouted bed (78–89%) and the lower one is obtained from the screw extruder (74–78%). This can be seen easily at 140 °C where the quantity of soluble protein in 0.2% KOH solution ranges between 82% and 84% for the spouted bed and infrared and becomes lower for the extruded soybeans with a value of 73%. The lower soluble proteins are attributed to the grounded soybeans absorbing the heat uniformly, unlike the other two techniques where the full kernels retard the heat penetration. Moreover, this effect results in a higher degree of urease inactivation, along with shorter treating time, when compared to the other heating techniques at the same temperature. To obtain a higher protein solubility, while maintaining an adequate level of urease inactivation, the extruder should not be operated at a temperature higher than 130 °C. The results of heat treatment by the spouted bed and infrared radiation indicated that the infrared seems to be a more attractive technique since the rates of water transport and urease inactivation using this approach are enhanced, along with a high soluble protein content.

Fig. 12 also shows the influence of temperature on the protein solubility, indicating the lower amount of soluble proteins associated with higher temperature. This is

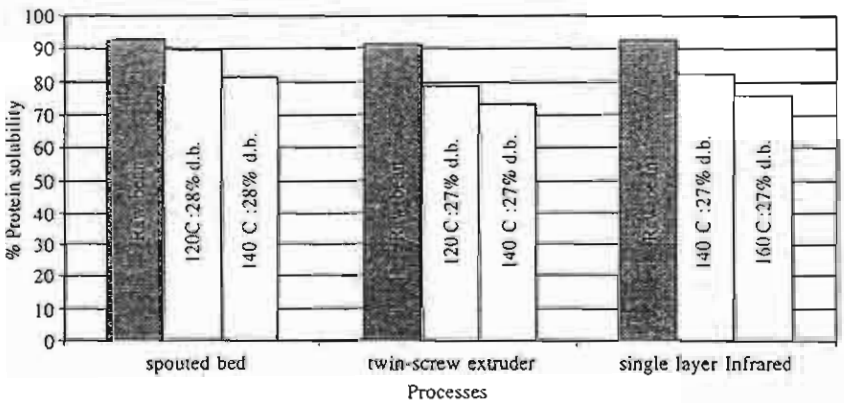

Fig. 12. Comparisions of the percentage of protein solubility between two-dimensional spouted bed, single layer infrared dryer and twin-screw extruder (lab-scale).

expected since when more thermal energy is transferred, the treating temperature is increased.

The change in protein solubility of dry soybeans after treating with the single-screw extruder, micronizer and fluidized bed dryer is shown in Tables 4–6, respectively. The protein solubility of soybeans from each heat treatment technique varies in a range of 73–85%, implying properly cooked soybeans. The soluble proteins of treated soybeans, when compared with those obtained from the extruder and fluidized bed, are relatively higher with the micronizer. From a qualitative point of view, these results are in accordance with the one from the lab-scale infrared dryer as illustrated in Fig. 12, showing higher protein solubility.

3.4. Lysine

Some interesting conditions of each process for inactivating urease enzyme were chosen to determine the remaining lysine as follows: 130 °C, 18% d.b. and 2.2 min for the twin-screw extruder; 140 °C, 14% d.b. and 10 min for the fluidized bed dryer; 140 °C, 14% d.b. and 30 min for the spouted bed dryer; and 160 °C, 18% d.b. and 12 min for the single layer infrared dryer. Table 7 shows the remaining lysine in the soybeans after treatment with the twin-screw extruder, fluidized bed, spouted bed and infrared driers. The percentage of lysine was 5.25% for untreated soybeans and was decreased by 0.8–1.2% in each heat treatment technique. The statistical analysis using a t-test approach indicated that the amounts of remaining lysine from such techniques were insignificantly different ($p < 0.05$).

Table 5
Full-fat soybean analysis after passing the micronizer (commercial-scale)

Time (min)	Product temperature (°C)	Moisture content (% d.b.)		Urease activity (pH change)	Protein solubility (%)
		Inlet	Outlet		
15	121	11.6	6.9		
30	120	11.5	6.8	0.10	83.5
45	122	11.6	7.0		
60	120	11.5	6.9	0.10	84.8
75	119	11.5	7.1		
90	120	11.6	7.1	0.10	85.9
105	121	11.6	6.7		
120	121	11.5	6.9	0.12	74.1
135	122	11.6	7.0		
150	119	11.6	7.0	0.16	76.8
165	120	11.6	6.9		
180	120	11.5	6.9	0.16	82.2

Table 6
Full-fat soybean analysis after fluidized bed heating process (commercial-scale)

Time (min)	Moisture content (% d.b.)		Urease activity (pH change)	Protein solubility (%)
	Inlet	Outlet		
15	11.8	0.8		
30	11.9	0.9	0.25	77.6
45	11.9	1.2		
60	12.3	1.3	0.21	74.4
75	11.9	1.0		
90	11.8	1.0	0.26	74.4
105	12.1	1.4		
120	12.3	1.6	0.27	75.6
135	12.3	1.5		
150	12.4	1.6	0.24	72.6
165	12.3	1.4		
180	12.3	1.4	0.26	74.6

3.5. Energy consumption

Table 8 shows the energy consumptions of commercial-scale equipment, i.e. extruder, micronizer and fluidized bed dryer for inactivating the urease in the dry soybeans. The electrical energy consumption represented in the table was calculated by multiplying by a factor of 2.6, a conversion factor for converting secondary to primary energy, with the experimentally measured electrical energy. It can be seen that the extruder consumed about 928 MJ/ton of product, which is 1.5 times of the thermal energy utilized. The opposite results were obvious with the fluidized bed dryer and micronizer where both types of equipment use high levels of thermal energy, with amounts of 550 MJ/ton of product for the micronizer and 911 MJ/ton of product for the fluidized bed.

In calculating the energy cost, we assumed that LPG gas cost was 20 baht/kg and electricity cost was 3 baht/kW h (42.3 baht = 1$). The calculated total energy costs were 260, 429, 547 baht/ton of product for the micronizer, fluidized bed dryer, single-screw extruder, respectively, the first technique providing the lowest operating cost. The energy cost for the fluidized bed was relatively high since the industrial dryer did not have an air recycling system although the exhaust air had a temperature higher than 100 °C and, therefore, a high reuse potential. The ineffectively utilized energy consumption is a consequence. However, if the exhaust air was fully recycled, the thermal energy might possibly have savings of 74%, compared to no air recirculation. The resulting total energy cost would be reduced and become lower than that spent in the micronizer and extruder by approximately 39% and 71%, respectively.

In addition to the energy cost, attention should be paid to the equipment cost as well. As informed by the feed milling industries, fluidized bed dryer, micronizer and extruder, all of which have a capacity of 1–1.5 ton/h, cost 375,000, 13,000,000 and 3,200,000 baht, respectively (SPM animal feed and Saha farm company limited). According to this information including the energy cost and the quality of treated soybeans, it is likely that

Table 7
Percent lysine in soybean after treatment for twin-screw extruder, fluidized bed, spouted bed, and single layer infrared dryer (lab-scale)

Heating processes	% Lysine
Untreated soybean	5.25
Heat treatment with two-dimensional spouted bed dryer[a]	4.15
Heat treatment with single layer infrared dryer[b]	4.05
Heat treatment with fluidized bed dryer[c]	4.45
Heat treatment with twin screw extruder[d]	4.15

[a] Heating temperature of 140 °C and initial moisture content of 14% d.b. for 30 min.
[b] Heating temperature of 160 °C and initial moisture content of 18% d.b. for 12 min.
[c] Heating temperature of 140 °C and initial moisture content of 14% d.b. for 10 min.
[d] Heating temperature of 130 °C and initial moisture content of 18% d.b. for 2.2 min.

Table 8
Energy consumption of commercial-scale extruder, micronizer, and fluidized bed soybean dryer (FBD)

Items	Extruder	Micronizer	FBD	FBD (assumed fully recycle)
Testing hours	3	3	3	
Capacity (ton/h)[a]	1	1.5	2	
Treatment temperature (°C)[a]	110	120	148	
Inlet moisture content (% d.b.)[a]	13	12	12	
Outlet moisture content (% d.b.)[a]	12	7	1	
Electrical energy consumed (MJ/ton of product)	928	94	204	204
Thermal energy consumed (MJ/ton of product)	625	550	911	233

[a] Average value.

fluidized bed technique is the most attractive alternative technique for replacing conventional methods such as extrusion and infrared radiation.

4. Conclusions

The rate of water removal in soybean during the course of drying by spouted bed and infrared techniques shows a remarkable difference, the latter exhibiting more potential. Such difference is shown by the drying constant, which can be statistically determined by the semi-empirical drying equation. The drying constant was correlated with moisture content and temperature in a modified Arrhenius form. Both factors also importantly affect the urease inactivation where high moisture content and temperature induce rapid inactivation for the soybeans treated by the spouted bed and infrared radiation whilst the first factor results in slow inactivation for the extruded soybeans. The results of the soybeans treated by spouted bed, extruders, fluidized bed and infrared radiation show that each heat treatment technique appears to be capable of satisfactorily inactivating urease, but provides radical differences in the amounts of soluble proteins, the highest protein solubility being produced by the infrared treatment whilst the lowest one was obtained by extrusion. The amounts of lysine remaining after treatment by the different techniques were similar. The experimental results from the feed milling industries showed that the highest total energy used for treating soybeans was required by the extruder followed by the fluidized bed technique with the micronizer requiring the least amount. There is a high possibility of using the fluidized bed with an air recirculation system for inactivating anti-nutritional factors and improving energy utilization.

Acknowledgements

The authors would like to thank the Thailand Research Fund for the financial support this work. In addition, we wish to thank the SPM animal feed company limited and the Saha farm company limited for their cooperation while working at industrial sites.

References

AACC. *Approved method of the American Association of Cereal Chemist (9th ed.)*. St. Paul, MN: AACC, 1995.
AOCS. *Official and Tentative Methods of the American Oil Chemists' Society (3rd ed.)*. Campaign, IL: AOCS, 1984.
ASA. *Fullfat Soybeans Handbook of American Soybean Association*. Singapore, 1990.
Camire, M. E., Camire, A., & Krumhar, K. (1990). Chemical and nutritional changes in foods during extrusion. *Critical Review in Food Science and Nutrition, 29*, 35–57.
Cheong, Y.L. (1997). Fullfat soybean meal production and utilization. *Technical Bulletin of American Soybean Association*, Singapore.

Faber, J. L., & Zimmerman, D. R. (1973). Evaluation of infrared-roasted and extruder-processed soybeans in baby pig diets. *Journal of Animal Science, 36*, 902–907.

Fasina, O., Tyler, B., Pickard, M., Hua Zheng, G., & Wang, N. (2001). Effect of infrared heating on the properties of legume seeds. *International Journal of Food Science and Technology, 36*, 79–90.

Hensen, B. C., Flores, E. S., Tanksley, T. D., Jr., & Knabe, D. A. (1987) Effect of different heat treatments during processing of soybean meal on nursery and growing pig performance. *Journal of Animal Science, 65*, 1283–1291.

Liener, I. E. (1994). Implications of antinutritional components in soybean foods. *Critical Review in Food Science and Nutrition, 34*. 31–67.

López, A., Piqué, M. T., Romero, A., & Aletá, N. (1998). Modelling of Walnut Sorption Isotherms. *Italian Journal of Food Science, 1*(10), 67–74.

Mustakas, G. C., & Griffin, E. L., Jr. (1964). Production and nutritional evaluation of extrusion-cooked full-fat soybean flour. *The Journal of the American Oil Chemist' Society, 41*, 607–614.

Osborne, T. B., & Mendel, L. B. (1917). The use of soybean as food. *Journal of Biological Chemistry, 32*, 369.

Osella, C. A., Gordo, N. A., González, R. J., Tosi, E., & Ré, E. (1997). Soybean heat-treated using a fluidized bed. *Lebensmittel-Wissenschaft & Technologie, 30*, 676–680.

Savage, W. D., Wei, L. S., Sutherland, J. W., & Schmidt, S. J. (1995). Biologically active components inactivation and protein insolubilization during heat processing of soybeans. *Journal of Food Science, 60*, 164–168.

Soponronnarit, S., Swasdisevi, T., Wetchacama, S., & Wutiwiwatchai, W. (2001). Fluidised bed drying of soybeans. *Journal Stored Products Research, 37*, 133–151.

Vandergrift, W. L., Knabe, D. A., Tanksley, T. D., Jr., & Anderson, S. A. (1983). Digestibility of nutrients in raw and heated soyflakes for pigs. *Journal of Animal Science, 57*(5), 1215–1224.

White, C. L., Greene, D. E., Waldroup, P. W., & Stephenson, E. L. (1967). The use of unextracted soybeans for chicks. *Poultry Science, 46*, 1180–1185.

Wright, K. N. (1981). Soya meal. *JAOCS*, 294–300.

Available online at www.sciencedirect.com
SCIENCE DIRECT®
PERGAMON
Journal of Stored Products Research 40 (2004) 379–393
Journal of STORED PRODUCTS RESEARCH
www.elsevier.com/locate/jspr

Methodology for enhancing drying rate and improving maize quality in a fluidised-bed dryer

Somkiat Prachayawarakorn[a,*], Somchart Soponronnarit[b], Somboon Wetchacama[b], Kongsak Chinnabun[b]

[a] *Department of Chemical Engineering, Faculty of Engineering, King Mongkut's University of Technology Thonburi, Suksawat 48Rd, Tungkru, Bangkok 10140, Thailand*

[b] *School of Energy and Materials, King Mongkut's University of Technology Thonburi, Suksawat, 48Rd, Tungkru, Bangkok 10140, Thailand*

Accepted 30 January 2003

Abstract

A theoretical diffusion model for a single maize (*Zea mays* L.) kernel has been developed to describe moisture migration during drying and tempering stages. The effective diffusivity was determined experimentally at a range of temperatures between 90°C and 170°C with initial moisture contents of 37% and 43% dry-basis. The functional relationship between the diffusivity and temperature is analogous to a modified Arrhenius equation.

Two-stage drying including tempering between stages provides not only faster removal of moisture, but also a reduced number of stress cracks when compared to single-stage drying. However, the colour of the maize appears darker and more intense with longer tempering periods. To maintain maize quality and to reduce energy consumption, the results from the experiments and simulations are limited to temperatures of less than 150°C; high-moisture maize should be dried to 23% dry-basis and then tempered for 40 min.

The ambient-air velocity for cooling the tempered maize in a range between 0.075 and 0.375 m/s does not affect the maize quality as measured by the number of stress cracks and colour.

Keywords: Ambient-air ventilation; Diffusion model; Fluidised bed; Quality; Tempering

1. Introduction

The main production of maize (*Zea mays* L.) in Thailand occurs in the rainy season. During this period, the moisture content of harvested maize is between 20% and 23% wet-basis. On some

*Corresponding author. Tel.: +66-2-4709220.
E-mail address: somkiat.pra@kmutt.ac.th (S. Prachayawarakorn).

0022-474X/03/$ - see front matter © 2003 Elsevier Science Ltd. All rights reserved.
doi:10.1016/S0022-474X(03)00029-8

occasions, it can be up to 25% wet-basis. A rapid moisture-removal rate is a necessary step in the prevailing hot and humid climate to achieve a safe moisture level and to inhibit the growth of microorganisms such as *Aspergillus flavus* Link ex Fr. and *Aspergillus parasiticus* Speare which are frequently found in maize from cultivation areas (Siriacha et al., 1991). Hot-air drying is likely to be an appropriate approach. Amongst the commercial dryer types, the fluidised-bed dryer is one that can suitably be applied (Mourad et al., 1995; Soponronnarit et al., 1997a).

With this technique, a stream of hot air is blown through a bed of solid particles which then behave like a liquid and can flow randomly along a bed with fluid-like properties. Solid particles are in intimate contact with the drying medium so that the temperature is rather uniform throughout the bed, although dispersion results in the moisture contents of individual grains being non-uniform. This provides advantages in that the inlet air temperature and superficial air velocity can be as high as possible. The resulting heat and mass transfer between solid and drying air are extreme, and hence some portions of the moisture concentrated near the grain surface can be transported rapidly through the environment whereas the inner surface is still wet, producing a large moisture gradient inside the grain. The moisture of the kernel is very difficult to remove in spite of the high convective mass transfer and the high capability of drying air, thus requiring rapid consumption of energy. In addition to energy consumption, such high drying rates in the fluidised bed may result in serious detrimental effects on maize quality. Thus, when maize is subjected to hot air for extended times, the dried maize surface becomes more and more brittle and eventually cracks or fractures. Soponronnarit et al. (1997b, 2001) investigated the effect of high temperatures (more than 100°C) on the physical damage to maize and soybean and reported that significant increases in stress cracks and in breakability occurred at reduced moisture contents.

Similarly, some early work on maize drying using a fixed-bed dryer showed that stress cracks increased with drying temperature, and conversely, reduced with increased humidity (Thompson and Foster, 1963; White and Ross, 1972; Otten et al., 1984; Estrada and Litchfield, 1993; Davidson et al., 2000). In their work, the temperature was in a range of 40°C to 100°C.

In addition to experimental studies, a theoretical framework has also been developed to explain qualitatively how crack generation develops in the porous materials while the material is being dried. It appears that moisture gradients are the main cause of the generation of the shrinkage stresses (Musielak, 2000). The kernels are in tension near the surface of the dried body, and in compression at the centre of the solid. If the relative humidity of the drying medium decreases with the increased temperature, then the stresses are considerably higher at higher values of the drying-medium temperatures.

In addition to stress cracking and breakage, the change in colour of the kernel caused by thermal effects is also important, particularly when drying involves very high temperatures. The colours in terms of a (red) and b (yellow) values measured on the Hunter scale were significantly affected by drying time (Soponronnarit et al., 1997b). The change of colour may result in a rapid drop in price and it is rejected by the food industries if premium quality is needed.

These considerations motivated us to explore methods of improving the process of fluidised-bed maize drying. One common approach used in the grain industry is tempering between drying stages. Some authors refer to this technique as dryeration. In the tempering stage, the maize leaving the dryer is kept in a closed bin with no air ventilation. During this period, moisture will not evaporate through the grain surface but is redistributed to achieve a uniform moisture content

throughout the kernel. Drying of paddy with tempering was investigated by Steffe and Singh (1980) who reported that head-rice yield could be improved as compared with single stage drying.

In the process of tempering, basic information that is needed in practice is how long the grain should be tempered to ensure a uniform moisture content. This is accomplished by formulating a mathematical model that enables the simulation of moisture movement inside the kernel. The model should be validated by experiments so that it can conveniently be used for engineering calculation.

The drawback of either semi-empirical or empirical models, which have frequently been used by some authors (Satayaprasert and Vanishsriwatana, 1992; Soponronnarit et al., 1997c), is that they do not provide the details of changing local moisture content inside the maize with time. Consequently, after the end of the first drying period, the spatial concentration profile is not known, thereby not allowing prediction of the change of moisture content during tempering. In the present work, we have developed a theoretical diffusion model that enables the moisture-content distribution to be determined during both drying and tempering. This allows investigation of the uniformity of moisture concentration everywhere inside the maize kernels after they have been dried for a given period. For simplicity, we used a sphere model to describe the maize kernel geometry. The effective diffusion coefficient was assumed to be the same for each component of the maize kernel, such as endosperm and pericarp. In addition to developing the mathematical model, we also examined how the tempering periods and cooling rates affect the quality of maize in terms of stress cracking and colour.

Since the establishment of commercial fluidised-bed dryers in Thailand, some industries have used this dryer type for maize drying. As high an operating temperature as possible is usually adopted to achieve the highest throughput and to avoid aflatoxin B-1 production, which is prevalent in tropical regions. Therefore, the principal experiments were conducted at the high end of the temperature range. The results of this work will therefore be of value in practical applications.

2. Mathematical model

In this work, the maize kernel is assumed to be composed of a homogeneous body at the macroscopic level, and the volume of maize kernel does not change during drying and tempering processes. When the maize is immersed in the drying air, the liquid starts diffusing through the maize surface, neglecting the convective effect inside the maize kernel, so that Fick's second law of diffusion can then be applied to describe the moisture movement inside the sphere-shaped maize as given by the following equation:

$$\frac{\partial M}{\partial t} = D_{eff}\left(\frac{\partial^2 M}{\partial r^2} + \frac{2}{r}\frac{\partial M}{\partial r}\right) \tag{1}$$

where M is the moisture content of maize in dry-basis units, D_{eff} is the effective diffusion coefficient (m^2/s) accounting for heterogeneous media, t is the drying time (s) and r is the distance in the radius direction (m^2).

Initially, the moisture content is assumed to be spatially uniform. When the maize is being subjected to drying, moisture around the exterior surface evaporates immediately and approaches

equilibrium with the surrounding air. This behaviour is substantially correct for drying maize at a high superficial air velocity and a high inlet temperature. Typically, as in the drying of other porous solids, the water content is removed most quickly from the peripheral regions of the kernel and more slowly from the interior. The initial and boundary conditions of internal resistance are:

$$t = 0, \quad 0 \leqslant r \geqslant a, \quad M = M_{in} \tag{2}$$

$$t > 0, \quad r = 0, \quad \frac{\partial M}{\partial r} = 0 \tag{3}$$

$$t > 0, \quad r = a, \quad M = M_{eq} \tag{4}$$

where M_{in} is the initial moisture content, M_{eq} is the equilibrium moisture content and a is the equivalent radius of sphere (m). The moisture profile along the radius positions when Eq. (1) is solved algebraically with the above initial and boundary conditions is given by the following equation:

$$\frac{M(r,t) - M_{eq}}{M_{in} - M_{eq}} = \frac{2a}{\pi} \sum_{p=1}^{\infty} \frac{(-1)^n}{rp} \sin \frac{p\pi r}{a} \exp\left(-\frac{p^2 \pi^2 D_{eff} t}{a^2}\right) \tag{5a}$$

After integrating the analytical solution of Eq. (5a) over the volume of the sphere and dividing by the total volume, the average moisture content throughout the kernel is expressed as

$$MR(t) = \frac{6}{\pi^2} \sum_{p=1}^{\infty} \left(\frac{1}{p^2}\right) \exp\left[-p^2 \pi^2 \frac{D_{eff}}{a^2} t\right] \tag{5b}$$

where p is the number of series terms, $MR(t)$ is the ratio of the remaining driving force of concentration to total driving force of concentration, $(M(t) - M_{eq})/(M_{in} - M_{eq})$. We found that 5 or 6 terms of the infinite series represented by Eq. (5b) were sufficient to represent the results over the drying period. The moisture equilibrium equation for maize is (Pudpong et al., 1990)

$$1 - RH = \exp(-3.074 \times 10^{-5}(T + 273.15)(100 M_{eq})^{1.8156}) \tag{5c}$$

where RH and T (°C) are the relative humidity and temperature of air, respectively. The proposed equation was obtained experimentally in a range of temperatures and relative humidities between 35°C and 65°C and 10% and 90%, respectively. Such conditions were lower than the range used in the present work, but it can still be used for calculating the moisture reduction as will be seen in Fig. 3 because of the very low equilibrium moisture content in our experimental conditions.

After passing through the fluidised bed, maize was collected in an airtight container maintained at the same temperature as that of the grains. This is known as tempering. To predict the change of moisture concentration profiles during tempering, the concentration gradient along the radius at the end of the drying period must be known. They are used as initial values at the beginning of the tempering process. In addition, the maize surface is assumed to be impermeable to moisture transport throughout the tempering period. The initial and boundary conditions during the tempering period are given by the following equations:

$$t = 0, \quad 0 \leqslant r \leqslant a, \quad M = M(r), \tag{6}$$

$$t > 0, \quad r = 0, \quad \frac{\partial M}{\partial r} = 0, \tag{7}$$

$$t > 0, \quad r = a, \quad \frac{\partial M}{\partial r} = 0 \tag{8}$$

Due to the complexity of Eq. (1) with the above-mentioned boundary conditions, a numerical solution is sought. A sphere is divided into N intervals and the distance between the nodes is h (m), and the time step used in calculation is k (s). Thus, a finite difference approximation of Eq. (1) is expressed by

$$\gamma M_i^{j+1} - \beta M_{i-1}^{j+1} - \sigma M_{i+1}^{j+1} - \beta M_{i-1}^{j} - \psi M_i^j - \sigma M_{i+1}^j = 0 \tag{9}$$

where

$$\alpha = \frac{kD_{eff}}{2h^2} \tag{10}$$

$$\beta = \alpha\left(\frac{i-2}{i-1}\right) \tag{11}$$

$$\gamma = 1 + 2\alpha \tag{12}$$

$$\sigma = \alpha\left(\frac{i}{i-1}\right) \tag{13}$$

$$\psi = 1 - 2\alpha \tag{14}$$

Subscripts i and superscripts j refer, respectively, to the spatial nodal grid index and the nodal temporal grid index. Eq. (9) is used to calculate the internal node concentrations starting from $i=2$ until N, the number of intervals in the sphere. To solve the boundary conditions given by Eqs. (7) and (8), substituting the Crank–Nicolson formula yields, respectively, the following equations:

for $i = 1$ (at sphere centre),

$$(1 + 6\alpha)M_1^{j+1} - (1 - 6\alpha)M_1^j - 6\alpha(M_2^{j+1} + M_2^j) = 0 \tag{15}$$

for $i = N + 1$ (at the impermeable surface),

$$(1 + 2\alpha)M_{N+1}^{j+1} - (1 - 2\alpha)M_{N+1}^j - (2\alpha)(M_N^{j+1} + M_N^j) = 0 \tag{16}$$

Values of parameters required to simulate the change in moisture profile during tempering by such equations can be summarised as follows:

1. An equivalent radius for the maize kernel is 4 mm.
2. The effective diffusion equation for maize as a function of moisture content and inlet-air temperature is expressed as

$$D_{eff} = 4.70 \times 10^{-5} \exp(-2.971M)\exp\left(-\frac{4171.3}{273 + T}\right) \tag{17}$$

where T is the inlet-air temperature (°C). Eq. (17) is obtained from the drying experiments at temperatures between 90°C and 170°C. The details will be discussed below.

3. Materials and methods

3.1. Drying kinetics

A batch-fluidised-bed dryer was used to study the drying kinetics and quality of maize. To fully understand the mechanism of moisture transfer inside the grain, a maize bed depth of 2 cm was used throughout these experiments. If the bed depth is too thick, then there may be transfer of water between kernels and a more elaborate model would be needed. However, this is not the main subject of our work. The superficial air velocity was limited to 3 m/s. The chosen velocity, which was beyond the minimum fluidisation velocity of maize (1.8 m/s; Soponronnarit et al., 1997c), ensured that the convection resistance to mass transfer would be insignificant. To determine the effective diffusion coefficient, the experiments were carried out at temperatures of 90°C, 110°C, 130°C, 150°C and 170°C with two levels of initial moisture content, 27% and 30% wet-basis. To obtain the desired moisture content, the maize was rewetted and kept in a temperature-controlled room between 5°C and 10°C for 7 days to allow for water to penetrate into the grains. Samples drawn from the dryer every minute were then placed in a hot-air oven at a constant temperature of 103°C for 72 h to determine their moisture content, using the method of the Association of Official Agricultural Chemists (Anon., 1960).

3.2. Tempering

After a first-stage drying at 150°C for 6 min for 43% dry-basis initial moisture content and 4 min for 37% dry-basis, maize was placed in a well-sealed container. During this stage, the maize was maintained at the same temperature as the maize leaving the bed for periods of 10, 20 30, 40 and 50 min. The tempered maize was then dried by the fluidised-bed dryer under the same drying conditions as employed previously for periods of 5 min. Eventually, the maize was tested for physical damage.

To study the effect of cooling rates, the maize dried under the conditions described and tempered for 40 min was ventilated immediately by ambient-air velocities of 0.075, 0.15, 0.225, 0.3 and 0.375 m/s without drying at the second stage. The reason for selecting this tempering period is explained below.

Before these experiments, the fresh maize was shelled carefully by hand to ensure that every kernel was sound and not cracked.

3.3. Quality tests

The amount of stress-cracked grain and the colour were of particular interest in testing maize quality in the rapid-drying approach using high temperature. For the stress cracks, visual inspection under light was employed using a 200 g sample of maize. Each kernel was assigned to one of two classes: cracks (multiple and single) and completeness. The percentage in each class was normalised by dividing the weight of maize kernels in each category by the total weight. Multiple cracking was often found in this work. A colour meter, Juki JP 7100p, was used to determine the grain surface colours. a, b and L values in the Hunter system correspond to red, yellow and lightness, respectively.

4. Results and discussion

4.1. Effective diffusion coefficients

Fig. 1 shows the moisture reduction of maize with time for different inlet-air temperatures, indicating that larger amounts of moisture can be removed when the maize is dried at higher inlet-air temperatures. During the early drying period, the slope of the drying curve is very steep and it continually declines with a longer drying time, suggesting that the water inside the kernel is difficult to remove and that internal diffusion is the main factor in controlling the moisture movement inside the maize kernel.

Moisture diffusion depends strongly on the temperature and frequently also on the moisture content. The dependence of effective diffusivity on temperature is often modelled by an equation of Arrhenius form:

$$\text{Model 1}: \quad D_{eff} = A_1 \exp\left\{\frac{-C_1}{R(T+273)}\right\} \tag{18}$$

where A_1 (m^2/s) is called pre-exponential factor, C_1 (kJ/kmol) is the activation energy and R (kJ/kmol/K) is the universal gas constant. In the case where effective diffusivity is independent of the moisture content, A_1 has a constant value. In contrast, when the moisture content contributes to an effective diffusion coefficient, A_1 varies with moisture content. In the absence of a theoretical explanation of the changing value of A_1 with moisture content, an empirical equation has often been used (Mulet et al., 1989; Ulku and Uckan, 1986). In the present work, the following diffusion equation including Eq. (18) was used to correlate the effective diffusion coefficient with inlet temperature and moisture content:

$$\text{Model 2}: \quad D_{eff} = A_2 \exp(B_2 M)\exp\left[-\frac{C_2}{R(273+T)}\right] \tag{19}$$

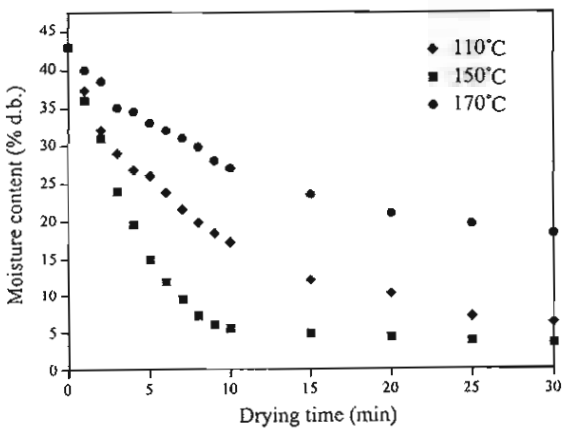

Fig. 1. Change of moisture content at different inlet-air temperatures during first-stage drying (initial moisture content of 43% dry-basis).

Table 1
Coefficients of diffusion models

Model	A	B	C	Coefficient of determination
1	1.992×10^{-4}	NA	599.4	0.9568
2	4.700×10^{-5}	−2.971	501.7	0.9734

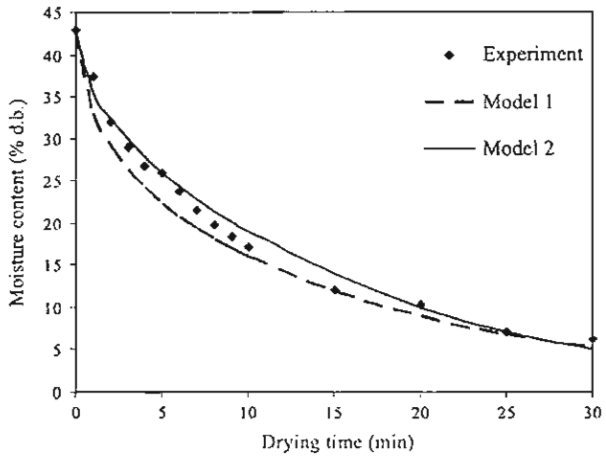

Fig. 2. Comparison of predicted moisture content from diffusion models with the experimental results (inlet-air temperature of 150°C).

A non-linear regression was applied to determine the coefficients in each model by substituting the above diffusion equations into Eq. (5b). The accuracy of the models was evaluated by examining the values of the coefficient of determination (R^2), which was defined as

$$R^2 = 1 - \frac{\sum_{i=1}^{z}(M_{\text{calculated}} - M_{\text{experiment}})^2}{\sum_{i=1}^{z}(M_{\text{experiment}})^2 - \sum_{i=1}^{z}(M_{\text{experiment}})^2/(z-k)} \tag{20}$$

where z and k are the numbers of data points and parameters in the diffusion model, respectively. The coefficients obtained from the fitting are shown in Table 1.

As seen from Table 1, the activation energy for maize varies in the range of 500–600 kJ/kmol, depending upon the diffusion model employed. Model 2 adequately describes moisture reduction over a long drying period as represented in Fig. 2.

4.2. *Effects of tempering period on moisture reduction*

The purpose of collecting the moisture contents for two-stage drying was to validate the data with the theoretical drying–tempering equations. In predicting moisture content at the second stage of drying, the moisture profile along the radius at the end of tempering was used as the initial condition for calculating the moisture reduction in this stage. It is shown in Fig. 3 that the

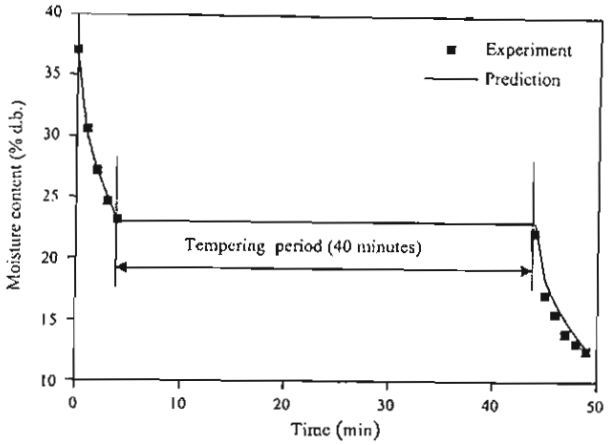

Fig. 3. Comparison of simulated moisture content with the experimental results for two-stage drying including tempering between stages (inlet-air temperature of 150°C).

agreement between the proposed drying–tempering equations and the experimental results is very good.

In the tempering process, large differences in moisture content between the surface and the centre of maize kernel during the early period can be encountered. After a sufficiently long period, the moisture redistributes and ultimately equalises throughout the kernel. To evaluate the time for moisture balance during such stage, a tempering index, TI, was recommended. The definition of this index is expressed by

$$TI = \frac{M_s(t) - M_s(t=0)}{M_s(t=\infty) - M_s(t=0)} \tag{21}$$

where M_s is the surface concentration and t is the tempering time (s). The tempering index was introduced initially by Sabbath (1970). The surface concentration after an infinite tempering period is equivalent to the mean concentration at the end of the first drying pass that is calculated by the following equation:

$$M_s(t=\infty) = \bar{M} = \frac{\int_0^a M(r) r^2 \, dr}{\int_0^a r^2 \, dr} \tag{22}$$

where $\bar{M}$ is the mean concentration, $M(r)$ is the moisture profile, r is the distance along the radius (m) and a is the radius of sphere (m). This equivalence is a result of the assumption that there is no moisture loss from the surface during the tempering.

The tempering–drying models were utilised to study the effect of tempering period on moisture removal. In our case study, maize having an initial moisture content of 43% dry-basis was dried at an inlet temperature of 150°C for 6 min followed by tempering at different periods, with subsequent drying at the same temperature as the previous one. The simulation results clearly indicate the advantages of having the tempering stage in the drying process as it not only reduces the drying time but also reduces the energy consumption. In Fig. 4, we plotted only the moisture content with the drying time, ignoring the tempering time. It is shown that as the tempering period

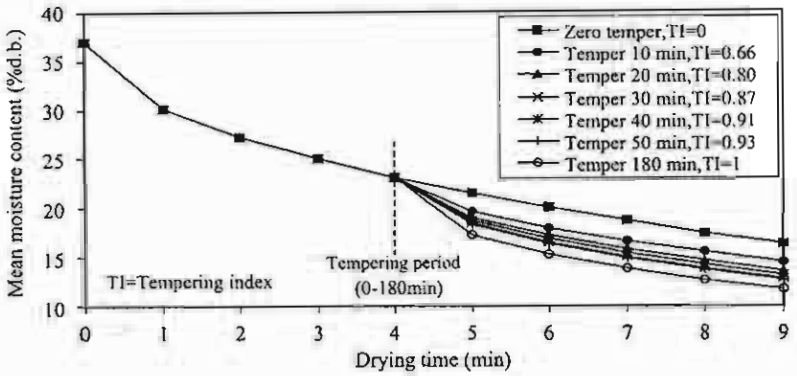

Fig. 4. Simulated results of the effect of tempering periods on moisture removal for two-stage drying (inlet-air temperature of 150°C and initial moisture content of 43% dry-basis).

is provided between two-stage drying, better moisture transport is accomplished. When predicting the moisture content at the start of second-stage drying, the tempering time is an important factor in determining the final moisture content. As shown in Fig. 4, as the tempering period increases from 0 to 180 min, the final moisture content decreases from 18.4% dry-basis to 13.7% dry-basis. This can be explained by the fact that tempering results in moisture transport from the interior to the surface of kernel, and consequently, the water near the surface can be removed easily when subjected to drying conditions again.

As indicated in Fig. 4, when maize was tempered for more than 40 min, corresponding to a tempering index higher than 0.9, the reduction of moisture content at the second stage is almost of the same magnitude as the case of maize tempered for 180 min. It seems that the moisture gradient becomes insignificantly different and does not affect the drying rate. For 37% dry-basis initial moisture content, the results of simulation are similar to Fig. 4.

In the remaining sections, we are concerned with how the grain quality is affected when the tempering stage was included in the process, by comparison with single-stage drying. The experiments for testing maize quality were limited to 150°C in order to maintain the drying capacity as high as possible. The effect of relative humidity on the stress cracks has not been considered since the relative humidity was very low (<5%) at high temperatures. In fact, this factor is also important for low-temperature drying (Estrada and Litchfield, 1993), reducing stress cracking with higher humidity.

4.3. Effect of tempering periods on maize qualities

In studying the effect of tempering on stress cracks and colour, maize was dried first to 19% or 18% dry-basis and then tempered for different periods, with subsequent drying. The final moisture content in all cases varied in a small range between 13% and 16% dry-basis, depending upon tempering period.

Fig. 5 shows the percentage of stress-cracked grain by weight against tempering periods for two initial moisture contents, 37% and 43% dry-basis. Note that zero tempering means that the moist

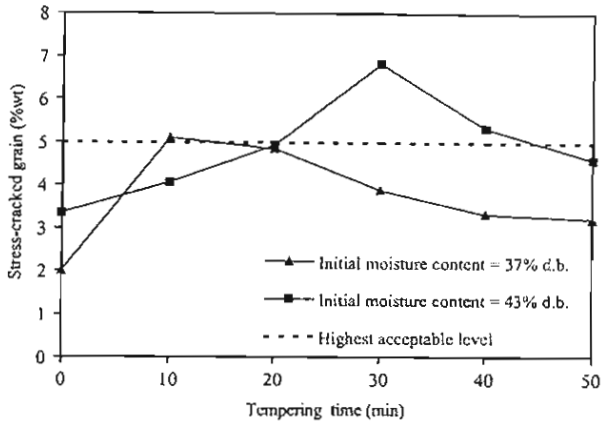

Fig. 5. Percentage of stress-cracked grain at different tempering periods (inlet-air temperature of 150°C for first-stage drying).

maize was dried to the desired moisture content by single-stage drying, and a standard value for cracking that is acceptable should not be higher than 5% as recommended by Soponronnarit et al. (1997b). In reducing moisture content to 15% dry-basis with no tempering, initial moisture content is one of the factors contributing to stress cracking. As shown in Fig. 5, the stress cracks for initial moisture contents of 37% and 43% reach, respectively, 3.8% and 6.2% of the kernels by weight when they are zero at the beginning. The latter would be graded as poorer quality maize. The cracked maize is caused by the non-uniform shrinkage within the maize kernel inducing stresses higher than the failure strength of the kernel. Cracking first manifested itself at the surface and then progressed inwards as the drying process continued.

When two-stage drying with tempering between stages was employed, however, stress cracking was reduced to an acceptable level. In addition, tempering for any longer time did not reduce the severity of stress cracking. This trend also appeared in the case of maize with lower moisture contents.

At present, the standard colour of yellow maize kernels used in the grain industry in Thailand has not been formally established as a criterion of quality. Traders use their experience and expertise to consider colour quality. According to Soponronnarit et al. (1999), the criterion has been established based on the maize samples that passed the quality test in the commercial market. The premium quality of colour is as follows: L and b should not be lower than 47.7 and 23.5, respectively, and a should not be higher than 9.7. Fig. 6 shows the maize surface colour represented in the form of L, b and a values, after it has passed the second stage of drying from initial moisture contents of 37% and 43% dry-basis. The data shown in this figure were obtained at the same conditions as in Fig. 5 indicating that colours do not change significantly with the increased tempering period from those of untempered maize. L decreases continuously with increased tempering period and the values of a and b are almost constant in the early period with subsequent higher values after 30 min. According to these results, both the tempering period and heat used to maintain temperature during tempering cause the poorer colour. However, the colour quality of tempered maize is still better than the standard level.

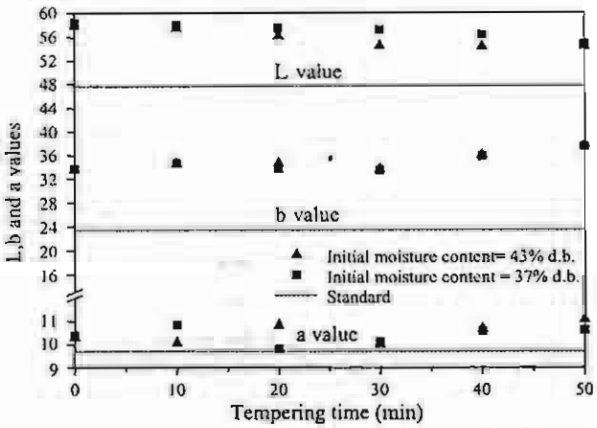

Fig. 6. Colours of maize surface at different tempering periods (values of L, b and a represent lightness, yellowness and redness, respectively).

4.4. *Effect of cooling rate on maize qualities*

After maize was tempered for 40 min, it was assumed that the moisture-content gradient inside the kernel was very small, corresponding to a tempering index of 0.9 as previously shown in Fig. 4. The tempered maize was subsequently cooled at different cooling rates. It was found that the cooling rate insignificantly affected the drying rate, implying that internal diffusion controlled moisture movement. The moisture content can be reduced by 2 points from 22.5% dry-basis down to 20% or 21% dry-basis during cooling, higher than the desired value of 16% dry-basis for safe storage. In view of this, the moisture gradient inside the kernel shows an insignificant variation, whereas the temperature gradient due to cooling was more pronounced. Such large gradients of temperature may lead to stress cracks in the maize kernel. Fortunately, this plays a minor role in the cracking of maize as evidenced by Fig. 7 which shows that the percentage of cracked maize changes slightly with the degrees of cooling rate, 3.3–4.7% for 37% moisture content and 4.0–5.3% for 43% moisture content. This can be explained by the shrinkage of the maize kernel due to moisture removal during the cooling period being very small and thus the stress that appears in this period is low. This behaviour is somewhat similar to drying during the very early period, in which the amount of moisture removed from the material is very small, so that physical damage in terms of breaking and cracking is small (Soponronnarit et al., 2001; Soponronnarit and Prachayawarakorn, 1994).

The data represented in Fig. 8 were obtained under identical conditions to those in Fig. 7. The cooling rates do not cause discolouration of maize kernels: the values of a, b and L are unchanged.

5. Conclusions and recommendations

- Moisture movement inside the maize kernel during drying is controlled by internal diffusion. The effective diffusivity depends on the temperature and moisture content and can be described adequately by the modified Arrhenius equation.

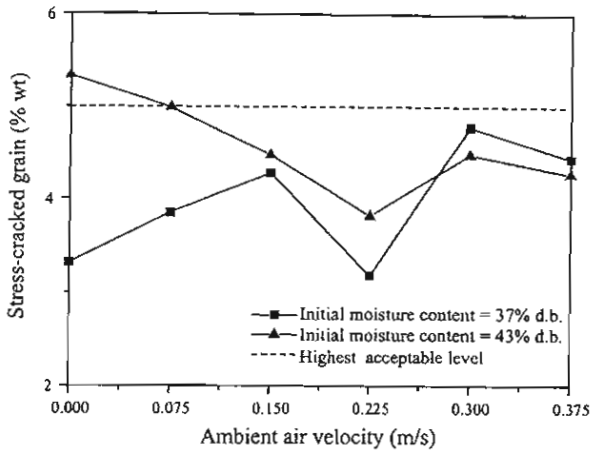

Fig. 7. Effect of cooling rates on stress-cracked grain (inlet-air temperature of 150°C for first-stage drying and tempering period of 40 min).

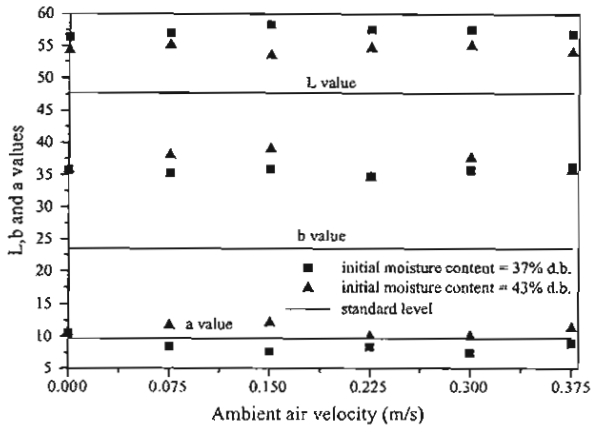

Fig. 8. Influence of cooling rates on maize surface colour (inlet-air temperature of 150°C for first-stage drying and tempering period of 40 min).

- A theoretical diffusion equation for a single sphere, that assumes the maize kernel is homogeneous at the macroscopic level, is used to simulate drying and tempering. The proposed equation is validated for moisture data over the range of the first and second drying stages in fluidised-bed drying
- The tempering period is the most important factor determining the extent of moisture removal during the second drying period. The amount of moisture removal is enhanced when the tempering stage is completed, allowing uniformity of concentration throughout the maize kernel. In reducing the moisture content from 37% or 43% dry-basis to 23% dry-basis using an inlet temperature of 150°C and drying periods of 4 or 6 min depending on its moisture content, a tempering period of 40 min is sufficiently long to provide the most efficient energy utilisation.

To be useful for the grain industry, more research work is needed to explore the appropriate tempering time for a wider range of inlet-air temperatures and initial moisture contents.

- Tempering reduces maize cracking but a longer tempering period causes the colour of maize to become more intense and darker.
- Ambient-air velocity in the range of 0.075–0.375 m/s flowing through the tempered maize insignificantly affects the above-mentioned maize qualities.

Acknowledgements

The authors thank The Thailand Research Fund for financial support of this work.

References

Anon., 1960. Official and Tentative Methods of Analysis of the Association of Official Agricultural Chemists, 9th Edition. Association of Official Agricultural Chemists, Washington, DC.

Davidson, V.J., Noble, S.D., Brown, R.B., 2000. Effects of drying air temperature and humidity on stress cracks and breakage of corn kernels. Journal of Agricultural Engineering Research 77, 303–308.

Estrada, J.A., Litchfield, J.B., 1993. High humidity drying of corn: effect on drying rate and product quality. Drying Technology 11, 65–84.

Mourad, M., Hemati, M., Laguérie, C., 1995. The drying of corn in a flotation fluidised-bed: an experimental study of the drying rate. Chemical Engineering Journal 59, 221–228.

Mulet, A., Berna, A., Rossello, C., 1989. Drying of carrots. I. Drying models. Drying Technology 7, 536–557.

Musielak, G., 2000. Influence of the drying medium parameters on drying induced stresses. Drying Technology 18, 561–581.

Otten, L., Brown, R.B., Reid, W.S., 1984. Drying of white beans—effect of temperature and relative humidity on seed coat damage. Canadian Journal of Agricultural Engineering 26, 101–104.

Pudpong, A., Soponronnarit, S., Tia, V., 1990. The study of parameters for corn drying. Thailand Engineering Journal 4, 95–101.

Sabbath, M.A., 1970. Convective heat transfer coefficient and tempering effects on cooling rate of shelled corn. Ph.D. Thesis, Purdue University, Lafayette, IN.

Satayaprasert, C., Vanishsriwatana, V., 1992. Drying corn in fluidised-bed. Thailand Engineering Journal 44, 76–79.

Siriacha, P., Tanboon-Ek, P., Buangsuwon, D., 1991. Aflatoxin in maize in Thailand. In: Champ, B.R., Highley, E., Hocking, A.D., Pitt, J.I. (Eds), Fungi and Mycotoxins in Stored Products: Proceeding of an International Conference, Bangkok, Thailand, 23–26 April, ACIAR Proceedings No. 36, pp. 187–193.

Soponronnarit, S., Prachayawarakorn, S., 1994. Optimum strategy for fluidised-bed paddy drying. Drying Technology 12, 1667–1686.

Soponronnarit, S., Kittiporn, K., Prachayawarakorn, S., 1997a. Appropriate operating parameters for fluidised-bed corn drying. Regional Energy Resources Information Center International Energy Journal 19, 1–13.

Soponronnarit, S., Pongtornkulpanich, A., Prachayawarakorn, S., 1997b. Maize quality after drying by fluidisation technique at high temperature. Drying Technology 15, 2577–2586.

Soponronnarit, S., Pongtornkulpanich, A., Prachayawarakorn, S., 1997c. Drying characteristics of maize in fluidised-bed dryer. Drying Technology 15, 1603–1615.

Soponronnarit, S., Wetchacama, S., Swasdisevi, T., Chotijukdikuld, P., 1999. Effects of drying, tempering and ambient air ventilation on quality and moisture reduction of corn. Drying Technology 17, 1227–1238.

Soponronnarit, S., Swasdisevi, T., Wetchacama, S., Wutiwiwatchai, W., 2001. Fluidised-bed drying of soybeans. Journal of Stored Products Research 37, 133–151.

Steffe, J.F., Singh, R.P., 1980. Theoretical and practical aspects of rough rice tempering. Transactions of the American Society of Agricultural Engineers 23, 775–781.

Thompson, R.A., Foster, G.H., 1963. Stress cracks and breakage in artificially dried maize. USDA Marketing Research Report 631, pp. 139–142.

Ulku, S., Uckan, G., 1986. Corn drying in fluidised-beds. In: Mujumdar, A.S. (Ed.), Drying'86. 2. Hemisphere. Springer, London, New York, pp. 531–536.

White, G.M., Ross, I.J., 1972. Discoloration and stress cracking in white corn as affected by drying temperature and cooling rate. Transactions of the American Society of Agricultural Engineers 15, 504–507.

DRYING TECHNOLOGY
Vol. 22, No. 4, pp. 719–743, 2004

Characteristics of Rice Dried in Superheated-Steam Fluidized-Bed

Chaiyong Taechapairoj,[1,*] Somkiat Prachayawarakorn,[2] and Somchart Soponronnarit[1]

[1]School of Energy and Materials and
[2]Faculty of Engineering, King Mongkut's University of Technology, Thonburi, Suksawat, Bangkok, Thailand

ABSTRACT

Characteristic properties of rice in a superheated-steam fluidized-bed dryer have been investigated using RVA, DSC, and SEM. The experimental results have shown that the reduction in moisture content from 41–42.5 to 25% d.b. using steam temperatures of 150–170°C was initially linear with drying time followed by the exponential decay when the moisture content was below 25% d.b. During the latter period, the water transport was controlled by the internal diffusion. Condensation of steam, along with the use of high temperature, enabled the development of gel layer as obvious from SEM. The formed gel layer caused the very low effective diffusivity

*Correspondence: Chaiyong Taechapairoj, School of Energy and Materials, King Mongkut's University of Technology, Thonburi, Suksawat 48 Road, Bangkok 10140, Thailand; E-mail: chaiyong_t@yahoo.com.

DOI: 10.1081/DRT-120034259

0737-3937 (Print); 1532-2300 (Online)
www.dekker.com

when compared with the case of no gel formation in paddy kernel. The pasting properties and DSC measurements have shown that paddy dried at a higher temperature and a thinner bed depth provided a greater extent of gelatinization during the drying time, the first factor showing a profound effect. Kinetics of gelatinization is reasonably described by the zero-order reaction. For the paddy quality, the head rice yield was 70% higher than the reference value and color of white rice became yellow and low luminous after reducing moisture content to 18% d.b. The percentage of white belly was less than 1.5%.

Key Words: Gelatinization; Superheated steam; White belly.

INTRODUCTION

Parboiled rice is made from fresh paddy, which is subjected to a hydrothermal treatment. In the traditional parboiling process, paddy is steeped in water until attaining the moisture content between 42 and 54% dry basis (d.b.). This stage is taken overnight or longer in water at ambient temperature. It is then followed by boiling or steaming the steeped rice at 100°C to gelatinize the starch, resulting in the grain swelling and the hull's lemma and palea separating. The parboiled rice is then cooled and dried before storing and milling. In the modern process, the stages are similar to the first one, except for the soaking stage in which paddy is immersed in hot water in order to reduce the sour odour and accelerate transport of water into kernel.[1] During steaming, the nutrients from the bran layer penetrate into the endosperm and consequently, some of the vitamins existing inside the rice kernels are sealed due to the formation of gel layer.[2] Parboiled rice is therefore a more nutritious form of rice than the white rice.

However, the above-mentioned parboiling processes are not very convenient in practice since they consist of many steps. An attempt to reduce them is a main objective in the present work and a possible way is that of using superheated-steam. With this medium, we expect that both steaming and drying stages can be integrated into a single stage if the gelatinizing condition and moisture removal stage are well organized. The superheated-steam drying has been widely recognized in many applications.[3–5] Recent studies have reported some advantages of superheated-steam drying[6,7]: high drying rate and deodorization of products.

The purpose of the present work is to produce the rice parboiling by using superheated-steam as a drying media in fluidized-bed dryer. The characteristics of dried paddy such as pasting properties, microstructure, and lipid content are investigated. In addition, the head rice yield and whiteness of paddy are also determined.

MATERIALS AND METHODS

Sample Preparation

Long grain paddy of Chainat1 (CNT1) variety from the Rice Experiment Station at Ayutthaya Province, Thailand, was used in the present investigation. In preparation, it was followed by a traditional method where paddy was cleaned and soaked at a temperature of 80°C for 3.5 h. Then, the water was drained out and the paddy was tempered at the same tank for 1 h prior to drying.

Drying

After soaking, paddy samples were dried with a batch superheated steam fluidized dryer as shown in Fig. 1. The system of the fluidized-bed dryer consists of five main components: a cylindrical chamber with a 15 cm inner diameter and a 100 cm height, a 13.5 kW electrical heater for converting saturated steam to the superheated steam, a backward-curved blade centrifugal fan driven by a 2.2 kW motor, a reverse flow cyclone, and a small boiler with a 31 kg/h capacity of generated steam. A PID controller with an accuracy of ± 1°C was used to control steam temperature. Before using steam for drying, hot air was used for warming up the system until the temperature in every part reached the desired temperature. Then, the steam was replaced accordingly. The steam generator was generated the saturated steam at 106 kPa (absolute pressure) with the corresponding temperature of 100°C. When the saturated steam was flowed through the electrical heaters, the additional heat was supplied to raise the steam temperature up to the required level. It was subsequently flowed through the fluidized bed dryer. The dust particles and the immature grains being suspended in the exhaust steam were collected at the cyclone. Finally, the cleaning exhaust steam was reused again.

The experimental conditions were set up as follows: initial moisture contents of 41–42.5% d.b., bed depths of 10–15 cm, superheated steam

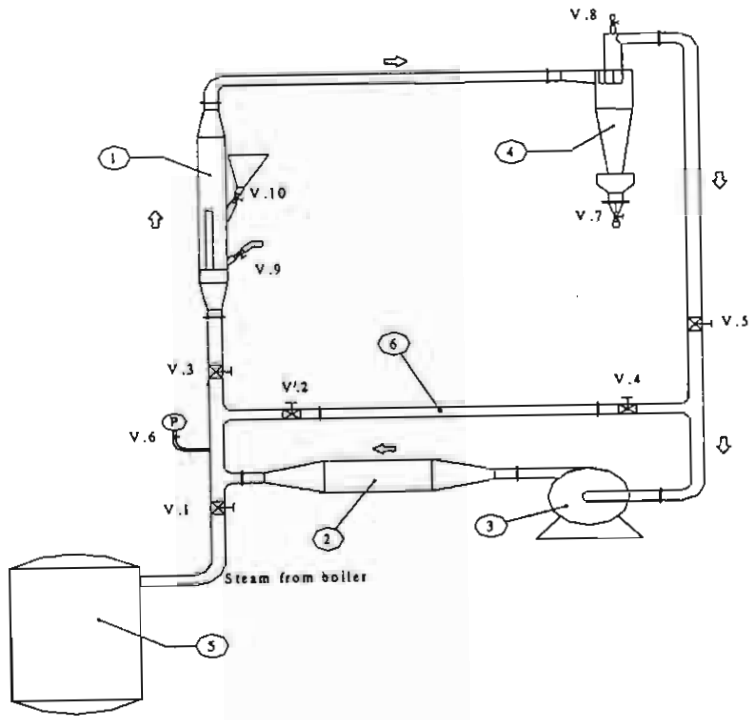

Figure 1. A schematic diagram of the superheated-steam system: (1) fluidized bed dryer; (2) heater; (3) fan; (4) cyclone; (5) boiler; (6) bypass line; P = pressure guage, and V = valve.

temperatures of 150–170°C, a fixed superficial velocity of 3.1 m/s. Temperatures at different positions of drying chamber were measured by Chromel-Alumel thermocouples (Type K) connected to a data logger with an accuracy of ± 1°C. The paddy, with a mass 1 kg, was dried until reaching the predetermined time and then withdrawn from dryer at the valve V.9 to determine the moisture content and grain temperature. In grain temperature measurement, the paddy kernels were fully packed in a well-insulated container. After that, the sample was kept in polypropylene bag and left in the environment condition until the grain temperature approached ambient temperature. Then, it was spread on a sieve and ventilated by an ambient airflow rate until its moisture content reached 16% dry basis. Finally, a 300 g sample was kept in a seal plastic bag for 2 weeks before testing head rice yield, whiteness and white belly.

The moisture content of paddy was determined by an electrical air oven at a temperature of 103°C for 72 h. Paddy quality in terms of head rice yield and whiteness was determined quantitatively and compared to the reference sample (paddy dried by the ambient air). The methods were followed with the guideline of the Ministry of Agriculture and Cooperatives, Thailand. Head rice is defined as milled rice having kernel length at least three-fourths of its original length. The head rice yield was calculated from the mass of white rice that remains as head rice after milling divided by the mass of paddy sample.

The color of rice samples was measured by a Kett digital whiteness meter (Model C-300). Before measuring the color of sample, the whiteness meter was calibrated with a white colored reference, presenting a standard value of 86.3.

Scanning Electron Microscopy

Structural changes of kernels were investigated by scanning electron microscopy (SEM) (S-4500, Hitachi, Tokyo, Japan). The rice kernel was broken along the cross-sectional axis. Samples were placed on adhesive tape attached to a circular aluminum specimen stub, coated with gold layer using a sputter-coater (Hitachi E-1010 10N, Tokyo, Japan), and photographed at an accelerator potential of 15 kV.

RVA Measurement

All rice flour samples were prepared by grinding rice with a laboratory model hammer mill (Retsch Mühle, type SK1, Germany) with a mesh opening of 800 μm. Pasting properties of rice flour were determined by a Rapid Visco Analyser model-4 (Newport Scientific Pty Ltd., Warriewood, Australia) utilizing Thermocline. Following AACC Method 61-02,[8] the sample (3 g, 14% moisture basis) was mixed with distilled water in a RVA aluminum canister to make the total weight of slurry 28 g. The mixture was stirred at 900 rpm for 10 s and then changed to 160 rpm. The mixture was held at 50°C for 1 min and then heated to 95°C at 12°C/min. After that, holding at 95°C was 2.5 min, followed by cooling down to 50°C at 12°C/min and kept for 2.1 min. These tests were done in duplication. A plot of paste viscosity in arbitrary RVA unit (RVU) vs. time was used to determine the peak viscosity (PV), temperature at peak viscosity (P_{temp}), trough final viscosity (FV), breakdown viscosity (BKV = PV − trough), and setback viscosity

(SBV = FV – trough). The first point at which the viscosity increases to 1 RVU/s or faster is defined as the onset gelatinization temperature of rice flour (P_{Temp}). Peak viscosity (PV) indicates the water-biding capacity of mixture. It is often correlated with the final product quality, and also provides an indication of the viscous load likely to be encountered by a cook. Breakdown viscosity measures the degree of disintegration of the granules or paste stability. Setback viscosity is a measure of gelling or retrogradation tendency.[9]

Lipid Content

Lipid content was determined using the method of Folch et al.,[10] with some modifications for the rice flour extraction. Parboiled rice flour was extracted with chloroform–methanol (2:1 by volume). The suspension was shaken for 5 min and settled for 30 min before decanted through folded filter paper. Filtrate was added with one-fourth of water and shaken to create two immiscible liquid phases. The lower and upper phases were composed of chloroform–methanol–water in the corresponding proportions of 86:14:1 and 3:48:47 (by volume), respectively. The final lipid extract was evaporated at 35°C under stream of oxygen-free nitrogen.

Differential Scanning Calorimetry Analysis

Gelatinization properties of parboiled rice flours were analyzed by using a differential scanning calorimeter (DSC Pyris-I, Perkin-Elmer, Norwalk, CT, USA). The calibration was periodically performed using indium (heat of fusion of 28.41 J/g and 156.66°C of melting temperature). Flour samples (~3 mg each) were weighed in sample pans, mixed with distilled water (~9 μL). The sample pan was sealed and allowed to stand for 1 h at room temperature.[11] The sample was held isothermally at 30°C for 1 min, and then scanned at a heating rate of 5°C/min until the temperature raise to 100°C. The calorimetric measures were made by duplications. The enthalpy change (ΔH) was evaluated using the Thermal Analyzer (TA) Instruments analysis software program. The degree of gelatinization (DG) of rice flour was calculated by the following equation[12]:

$$DG(\%) = [1 - (\Delta H_{pg}/\Delta H_{raw})] \times 100 \quad (1)$$

where ΔH_{pg} and raw ΔH_{raw} are the enthalpies of gelatinized and raw rice grains, respectively.

Drying Kinetics

In the present study, paddy kernels fully adsorbed water which is formed a thin liquid film around the external surface, namely unbound moisture. When exposed to superheated steam, this unbound water can be removed easily and water evaporation rate can thus be simply expressed by

$$\frac{d(M(t) - M_{eq}/M_{in} - M_{eq})}{dt} = k \quad (2)$$

where $M(t)$ is the moisture content at time t (d.b.), M_{eq} is the equilibrium moisture content, M_{in} is the initial moisture content, k is the drying constant (s^{-1}) and t is the drying time (s^{-1}). The drying constant depends upon the operating parameters.

When the moisture content has reached a value of M_c, the critical moisture content, the film thickness of moisture at the surface has been reduced by evaporation, so that further drying causes the formation of dry surface. This gives rise to the part of falling rate period in which the evaporation rate can be calculated by

$$\frac{M(t) - M_{eq}}{M_c - M_{eq}} = \frac{8}{\pi^2}\sum_{i=1}^{\infty}\frac{1}{(2i-1)}\exp\left[-(2i-1)^2\frac{\pi^2}{4b}\left(\frac{D_{eff}(t-t_c)}{b}\right)\right] + 4\sum_{i=1}^{\infty}\frac{1}{\alpha_i^2 R^2}\exp\left(-D_{eff}\alpha_i^2(t-t_c)\right) \quad (3)$$

where R is the radius of cylinder, b is the half thickness, t_c is the drying time at the critical point, and α_i are the positive roots of the equation $J_0(R\alpha_i) = 0$. Equation (3) was used by Poomsa-ad et al.[13] in order to describe the moisture transport inside paddy kernel, assuming cylindrical shape, which governs the drying behavior.

Gelatinization Kinetics

Food systems usually follow either a zero or first order kinetics.[14] A plot of C vs. t gives a straight line for zero-order reaction (Eq. (4)),

whereas for first-order reaction (Eq. (5)), a plot of log C vs. t yields a straight line. The slope of the line is equal to the rate constant.

$$-C = kt + C_0 \tag{4}$$

$$-\log C = kt + \log C_0 \tag{5}$$

where C and C_0 are the percentage of ungelatinized rice flour at time t and 0, respectively, k is the rate constant (s^{-1}) and t is the drying time (s).

The temperature dependence of the rate constant can be explained by an Arrhenius type relationship:

$$k = k_a \exp(-E_a/RT_{abs}) \tag{6}$$

where R is the universal gas constant and T_{abs} is the absolute temperature. The activation energy (E_a) can be obtained from the slope of the plot of ln k vs. the reciprocal of process temperature (T_{abs}). The regression results were shown that the determined activation energy was slightly changed with bed depth, showing 13% difference between the lowest and highest bed depths, whilst the value of k_a was very sensitive to the bed depth, the largest difference being 60% in present work, the activation energy is, therefore, assumed to be constant and the pre-exponential factor (k_a) is correlated with the following form:

$$k_a = F + GH_b + IHb^2 \tag{7}$$

where F, G, and I are the constant parameters and H_b is the bed depth (cm).

RESULTS AND DISCUSSION

Drying Curve

Figure 2 shows the relationship between the grain temperature, moisture content, and drying time. At the initial stage of drying, there is a region where the uptake of moisture into grains can be observed, typically of the order of 1–2% moisture content dry basis, since the flowing steam contacting with a low initial temperature of paddy is condensed. The amount of water uptake is slightly dependent on the steam temperature, as observed from the experiments.

Because of rapid release of heat vaporisation by condensation, the grain temperature rapidly increases. As shown in Fig. 2a, the grain temperature is slightly above 80°C in the first minute of drying time and

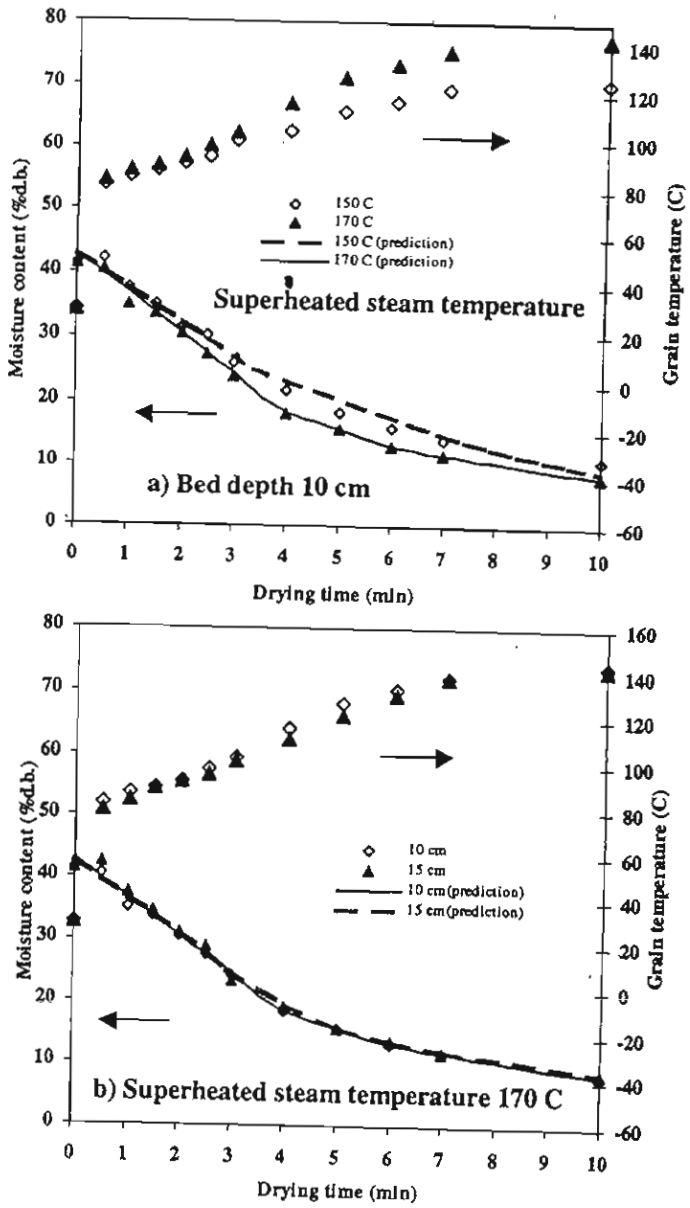

Figure 2. Variation in moisture content and grain temperature with time at different bed depths and inlet superheated-steam temperatures.

then relatively rises to 100°C in 3 or 4 min. During this period, more than a half of rice starch is gelatinized as can be seen in Fig. 6 and all of the heat is used to vaporise the water that exists inside the paddy and the condensing water that was not adsorbed by grains. Afterwards, the grain temperature rapidly increases and higher grain temperatures follow with higher steam temperatures, resulting in the relative difference of moisture content.

Due to very high initial moisture content, together with steam condensation, the moisture reduction of paddy at the early drying period is linear with time and it is described by the following equation:

$$MR = (0.08991V - 1.1886 \times 10^{-5}T - 2.268 \times 10^{-4}VT + 0.00314)\,t + 1.03674 \qquad (R^2 = 0.975) \tag{8}$$

where MR is the moisture ratio $(M(t) - M_{eq}/M_{in} - M_{eq})$, V is the specific mass velocity (kg steam s^{-1}/kg dry matter), T is the superheated steam temperature (K), and t is the time (s). The drying rate in this period is affected by the temperature and specific mass velocity: higher drying rates will follow with higher temperature and specific mass velocity, the first one being more important. Such linear decrease proceeds to the critical moisture content, after which it falls into the exponential decline. The critical moisture content of paddy was approximately 25% d.b. and independent of drying conditions. Equation (8) is valid at the temperature of 423–443K and the specific mass velocity of 0.024–0.038 kg $kg^{-1}_{dry\ matter}$ s^{-1}.

In the period of the exponential decline, the effective diffusivity of paddy was determined by using Eq. (3). Figure 3 shows the experimentally determined effective diffusivity at various bed depths and steam temperatures. The value of effective diffusivity is in the range of 3.0×10^{-10}–4.2×10^{-10} m^2/s for the temperatures of 150–170°C. As expected, the effective diffusivity increases with the increase of drying temperature. The bed depth does not remarkably affect the effective diffusivity obtained for each temperature, implying that the values obtained are the intrinsic ones. The experimental relationship between drying temperature and D_{eff} has been established using the Arrhenius-type equation,

$$D_{eff} = 3.02087 \times 10^{-7}\exp\left(\frac{-24318.4}{RT}\right), \qquad R^2 = 0.925 \tag{9}$$

Equation (9), with a R^2-value of 0.925 and an absolute mean error of 1.0025×10^{-11}, is reasonably fitted with the experimental data, as indicated by the solid line in Fig. 3.

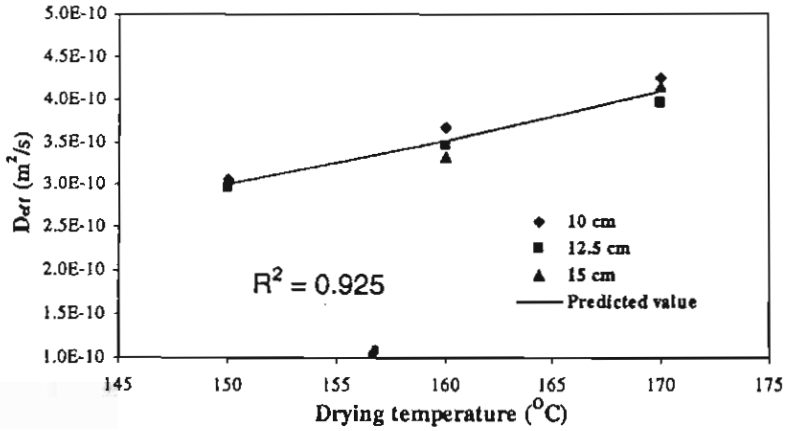

Figure 3. Experimental and predicted values of effective diffusivity (superheated steam).

Comparing to Poomsa-ad's work,[13] the effective diffusion of paddy is atleast 15 times lower when dried in the superheated steam than when dried in the hot air under the same dryer type. The effective diffusion of paddy dried in hot air fluidized-bed dryer[13] is given by

$$D_{eff} = 5.41141 \times 10^{-6}\exp\left(\frac{-28436.4}{RT}\right) \tag{10}$$

The prediction of moisture reduction of paddy using D_{eff} in Eqs. (9) and (10) is shown in Fig. 4 that the drying rate in the falling rate period for the use of superheated steam as drying medium is significantly lower over the drying time. The lower drying rate is due to the formation of gel layer starting from the exterior surface and moving towards the interior, thereby allowing the internal spaces to be reduced. This gel layer retards the diffusing water. The evidence of the gel formation will be discussed later with the results of differential scanning calorimeter and RVA measurements and morphology of rice kernel using scanning electron microscopy.

Pasting Behavior

Pasting curve of viscosity determined by RVA represents the viscosity of starch during heating cycle, which shows the molecular

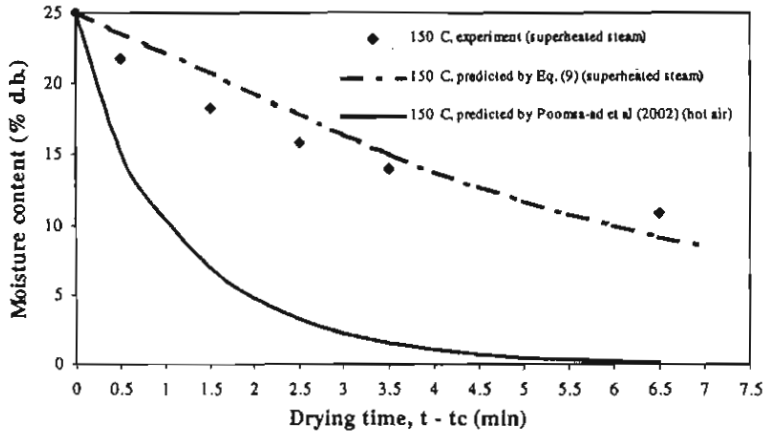

Figure 4. Comparison of predicted and experimental drying curve for paddy drying at 150°C.

events occurring in the starch granules. The integrity of starch granules and hydration properties resulting from the native properties of starch, or from the molecular interactions during drying can therefore be easily investigated by measuring the pasting properties of rice flour before and after treatments. The typical RVA viscographs and viscosity properties of pastes prepared from the raw rice and dried rice are shown in Figs. 5a and b. The pasting properties are significantly affected by the temperature, except for bed depth, and the characteristic properties are totally different from those of the raw rice. The rate of increasing viscosity of dried rice flour during heating period, as indicated by the slope, is very low when dried at 150, 160, and 170°C. The resulting gelatinization temperature becomes higher, approximately 90°C for the dried rice and 80°C for the raw rice, and the peak viscosity is lower. The higher gelatinization temperature is due to retrogradation of dried rice causing reassociation of starch molecules. Consequently, the reassociated starch structure is resistance to water penetration and thus required more energy for water absorption during the heating period in RVA testing.

Table 1 presents a summary of the effect of temperature on the pasting properties of treated rice flour. The PV, BKV, FV, and SBV of treated rice flour are remarkably smaller than those of the raw rice flour. The differences between the raw rice flour and dried rice flour increase with increase in temperature because the degrees of reassociation of starch molecules depend on the degree of heat treatment. This is indicated

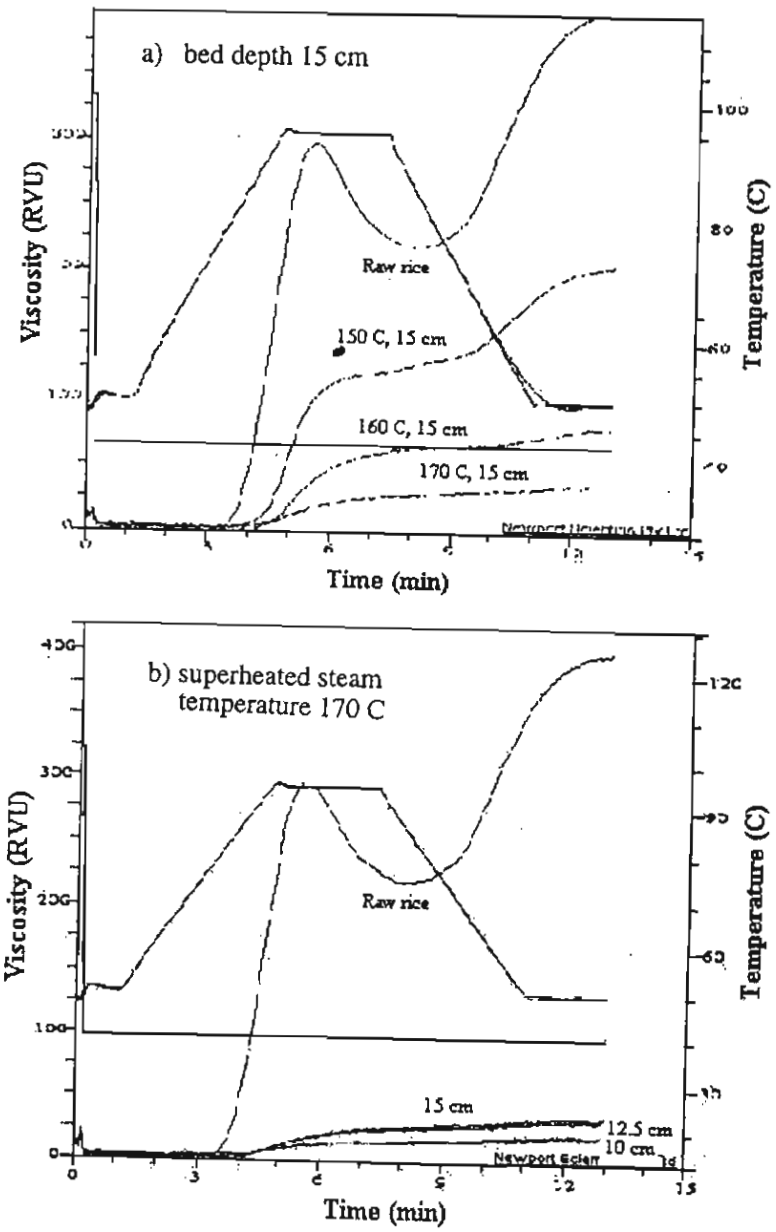

Figure 5. Viscograph of raw rice flour and rice flour dried by superheated steam.

Table 1. Pasting properties of raw and dried flour.

	PV (rvu)	Trough (rvu)	BKV (rvu)	FV (rvu)	SBV (rvu)	P_{Temp} (°C)
Raw rice	296	218	78	399	181	79.9
150°C 15 cm	120	113	7	205	92	89.7
160°C 15 cm	57	47	10	81	34	88
170°C 15 cm	25	20	5	35	15	89.7
170°C 12.5 cm	23	19	4	32	13	89.7
170°C 10 cm	14	12	2	21	9	89.7

by the decrease of PV and FV with increase in temperature. The treated samples possess low firmness texture, as indicated by the low FV and SBV.

Kinetics of Gelatinization

Figure 6 illustrated the DSC thermal curve for rice drying at temperature of 160°C and bed depth of 15 cm, showing the increase in degree of gelatinization of rice four with drying time. At the drying time of 5 min, heat flow line is almost parallel with x-axis, implying the nearly completed gelatinization of starch. Degree of ungelatinization of rice flour during superheated steam drying as a function of drying time at different temperatures and bed depths is shown in Fig. 7. A certain degree of starch gelatinization, approximately 20%, occurred before starting the experiment because of the soaking effect. The degree of ungelatinization is linearly decreased with drying time and is almost zero after the drying time passed by 5–6 min at steam temperatures of 150–160°C and 4 min at 170°C.

The experimental data were used to fit with Eqs. (4) and (5). The prediction results for the zero and first order reactions show in Figs. 7 and 8, respectively. The kinetics of gelatinization of paddy during drying in the superheated-steam fluidized-bed dryer is reasonably described by the zero-order kinetic reaction, as indicated by R^2 and absolute mean error values which are respectively 0.97 and 3.66 for the zero order whilst 0.80 and 45.3 for the first order. These findings oppose to the previous works reported in the literature as a first-order reaction.[15–19] The reason has not yet cleared. However, it might be possible that the gelatinization

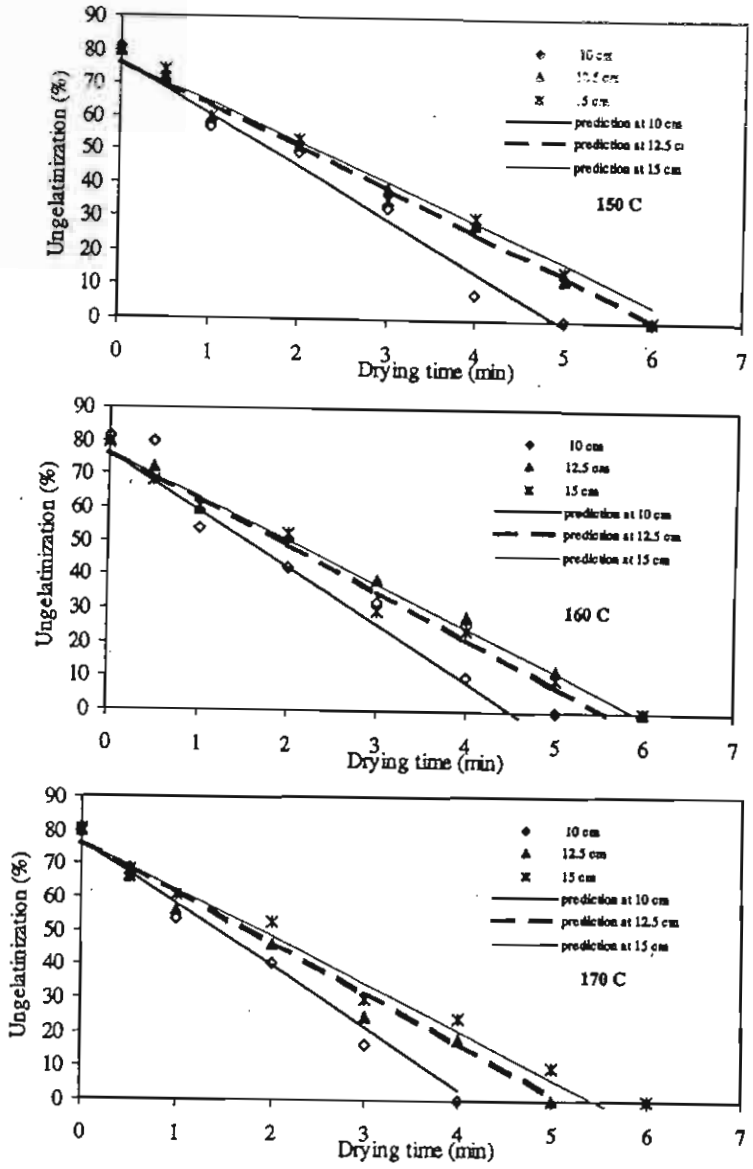

Figure 6. Zero-order reaction kinetics of gelatinization of rice at different temperatures and bed depths.

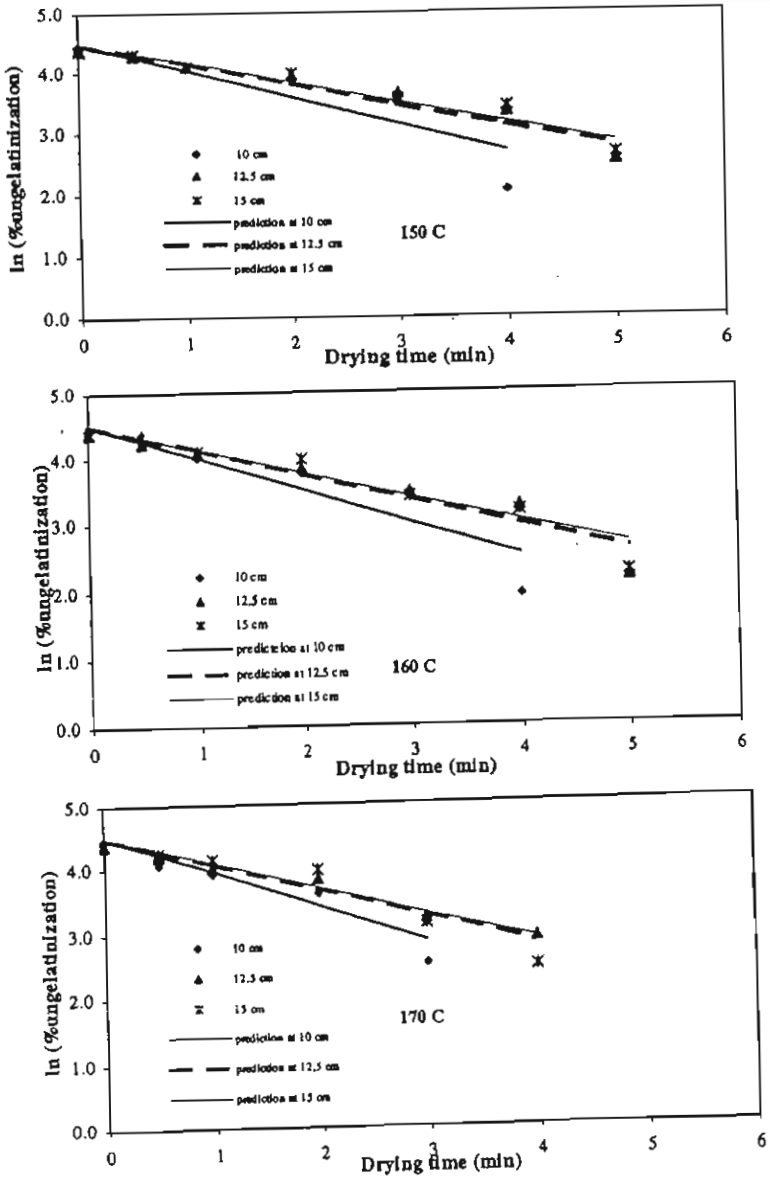

Figure 7. First-order reaction kinetics of gelatinization of rice at different temperatures and bed depths.

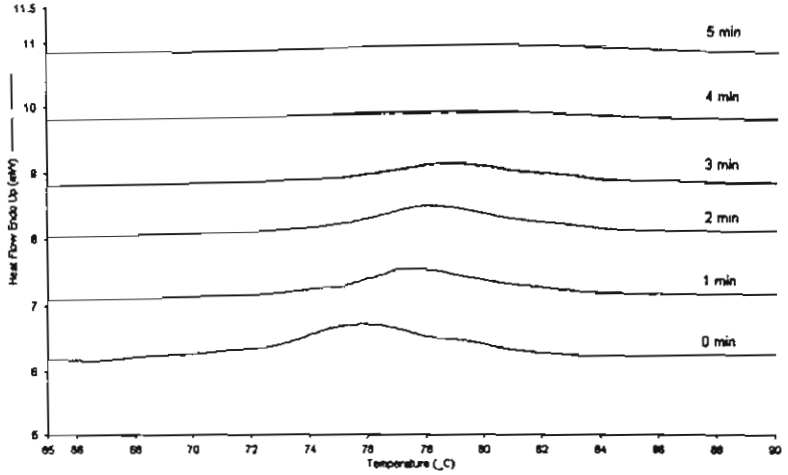

Figure 8. DSC thermal curves for rice drying at temperature of 160°C and bed depth of 15 cm. The water content of all samples was 70% (w/w).

Table 2. Zero-order reaction rate constant for the gelatinization of treated rice.

Drying temperature (°C)	Zero-order reaction rate constant, k (s^{-1})		
	10 cm	12.5 cm	15 cm
150	0.25	0.20	0.20
160	0.28	0.22	0.22
170	0.31	0.24	0.24

kinetics of starch granules they investigated was carried out in a limited range of slightly above normal boiling point temperature and the resulting time required for the complete gelatinization took longer than 20 min, but this work performed in a very shorter time, at least five times.

The apparent rate constants for the zero-order reaction (k) at various drying conditions are presented in Table 2. The apparent rate varies with the temperature and bed depth, the first factor showing a positive effect, in which the rate increases with temperature, whilst the latter shows a negative effect. The relationships between the apparent rate constant and

Table 3. Nonlinear regression analysis of zero-order and first-order

Model	I	G	J	E_a/R	R^2
Zero	−30.34026	3.1920113	−0.109836	−1518.626	0.97
First	−2.630565	0.3054912	−0.010674	−1654.481	0.80

the involving parameters are described by Eqs. (7) and (8), of which the constant parameters determined by the nonlinear regression are given in Table 3. The activation energy for paddy is in order of 12.63 kJ/mol in the temperature range of 150–170°C.

Scanning Electron Microscopy

The microstructure of the starch granules is shown in Fig. 9. Before drying as shown in Fig. 9a, the starch granules spreads throughout the cross-sectional surface. When dried at any drying temperature (150–170°C), the starch granules swelled, absorbed surrounding moisture, and gelatinized, leading to lose its granular appearance. The rice kernels were consequently observed as smoother appearance on the entire cross-sectional microstructure as represented in Figs. 9b–d.

Head Rice Yield

The relationship between head rice yield and final moisture content in the superheated-steam fluidized-bed dryer at different drying conditions is shown in Fig. 10. The head rice yield slightly changes when the paddy is dried from 41–42.5% to 18% d.b. The head rice obtained is in the narrow range of 65–70, which is 70% higher than that of the control samples. The higher head rice yield is because the swelling effect causes the starch granules approaching together and thus resistant to deformation by strengthening the intra-molecular binding forces. This explanation can be indicated by the low SBV, FV, and trough of dried rice flour in RVA measurement. However, when the moisture content reduces below 18% d.b., the head rice yield rapidly decreases. This may be caused by the prevalent contribution of stress forces taking place by moisture gradient, leading to fissure development inside the grain kernels.

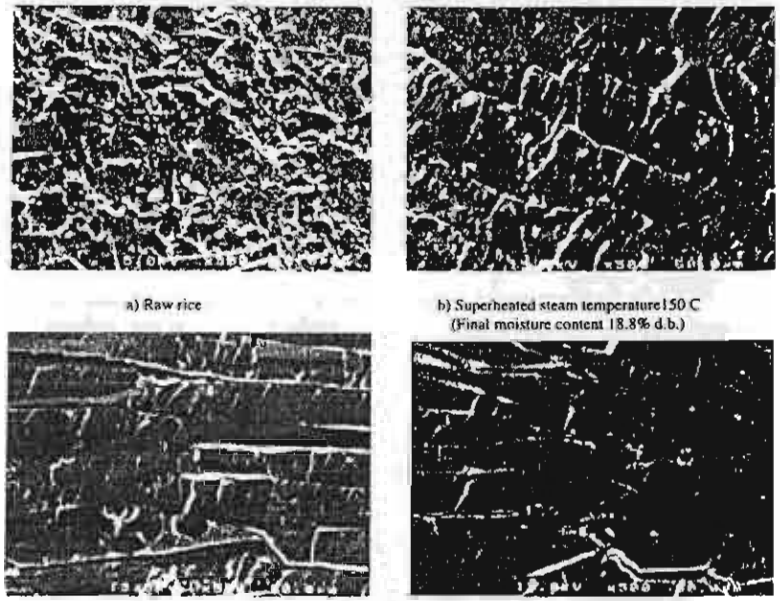

Figure 9. Effect of steam temperature on microstructure.

White Belly

Kernel that has an opaque white area higher than 50% of its total area is taken into account as white belly category, according to Thai Standard Rice.[20] The percentage of white belly shown in Fig. 10 was calculated by the number of white belly kernels divided by the total number of head rice kernels. The percentage of white belly kernels reduces with decrease in final moisture content or, in other words, with increase in drying time. When drying temperature is changed, the percentage of white belly is changed in a way that higher temperature provides the smaller number of white belly kernels as shown in Fig. 11a. The bed depth has a rather small effect, with the value lying between 1 and 2% for the bed depths of 10–15 cm as illustrated in Fig. 10b for 170°C. According to the white belly results, it may be indirectly used to indicate how well the grain kernels can be gelatinized, besides the accurate method.

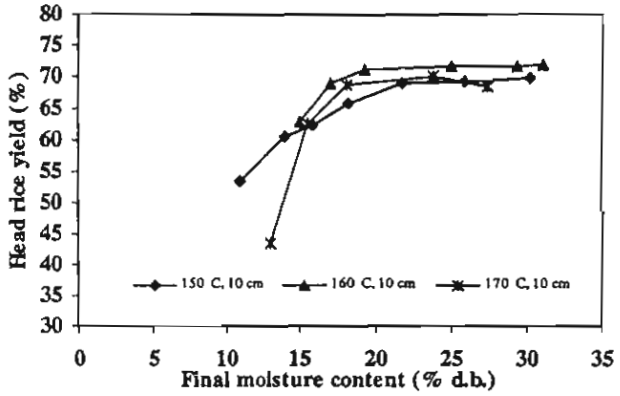

a) Bed depth 10 cm

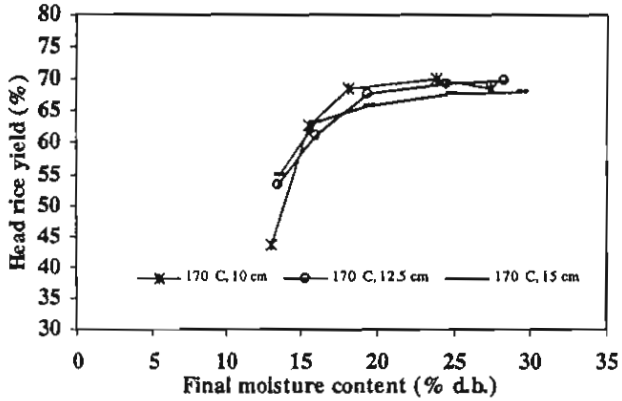

b) Superheated steam temperature 170 C

Figure 10. Relationship between head rice yield and final moisture content during drying in superheated steam (initial moisture content = 41.5–42.5% d.b.).

Rice Whiteness

The change of the color of samples at steam temperatures of 150, 160, and 170°C and initial moisture content of 42% d.b. is shown in Figs. 12a and b. The rice whiteness at the first 2 min of drying steeply drops from the original values, 41–43, to approximately 30. Such a rapid change

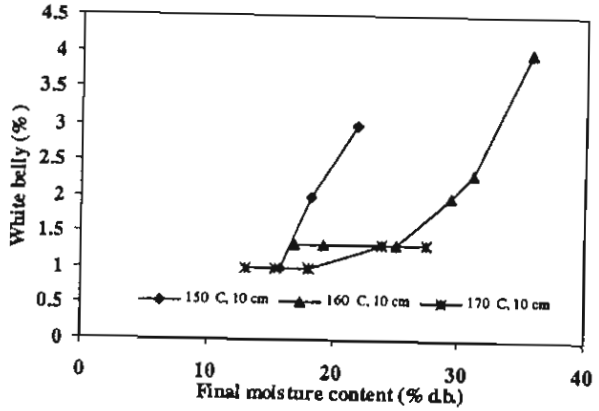

a) Bed depth 10 cm

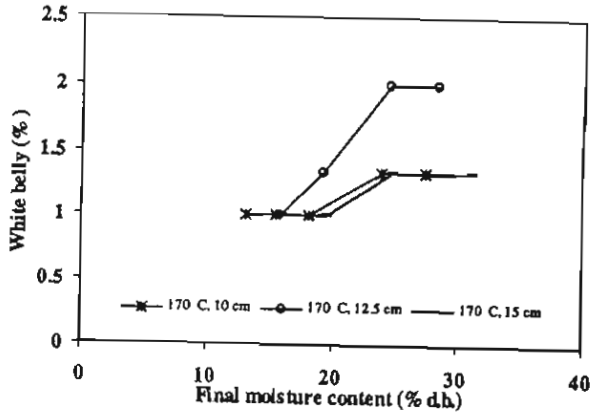

b) Superheated steam temperature 170 C

Figure 11. Relationship between percentage of white belly and final moisture content during drying in superheated steam (initial moisture content = 41.5–42.5% d.b.).

in the color is due to the steam condensation onto the paddy surface. The resulting bran and color pigments covered around kernel are dissolved and then adsorbed by the endosperm: the amounts of bran after milling for the dried samples are in order of 5.3–7.1%, which is approximately two times lower than the original value of the reference samples. In

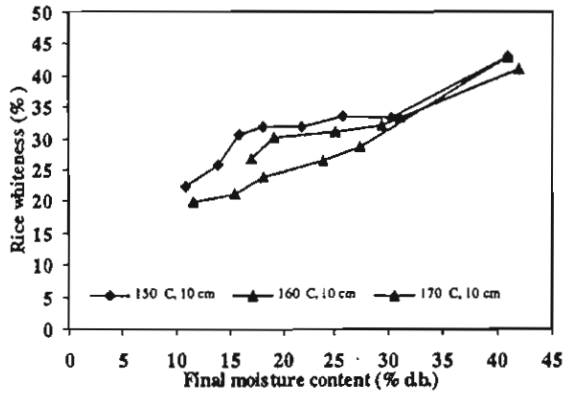

a) Bed depth 10 cm

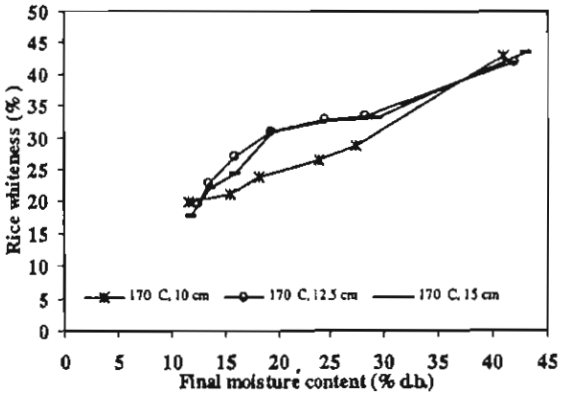

b) Superheated steam temperature 170 C

Figure 12. Relationship between rice whiteness and final moisture content during drying in superheated steam (initial moisture content = 41.5–42.5% d.b.).

addition to the result of bran, we also tested the lipid content as presented in Table 4, showing higher lipid contents in the dried rice than in the raw rice. This was due to the absorption of lipid from bran layer to endosperm of grain during drying as mention earlier. Thus, greater amount of lipid was removed with bran of raw rice compared to that of dried sample.

Table 4. Lipid content for dried rice at various temperatures and bed depths.

		Lipid content (%$g/g_{dry\ matter\ flour}$)
Raw white rice		0.2 ± 0.02
Rice		
150°C	10 cm	0.4 ± 0.03
	12.5 cm	0.23 ± 0.04
	15 cm	0.23 ± 0.04
160°C	10 cm	0.43 ± 0.03
	12.5 cm	0.3 ± 0.04
	15 cm	0.21 ± 0.03
170°C	10 cm	0.65 ± 0.02
	12.5 cm	0.35 ± 0.02
	15 cm	0.21 ± 0.03

In addition to the dissolved pigments, the color development might be caused by nonenzymatic Browning reaction. This reaction seems to be enhanced by high grain temperature as shown in Fig. 11a, where the higher temperature causes the lower whiteness. For the bed depth effect, the slightly low value of whiteness is obtained with the use of thin bed depth.

CONCLUSIONS

The characteristics of pasting properties of rice dried by superheated-steam fluidized-bed drying under temperatures, 150–170°C, and bed depths, 10, 12.5, and 15 cm, were determined. Drying rate was initially constant and exponentially decreased after the moisture content was lower than 25% d.b. During superheated steam drying, the gel formation occurred throughout the kernel resulting in the starch molecules closely packed together, as revealed by SEM micrograph. This provided the limitation of the water transport inside the paddy, resulting in low value of effective diffusivity when compared to the case of no gel development. DSC measurement indicated that the kinetics of gelatinization is described by the zero-order reaction. The values of peak viscosity, breakdown viscosity of dried rice were lower than those of the raw rice. Rice whiteness was apparently darkened at high temperature. In addition to such qualities, the percentage of white belly kernels decreased with the increase in inlet drying temperature. To maintain high head rice yield,

it is recommended that the final moisture content of paddy should not be dried lower than 18% dry basis.

ACKNOWLEDGMENTS

The authors would like to express their sincere thanks to the Thailand Research Fund for financial support, Faculty of Engineering and Industrial Technology Silpakorn University for supporting RVA instrument, Division of Agricultural Engineering, Department of Agriculture for testing quality of milling, and Pathum Thani Rice Research Center for testing the physical quality of rice. Phillip Semiconductor (Thailand) for supporting SEM instrument.

REFERENCES

1. Gariboldi, F. Rice parboiling. *FAO Agricultural Development Paper No. 97*; Food and Agriculture Organization of the United Nations: Rome, Italy, 1974.
2. Dimopoulos, J.S.; Muller, H.G. Effect of processing conditions on protein extraction and composition and on some other physicochemical characteristics of parboiled rice. Cereal Chemistry **1972**, *49*, 54–62.
3. Blasco, R.; Alvarez, P.I. Flash drying of fish meals with superheated steam: isothermal process. Drying Technology **1995**, *17* (4–5), 775–790.
4. Iyota, H.; Nishimura, N.; Nomura, T.; Konishi, Y.; Yoshida, K. *Effect of Initial Steam Condensation on Color Changes of Potatoes During Drying in Superheated Steam*, Proceedings of the 13th International Drying Symposium; Beijing, China, Aug 27–30, 2002; Vol. B, 1352–1359.
5. Looi, A.Y.; Golonka and Rhodes, M. Drying kinetics of single porous particles in superheated steam under pressure. Chem. Eng. J. **2002**, *87* (3), 329–338.
6. Iyota, H.; Nishimura, N.; Onuma, T.; Nomura, T. Drying of sliced raw potatoes in superheated steam and hot air. Drying Technology **2001**, *19* (7), 1411–1424.
7. Tatermoto, Y.; Mawatari, Y.; Sakurai, K.; Noda, K.; Komatsu, N. *Drying Characteristics of Pours Material in Superheated Steam Fluidized Bed*, Proceedings of the 13th International Drying Symposium; Beijing, China, Aug 27–30, 2002; Vol. A, 624–633.

8. AACC. *Approved Method of the American Association of Cereal Chemists*, 8th Ed.; American Association of Cereal Chemists: St. Paul, MN, 1995.
9. Dengate, H.N. Swelling pasting, and gelling of wheat starch. In *Advances in Cereal Science and Technology*; Pomeranz, Y., Ed.; American Associated Cereal Chemistry, St. Paul: MN, USA, 1984; Vol. 6, 49–82.
10. Folch, J.; Lees, M.; Sloane-Stanley, G.H. A simple method for isolation and purification of total lipids from animal tissues. J. Bio. Chem. **1957**, *226*, 497–509.
11. Normand, F.L.; Mashall, W.E. Differential scanning calorimetry of whole grain milled rice and milled rice and milled rice flour. Cereal Chemistry **1989**, *66* (4), 317–320.
12. Marshall, W.E.; Wadsworth, J.I.; Verma, L.R.; Velupillai, L. Determining the degree of gelatinization in parboiled rice: comparison of a subjective and an objective method. Cereal Chemistry **1993**, *70*, 226–230.
13. Poomsa-ad, N.; Soponronnarit, S.; Prachayawarakorn, S.; Terdyothin. Effect of tempering on subsequent drying of paddy using fluidization. Drying Technology **2002**, *20* (1), 195–210.
14. Arabshahi, A.; Lund, D.B. Consideration in calculating kinetic parameters from experimental data. J. Food Proc. Engng. **1985**, *7*, 239–251.
15. Okechukwu, P.E.; Rao, M.A. Influence of granule size on viscosity of cornstarch suspension. J. Texture Studies **1995**, *26*, 501–516.
16. Bakshi, A.S.; Singh, R.P. Kinetics of water diffusion and starch gelatinization during rice parboiling. J. Food Science **1980**, *45*, 1387–1392.
17. Suzuki, K.; Kubota, K.; Omichi, M.; Hosaka, H. Kinetic studies on cooking of rice. J. Food Science **1976**, *41*, 1180–1183.
18. Lund, D.B.; Wirakartakusumah, M. A model for starch gelatinization phenomena. In *Engineering and Food*; McKenna, B.M., Ed.; Engineering Science in the Food Industry: London, UK, 1984; Vol. 1, 425–435.
19. Turhan, M; Gunasekaran, S. Kinetic of in situ and in vitro gelatinization of hard and soft wheat starches during cooking in water. J. Food Eng. **2002**, *52*, 1–7.
20. *Ministry of Commerce*; Thai Standard Rice: Thailand, 1997 http://203.151.17.19/document/grain/english/standard.htm, last revised on 20 June 2002.

DRYING TECHNOLOGY
Vol. 22, No. 4, pp. 759–778, 2004

Drying Kinetics and Quality of Shrimp Undergoing Different Two-Stage Drying Processes

Yuvanaree Namsanguan,[1,*] Warunee Tia,[1] Sakamon Devahastin,[2] and Somchart Soponronnarit[1]

[1]School of Energy and Materials and
[2]Department of Food Engineering, King Mongkut's University of Technology Thonburi, Bangkok, Thailand

ABSTRACT

An innovative two-stage drying concept is presented in this article. The work considered drying of shrimp using a superheated steam dryer followed by a heat pump (SSD/HPD) or a hot air dryer (SSD/AD) both from drying kinetics and dried product quality points of view. The experiments were performed using the first-stage superheated steam drying temperature of 140°C while the second-stage heat pump drying (or hot air drying) was performed at 50°C. The moisture content of shrimp at the end of the superheated steam

*Correspondence: Yuvanaree Namsanguan, School of Engineering and Materials, King Mongkut's University of Technology Thonburi, 91 Pracha U-tid Road, Bangkok 10140, Thailand; Fax: 662-470-8663; E-mail: yuvanaree@yahoo.com.

DOI: 10.1081/DRT-120034261
0737-3937 (Print); 1532-2300 (Online)

drying stage was varied between 30 and 40% (w.b.). The effect of tempering between SSD/HPD was also investigated. Shrinkage, color, rehydration behavior, texture (toughness and hardness), and microstructure of dried shrimp were measured. The results showed that SSD/HPD dried shrimp had much lower degree of shrinkage, higher degree of rehydration, better color, less tough and softer, and more porous than single-stage SSD dried shrimp. It was also found that SSD/AD gave redder shrimp compared to shrimp dried in a single-stage superheated steam dryer. No improvement in terms of shrinkage and rehydration behavior was observed, however.

Key Words: Color; Hybrid drying; Rehydration behavior; SEM; Shrinkage; Texture.

INTRODUCTION

Shrimp is one of the most popular seafood products available. Traditionally, a production of dried shrimp is performed in a small-scale, mostly at a household level, and sun drying, roasting in an opened air, or alternating with dryer have been used mostly to dry shrimp. Due to very high domestic and export demands, however, a way to improve the dried shrimp production that would yield dried shrimp of superior quality at a high drying rate and lower energy consumption is desired. The preferred quality of dried shrimp is red-orange color, low shrinkage, little tough but rather soft.

The production of dried shrimp can be mainly divided into two steps: boiling raw shrimp in NaCl solution (in order to deactivate microbial growth) and then drying. For shrimp drying the use of a superheated steam dryer (SSD) seems very attractive since boiling and drying can be performed in a single step due to the use of superheated steam as the drying medium. Another advantage of using SSD to dry shrimp, and hence be able to eliminate the boiling step, is that there is no nutritional loss during boiling.[1] The color and shrinkage were also found to be better than shrimp dried in a conventional hot air dryer (AD). Other advantages of using SSD to dry shrimp include the ability to obtain the dried product that has lower degree of shrinkage, which is due to expanded vapor inside the product during rapid drying leading to a highly porous structure.[2–5] It is found, however, that although the higher steam temperature leads to more and larger pores, the elevated steam temperature corresponds to a higher modulus of deformation (hardness) of the dried product.

Albeit the above-mentioned advantages, the use of higher steam temperature may cause the thermal damage of food or some other biological products such as structural degradation, discoloration and protein denaturation.[6,7] Drying product at a higher steam temperature for an extended period of time may also damage its porous structure. In the case of meat product such as shrimp, thermal denaturation of muscle (myofibrillar proteins) and shrinkage of collagen experienced during dehydration can also result in a tightening and stiffening of its structure.

To alleviate the aforementioned problem, various new drying techniques have been proposed and reported over the past decade such as hybrid or multi-stage drying. For example, the two-step SSD/AD (superheated steam drying followed by hot air drying) was recommended by Chen et al.[7] for drying silk cocoon. Since all a product of improper silk quality was obtained when drying was conducted solely in superheated steam. Innovatively, combining a superheated steam dryer and a heat pump dryer (HPD) may have a potential for improving the quality of the final dried product as well as reducing the energy consumption due to enhanced drying rates. SSD can produce a product with high porous structure at a higher drying rate during the first stage of drying; HPD could then be used to maintain the shape and preserve the color of the drying product.[8–15]

The purpose of the present work was to study a two-stage SSD/HPD (superheated steam drying followed by heat pump drying). The effect of tempering between these two stages of drying was also investigated in order to possibly reduce the drying time. The drying characteristics, along with various quality attributes of dried shrimp, i.e., shrinkage, color, texture (toughness and hardness), rehydration behavior and microstructure, were investigated. In addition, SSD/AD was also investigated and compared with SSD/HPD and SSD/HPD with tempering.

MATERIALS AND METHODS

Equipment

Figure 1 shows a schematic diagram of the close-loop superheated steam drying system used in the present study. The unit consisted of a steam generator, a steam superheater rated at 13.5 kW, a $0.3 \times 0.3 \times 0.1$ m^3 cabinet dryer and a backward-curved blade centrifugal fan, which was used to circulate the drying steam through the dryer. Drying was performed at a pressure slightly above the atmospheric pressure.

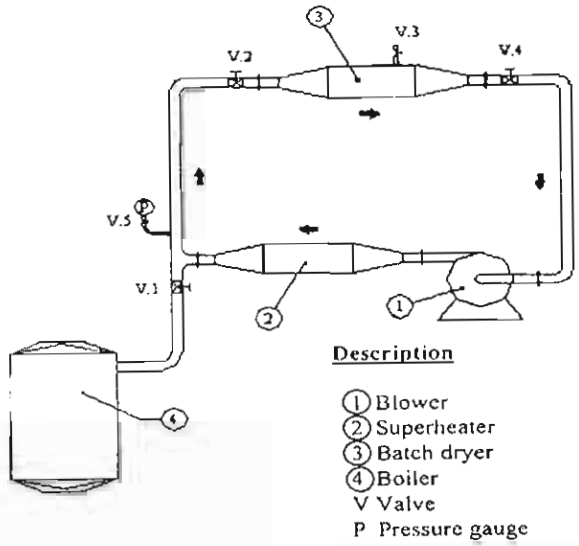

Figure 1. A schematic diagram of the superheated steam dryer used.

A schematic diagram of the close-loop heat pump dryer using R134a refrigerant, which was also used in the present study, is shown in Fig. 2. The unit consisted of a 0.5 kW reciprocating compressor, a 1 kW evaporator, a 1.8 kW internal condenser and a 1.1 kW external condenser. The evaporator bypass air ratio was fixed at 52%.

For air-drying experiments, drying was performed in an open-circuit hot air dryer. An AD unit used consisted of an air heater rated at 4 kW, a $0.4 \times 0.4 \times 0.4\ m^3$ cabinet dryer and a 1.5 kW centrifugal fan. Both steam and air (in HPD and AD) were forced to flow in parallel with a series of wire screens where the samples sat upon in each dryer. Temperatures of all drying media were measured by type-*k* thermocouples connected to a data logger with an accuracy of ±1°C.

Drying of Shrimp

One kilogram of raw shrimp (*Penaeidae*) was used in each drying test. Before drying raw shrimp was washed and dipped in NaCl solution (2% W/V) at room temperature for 30 min. The sample was then placed proportionally on three wire screens. The weight of shrimp was measured

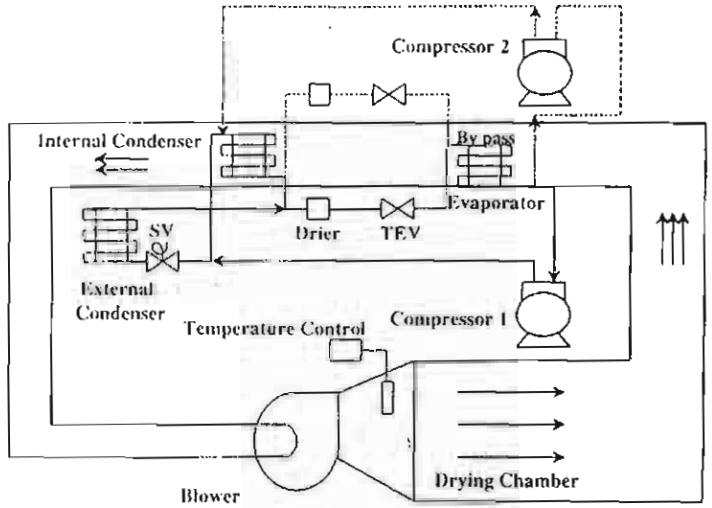

Figure 2. A schematic diagram of the heat pump dryer used (SV = solenoid value, TEV = thermostatic expansion value).

by a digital balance (an accuracy of ±0.1 g) at every 15 min interval during drying. Drying was carried out first in an SSD and later in an HPD. The inlet steam temperature of 140°C and the steam velocity of 2.08 ± 0.2 m/s were used in all experiments. For an HPD unit drying was performed at the drying air temperature and air velocity of 50°C and 0.91 m/s, respectively. The moisture content of dried shrimp after SSD was termed intermediate moisture content (IMC), and was varied between 30 ± 2.4 and 40 ± 2.1% (w.b.). For comparison shrimp was also dried solely using SSD. Another set of experiments involved using SSD/HPD but with a tempering period in between. During tempering shrimp was placed in a tightly sealed container and kept at 60°C with the tempering time of 60 min. Drying conditions used for the SSD/HPD with tempering experiments were the same as those used in the SSD/HPD experiments with no tempering.

Finally, drying was also carried out first in an SSD and later in an AD. For SSD/AD experiments, the first-stage drying conditions and IMCs were the same as those in SSD/HPD experiments. The air temperature and air velocity used in the second-stage air dryer were set at 50°C and 0.87 m/s, respectively.

Shrinkage Measurement

The measurement of shrinkage was performed by manually measuring the sizes of dried shrimp samples obtained from different drying processes (SSD, SSD/HPD, SSD/HPD with tempering, and SSD/AD) using a vernier (by measuring each sample at three positions: length, width, and thickness). The equivalent spherical diameter of each sample was then determined and compared. Ten samples were taken for measurement for each experimental condition. All experiments were performed in duplicate. Percentage of shrinkage was then calculated by:

$$\% \text{ shrinkage} = \frac{Z_o - Z_f}{Z_o} \times 100 \quad (1)$$

where Z_o and Z_f are respectively the sizes of shrimp at the beginning and at the end of each drying experiment.

Color Measurement

Colors of the dried samples were assessed using a colorimeter (Juki JP 7100, Juki Corporation, Tokyo, Japan). The color system used was Hunter Lab where "L" is a measure of lightness, "a" is a measure of redness (-a implies greenness), and "b" is a measure of yellowness (-b implies blueness). For each drying experiment color measurements were taken on five dried and deshelled samples at three positions: P1 (by the head) to P3 (by the tail). The average of 15 measurements of each color parameter (L, a, b) was reported. All experiments were performed in duplicate.

Texture Measurement

Texture of dried and deshelled samples was analyzed by shear test and uniaxial compression test. The shear test was carried out using a TA-XT2i Texture Analyzer (Stable Micro Systems, Haslemere, England). The force required to cut through an individual dried shrimp was measured using a Warner-Bratzler (WB) shear blade with an angular triangular slot cutting edge. The crosshead speed used was 2 mm/s and the distance travelled by the blade through the whole sample thickness and through the base plate slot was 20 mm. The maximum shear force was recorded. Three measurements were taken each at three positions (near head, center, and near tail). Fifteen samples were analyzed and the mean value of 45 measurements was reported.

A uniaxial compression test was performed using an Instron Universal Testing Machine model 4301 (Instron Limited, High Wycombe, England). The crosshead speed used was 50 mm/min and the specimens were compressed to 50% of their original thickness. The values of maximum force reported were the mean of 30 measurements.

The two textural tests were carried out by shearing and compressing the samples perpendicular to the muscle fiber axis and were performed in duplicate.

Microstructure Measurement

The microstructure of dried shrimp samples was analyzed by a JEOL Scanning Electron Microscope (model JSM-5600LV, JEOL Ltd., Tokyo, Japan) with an accelerating voltage of 10 kV. The samples were cut perpendicular to their body longitudinal direction and their cross sections (transverse sections) were observed.

Rehydration Measurement

Dried shrimp samples were rehydrated by immersing them in hot water at 100°C. The samples were drained and their sizes were measured by a vernier at 1 min interval for 10 min. The expanded size, due to absorbed water, was then expressed as the degree of rehydration. The slope of the plot between the degree of rehydration and the rehydration time was defined as the rate of rehydration.

All experiment data were analyzed using an analysis of variance (ANOVA). Differences among mean values were established using the Duncan test. Mean values were considered significantly different when $p < 0.05$.

RESULTS AND DISCUSSION

Drying Curves

The drying curves of shrimp undergoing SSD and two-stage SSD/HPD are shown in Fig. 3. By varying the intermediate moisture content

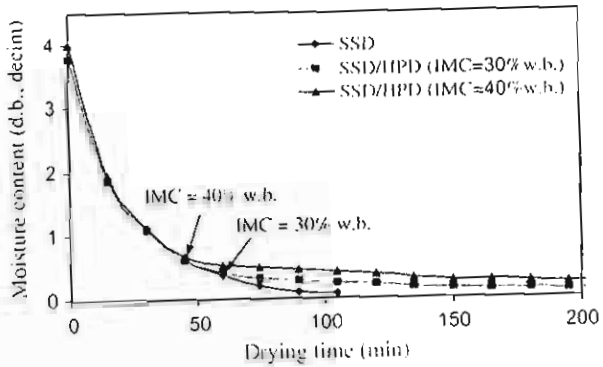

Figure 3. Drying curves of shrimp undergoing purely SSD and SSD/HPD. *(View this art in color at www.dekker.com.)*

(IMC) between 30 and 40% (w.b.), the final moisture content of shrimp of about 20% (w.b.) was reached in approximately 100 and 180 min, respectively. It can be seen from this figure that purely SSD resulted in the highest rate of moisture reduction as compared with the other drying techniques tested here. The moisture content of shrimp of about 20% (w.b.) was reached in approximately 70 min since the whole drying process was performed at a higher medium temperature.

To reduce the drying time of SSD/HPD, tempering between these two stages of drying was included. Figure 4 represents the effect of tempering on the second-stage HPD drying curves. After passing through the tempering stage, shrimp dried faster during the second-stage HPD. As shown in Fig. 4, the linearized second-stage HPD drying curves illustrate the effect of tempering on the second-stage drying rate by comparing the specific drying constant, K, which is equal to the slope of the plots between $\ln[M - M_{eq}]/[M_{in} - M_{eq}]$ against time, where M is the moisture content of shrimp and the subscripts "in" and "eq" are initial and equilibrium, respectively. Higher values of K were obtained for shrimp undergoing tempering for both IMC's (Figs. 4(a) and (b)) implying higher drying rates. The faster moisture removal is due probably to the redistribution of moisture inside the product. The moisture inside the shrimp body transported to the exterior surface and concentrated near this surface, so it could be removed more easily when drying was continued again. It was found that SSD/HPD with tempering could save about 14 and 12% of the net drying time for the corresponding IMCs of about 30 and 40% (w.b.), respectively.

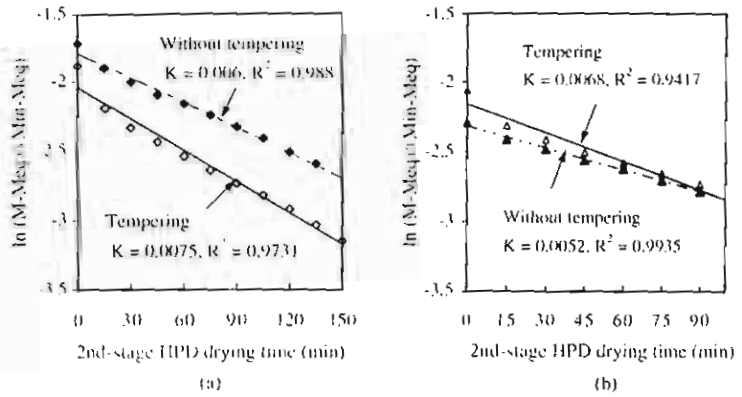

Figure 4. Linearized second-stage HPD drying curves: K = specific drying constant (dotted line were experimental and dashed line were calculated data). (a) IMC about 40% w.b., (b) IMC about 30% w.b. *(View this art in color at www.dekker.com.)*

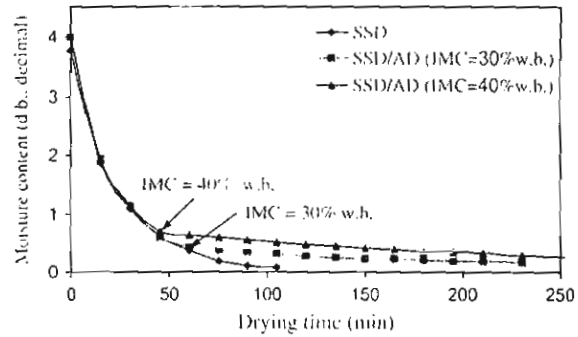

Figure 5. Drying curves of shrimp undergoing purely SSD and SSD/AD. *(View this art in color at www.dekker.com.)*

Figure 5 shows the drying curves for the case of SSD/AD. The moisture content of shrimp reached 20% (w.b.) in approximately 135 and 250 min for the corresponding IMCs of about 30 and 40% (w.b.), respectively. In terms of the drying time, as shown in Fig. 6, SSD/HPD was found to be 1.4–1.5 times faster than SSD/AD at the same IMCs. This is due to the use of low-humidity drying air in an HPD; SSD/HPD is thus a faster drying process compared with SSD/AD. Compared to

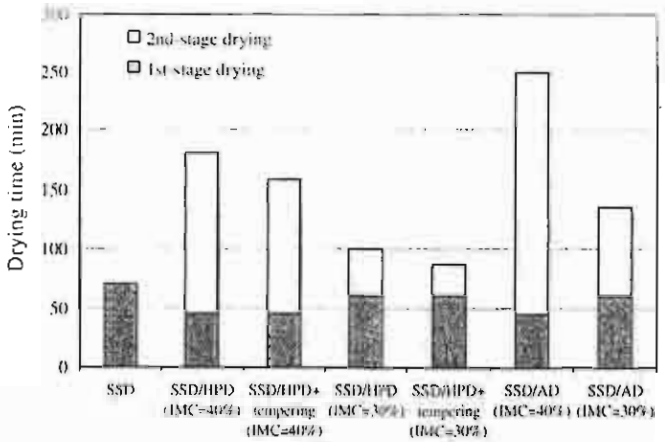

Figure 6. Net drying time of dried shrimp undergoing different drying techniques (reached to the final moisture content of about 20% (w.b.)). *(View this art in color at www.dekker.com.)*

purely SSD, it was observed that the drying time increased slightly in the case of SSD/HPD at lower IMCs but increased significantly in the case of SSD/AD at higher IMCs. For the same two-stage drying process, i.e., SSD/HPD or SSD/AD, it was found that the lower IMC used, the shorter the drying time required. For the same value of IMC used, the drying time required to reach the desired final moisture content differs significantly for the case of SSD/HPD and SSD/AD, however.

Shrinkage

During drying foods undergo volume changes either by shrinkage, which is due to the removal of water from the drying material or by expansion, which is due to the gas generation or pore formation.[16] Different drying techniques thus provide different degrees of volume changes. Normally, the muscle fibers shrink as they lose moisture during drying.

Table 1 shows the results of shrinkage of shrimp that underwent different drying techniques investigated. Shrinkage was found to be lower in the case of SSD/HPD as compared to the case of purely SSD. Although superheated steam drying is known to have a potential to

Table 1. Percentage of shrinkage of shrimp undergoing different drying techniques.*

Drying technique	Shrinkage (%)
SSD	37.50 ± 7.50^{b}
SSD/HPD (IMC ≈ 40% w.b.)	$31.20 \pm 5.67^{a,b}$
SSD/HPD + tempering (IMC ≈ 40% w.b.)	35.79 ± 4.64^{b}
SSD/HPD (IMC ≈ 30% w.b.)	21.47 ± 7.36^{a}
SSD/HPD + tempering (IMC ≈ 30% w.b.)	23.81 ± 6.39^{a}
SSD/AD (IMC ≈ 40% w.b.)	48.07 ± 8.87^{c}
SSD/AD (IMC ≈ 30% w.b.)	35.53 ± 7.19^{b}

*Data are means ± standard deviations.
[a,b,c]Means in the same column with different superscripts are significantly different ($p < 0.05$).

reduce the degree of shrinkage of the drying product due to the evolution of vapor inside the product that expands into cells, leading to a normally porous dried product.[12, 51] drying product at higher steam temperature for an extended period of time may damage the porous structure and hence leads to a less porous product when comparing with the product undergoing SSD/HPD. When separating drying into the first-stage drying at high steam temperature and the second-stage HPD at lower air temperature, it was observed that most pores or space network inside the products developed during superheated steam drying were better maintained during the second-stage HPD due to the use of lower air temperature. Using HPD as the second-stage drying thus helps maintaining the shape of product better than using only SSD.

Similarly, the degree of shrinkage of shrimp undergoing SSD/HPD with tempering was found to be lower than that of purely SSD; similar trends to SSD/HPD were observed, but tempering seemed to yield a product with slightly higher degree of shrinkage than that obtained from the process with no tempering. It is possible that some shrinkage occurred during the tempering period.

The degree of shrinkage of SSD/AD dried shrimp when IMC ≈ 40% (w.b.) was much higher, while that of SSD/AD when IMC ≈ 30% (w.b.) was found to be almost equal to that of purely SSD. It can be concluded that SSD/AD gives no improvement in terms of shrinkage of dried shrimp over that of purely SSD. A possible reason for this is that SSD/AD took longer drying time, especially at higher IMCs. Furthermore, hot air drying is normally known as the cause of shrinkage itself as confirmed

by several previous works such as those of Prachayawarakorn et al.[11] and Posomboon.[17]

It was also noticed that the lower the intermediate moisture content, the lower the degree of shrinkage. This may be ascribed to the fact that changing the process from SSD at higher moisture contents resulted in a lower degree of pore development. Thus, when the drying was continued with HPD, the materials shrink easier. Drying time is also a significant factor in determining the degree of shrinkage; it takes longer time to dry products with higher IMCs in an HPD so these products tend to shrink more than those with lower IMCs.

Colors

Dried shrimp samples that were processed by different drying techniques were distinguishable based on both visual and instrumental assessments of their colors. Instrumentally, as shown in Table 2, the "a" and "b" values of samples dried in both SSD/HPD and SSD/HPD with tempering were higher compared to samples dried in purely SSD while the values of "L" were lower. Since the intense red orange color indicates the good quality of dried shrimp, it can be said that SSD/HPD and SSD/HPD with tempering have a potential to improve the color of dried shrimp in terms of higher a and b values, and lower L value. In the case of SSD/HPD, it is possible that the two-stage drying process helps preventing color degradation, which may result from the use of higher steam temperature for an extended period of time in SSD; low drying

Table 2. Values of "a," "b," and "L" of dried shrimp samples.

Sample	Colors		
	a	b	L
SSD	6.05^{d}	12.80^{b,c}	41.98^{a}
SSD/HPD (IMC ≈ 40% w.b.)	10.82^{a}	13.64^{a,b}	34.89^{b}
SSD/HPD + tempering (IMC ≈ 40% w.b.)	11.47^{a}	14.95^{a}	36.48^{b}
SSD/HPD (IMC ≈ 30% w.b.)	6.80^{c,d}	13.12^{b}	36.32^{b}
SSD/HPD + tempering (IMC ≈ 30% w.b.)	7.33^{b,c}	13.28^{b}	35.18^{b}
SSD/AD (IMC ≈ 40% w.b.)	5.97^{d}	11.34^{c}	42.08^{a}
SSD/AD (IMC ≈ 30% w.b.)	8.19^{b}	9.75^{d}	35.25^{b}

^{a,b,c,d}Means in the same column with different superscripts are significantly different ($p < 0.05$)

temperature in the second-stage HPD helps preserving the color of the dried products. As confirmed by many researchers HPD itself is known to provide excellent product color[9,11,12,18] and hence is a good candidate for the second-stage drying. Switching the process from SSD to HPD at higher moisture contents yields products of better color since doing so implies shorter exposure of shrimp to the higher drying temperature. In this work, the initial values of a, b, and L were −0.42, −0.97, and 32.15, respectively.

Shrimp dried by SSD/HPD with tempering also possessed similar color trends to that dried by SSD/HPD; the two-stage drying with tempering yielded products that were redder and more yellow than products obtained from the process without tempering since tempering reducing the HPD drying time. Moreover, based on the sensory evaluation, it was found that shrimp undergoing SSD/HPD and SSD/HPD with tempering was more transparent and glossy than purely SSD samples. This is due to the shorter drying period at higher steam temperature.

On the other hand, SSD/AD gave reversed results compared to SSD/HPD. Shrimp that was dried using this technique seemed to have no color improvement compared to SSD. Since SSD/AD took longer time to dry shrimp due to the disadvantages of high humidity air, color could not be preserved. Dried shrimp that had an IMC ≈ 30% (w.b.) was markedly redder compared to that had an IMC ≈ 40% (w.b.), however. This is due to the shorter second-stage drying time at lower IMCs mentioned earlier.

In the case of pure hot air drying, the color of dried shrimp is not acceptable if high air temperatures (over 140°C) are used[17] while the color is not acceptable when the drying temperature is over 160°C for SSD.[11] A two-stage SSD/HPD is therefore a possible way to eliminate this limitation; a higher steam temperature is used only in the first-stage SSD to increase the drying rate while the rest of drying is conducted in a lower-temperature environment.

Texture

Textural properties of dried shrimp samples were measured in terms of shear strength or maximum shear force (Fig. 7) and maximum force in compression test (Fig. 8). The shear strength is an indicator of the toughness of the product whereas the compressive force is an indicator of the hardness. Shear strength can describe the maximum force needed to cut the product in human mouth by the front teeth while hardness measures the force needed to destruct the product by the molars.

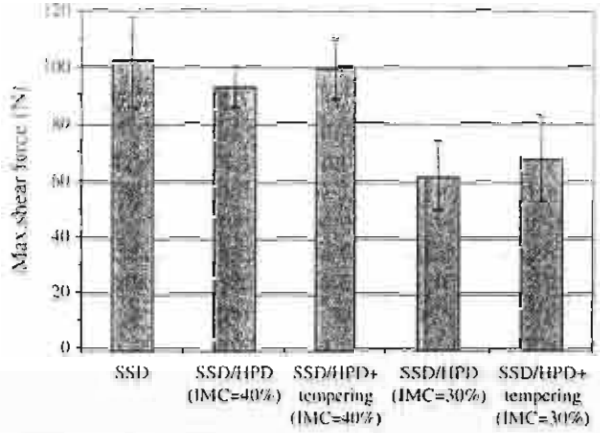

Figure 7. Shear strength of dried shrimp undergoing different drying techniques (vertical lines indicate standard deviations). *(View this art in color at www.dekker.com.)*

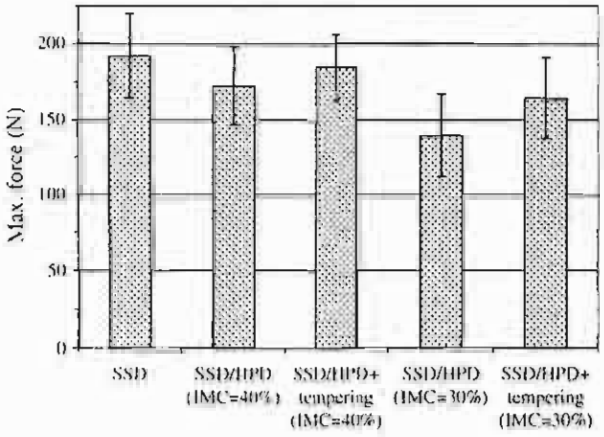

Figure 8. Hardness of dried shrimp undergoing different drying techniques (vertical lines indicate standard deviations). *(View this art in color at www.dekker.com.)*

From the experiments it was found that the shear strength required to cut dried shrimp undergoing SSD/HPD and SSD/HPD with tempering was lower than that required for SSD samples, especially when IMC $\approx 30\%$ (w.b.); the texture of SSD/HPD dried shrimp was less tough than

that of SSD samples (Fig. 7). Similarly, shrimp undergoing SSD/HPD and SSD/HPD with tempering was softer than that dried by purely SSD (Fig. 8). Evidently, toughness and hardness are closely related; a direct relationship was found between instrumental shear force (toughness) and compressive force (hardness) measurements for all different dried samples tested.

Based on the instrumental evaluation it was found that the texture of dried shrimp samples obtained from two-stage SSD/HPD with and without tempering was less tough and softer than that of samples obtained from the single-stage SSD. This is due to the shorter period of high-temperature drying, which leads to less tough and softer dried product. It is also known that temperature changes the solubility of the meat protein; high temperature in food processing often attributes to increased protein coagulation resulting in the toughening of the meat fibers.[19] The texture of dried shrimp also seems to have a direct relationship with shrinkage; the lower the degree of shrinkage, the less tough and softer the dried product.

Microstructure

Figure 9 shows the microstructure of dried shrimp samples obtained from different drying processes (SSD and SSD/HPD) while Figs. 10(a) and (b) compare the microstructure of dried samples undergoing SSD/HPD with and without tempering. Microscopically, all scanned sets of dried shrimp muscle tissue had nearly the same pattern in their structure organization. However, there was an enormous system of pore between the muscle fibers of shrimp undergoing SSD/HPD, especially at IMC $\approx 30\%$ (w.b.) (Fig. 9(c)) while there was much less pore space inside the muscle fibers of shrimp undergoing single-stage SSD (Fig. 9(a)). SSD samples seemed to have a tightening structure of muscle fibers due to its exposure to an extended period of high-temperature drying. For the effect of tempering it was observed that some shrinkage occurred during the tempering period. As shown in Fig. 10 shrimp undergoing SSD/HPD with tempering had less space inside its muscle fibers than samples that did not go through the tempering period.

Generally, dried products with more porous structure often have lower density as well as lower degree of shrinkage. As evidenced by SEM photographs and the results on shrinkage discussed earlier, larger pore space resulted in a lower degree of shrinkage. Besides, this pore space system affects the texture of shrimp; more space inside the muscle fibers resulted in a softer shrimp. SSD/HPD samples were thus the least tough

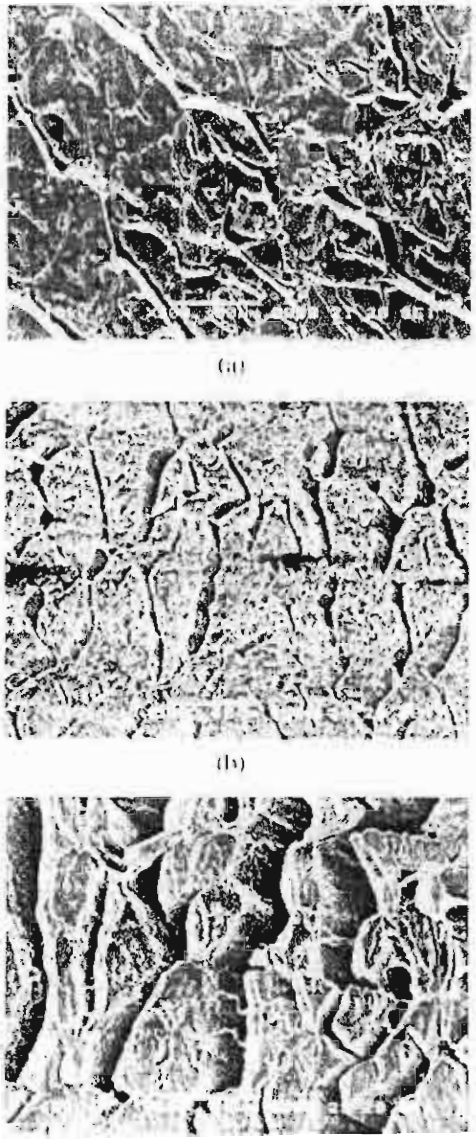

(a)

(b)

(c)

Figure 9. Effects of different drying processes on microstructure of dried shrimp (transverse sections). (a) SSD, (b) SSD HPD (IMC ~ 40% w.b.), and (c) SSD HPD (IMC ~ 30% w.b.).

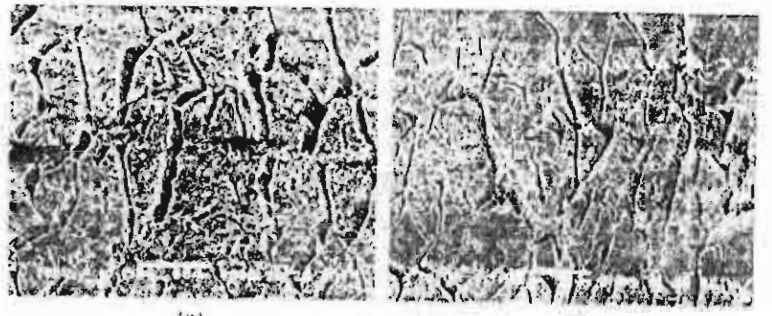

(a) (b)

Figure 10. Effects of tempering between SSD and HPD on microstructure of dried shrimp (IMC ~ 40% w.b.) (transverse sections). (a) SSD HPD and (b) SSD HPD with tempering.

and the softest. This is probably the reason for the direct correlation between shrinkage and textural properties of dried shrimp.

Rehydration Behavior

Figure 11 illustrates the rehydration behavior of dried shrimp samples obtained from different drying methods at rehydrating temperature of 100 C. The trends are similar for all sample sets tested. Higher rehydration rates were observed at the beginning of the process, as expected. Also, it was found that SSD HPD produced samples had higher degree of rehydration compared to samples dried using other techniques. An adversely relationship was also found between the degree of rehydration and that of shrinkage.

Generally, it is accepted that the degree of rehydration is dependent on the degree of cellular and structural disruption[20,21] and the nature of internal porous structure and mechanical properties of dried materials will influence the water uptake during their rehydration. The space system provides necessary avenues for conveying water to the muscle fibers, which are indispensible during rehydration.[22] Form SEM photographs, it is clear that the structural pattern of dried shrimp tissue is directly related to its rehydratability. SSD HPD dried shrimp had higher degree of rehydration than dried samples obtained from the other drying methods studied.

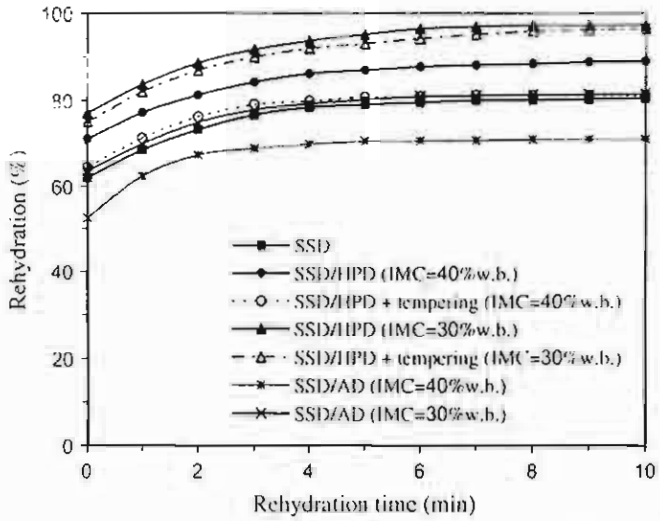

Figure 11. Rehydration curves of dried shrimp samples obtained from different drying processes. *(View this art in color at www.dekker.com.)*

CONCLUSION

SSD/HPD is a new alternative for two-stage drying, which has proved to yield a product of better quality; degree of shrinkage, rehydration potential, color, textural properties, and microstructure of shrimp undergoing this newly proposed drying scheme were greatly improved as compared to samples undergoing a single-stage SSD. An enormous system of pore space between the muscle fibers of sample undergoing SSD/HPD was also observed as compared to sample undergoing only SSD.

A two-stage drying (SSD/HPD) with a tempering period in between was also tested. It was found that the drying rate during the second-stage HPD could be improved when the tempering treatment between the two drying stages was included. In addition, a two-stage SSD/AD was tested and it was found that the process led to some quality improvement viz. redder products but no improvement was observed in terms of shrinkage and rehydration behavior.

An appropriate selection of drying conditions viz. drying temperature and intermediate moisture content between the two drying stages presents an effective way to improve dried product quality in many ways. For this study, the optimum IMC ≈ 30% (w.b.) was found to improve many attributes of quality of dried shrimp.

ACKNOWLEDGMENTS

The authors would like to express their sincere appreciation to the Thailand Research Fund (TRF) for supporting this study financially.

REFERENCES

1. Prachayawarakorn, S.; Soponronnarit, S.; Wetchacama, S.; Jaisut, D. Desorption isotherms and drying characteristics of shrimp in superheated steam and hot air. Drying Technology **2002**, *20* (3), 669–684.
2. Caixeta, A.T.; Moreira, R.G.; Castell-Perez, M.E. Impingement drying of potato chips. Journal of Food Process Engineering **2002**, *25*, 63–90.
3. Elustondo, D. Drying foodstuff with superheated steam. Drying Technology **2002**, *20* (1), 235–237.
4. Moreira, R.G. Impingement drying of foods using hot air and superheated steam. Journal of Food Engineering **2001**, *49*, 291–295.
5. Seyed-Yagoobi, J.; Li, Y.B.; Moreira, R.G.; Yamsaengsung, R. Superheated steam impingement drying of tortilla chips. Drying Technology **1999**, *17* (1–2), 191–213.
6. Mujumdar, A.S. Superheated steam drying. *Handbook of Industrial Drying*; Pub. Marcel Dekker Inc.: New York, 1995.
7. Chen, S.-R.; Chen, J.-Y.; Mujumdar, A.S. A preliminary study of steam drying of silkworm cocoons. Drying Technology **1992**, *10* (1), 251–260.
8. Sosle, V.; Raghavan, G.S.V.; Kittler, R. Low-temperature drying using a versatile heat pump dehumidifier. Drying Technology **2003**, *21* (3), 539–554.
9. Alves-Filho, O. Combined innovative heat pump drying technologies and new cold extrusion techniques for production of instant foods. Drying Technology **2002**, *20* (8), 1541–1557.
10. Chua, K.J.; Chou, S.K.; Ho, J.C.; Hawlader, M.N.A. Heat pump drying: recent developments and future trends. Drying Technology **2002**, *20* (8), 1579–1610.

11. Perera, C.O. *Modified Atmosphere Heat Pump Drying of Food Products*, Proceedings of the 2nd Asian-Oceania Drying Conference (ADC '01), Pulau Pinang, Malaysia, Aug 20–22, 2001; 469–476.
12. Strommen, I. *Heat Pump Drying, New Development and Applications*, Proceedings of the 2nd Asian-Oceania Drying Conference (ADC '01), Pulau Pinang, Malaysia, Aug 20–22, 2001; 102–113.
13. Prasertsan, S.; Saen-saby, P. Heat pump drying of agricultural materials. Drying Technology **1998**, *16* (1–2), 235–250.
14. Chou, S.K.; Hawlader, M.N.A.; Ho, J.C.; Wijeysundrea, N.E.; Chua, K.J. *Heat Pump Drying Systems*, Proceedings of the 4th ASEAN Science and Technology Week, Science and Technology: The Future of ASEAN, Bangkok, Thailand, Aug 21–Sept 1, 1995; 266–276.
15. Young, G.; Sirchall, S; Mason, R. *Heat Pump Drying of Food Products—Prediction of Performance and Energy Efficiency*, Proceedings of the 4th ASEAN Science and Technology Week, Science and Technology: The Future of ASEAN, Bangkok, Thailand, Aug 21–Sept 1, 1995; 240–247.
16. Rahman, M.S. Toward prediction of porosity in foods during drying: a brief review. Drying Technology **2001**, *19* (1), 1–13.
17. Posomboon, W. Processing Effect on Quality of Dried Shrimp. Master thesis, Asian Institute of Technology, Bangkok, Thailand, 1998.
18. Chua, K.J.; Mujumdar, A.S.; Chou, S.K.; Hawlader, M.N.A; Ho, J.C. Convective drying of banana, guava and potato pieces: effect of cyclical variations of air temperature on drying kinetics and color change. Drying Technology **2000**, *18* (4–5), 907–936.
19. Bouton, R.E.; Harris, P.V. The effect of cooking temperature and time on some mechanical properties of meat. Journal of Food Science **1972**, *37*, 140–144.
20. Krokida, M.K; Morinos-Kouris, D. Rehydration kinetics of dehydrated products. Journal of Food Engineering **2003**, *57*, 1–7.
21. Moorjani, M.N.; Dani, N.P. Textural and reconstitutional properties of freeze-dried shrimp. Food Technology **1968**, *22*, 886–888.
22. Wang, H.; Auerbach, E.; Bates, V.; Doty, D.M.; Kraybill, H.R. A histology and histochemical study of beef dehydration. IV. Characteristics of muscle tissues dehydrated by freeze-drying techniques. Food Research **1954**, *19*, 543–556.

DRYING TECHNOLOGY
Vol. 22, No. 7, pp. 1731–1754, 2004

Effect of Fluidized Bed Drying Temperature on Various Quality Attributes of Paddy

Supawan Tirawanichakul,[1,*] Somkiat Prachayawarakorn,[2] Warunee Varanyanond,[3] Patcharee Tungtrakul,[3] and Somchart Soponronnarit[1]

[1]School of Energy and Materials and
[2]Faculty of Engineering, King Mongkut's University of Technology, Thonburi, Bangkok, Thailand
[3]Institute of Food Research and Product Development, Kasetsart University, Bangkean, Bangkok, Thailand

ABSTRACT

As reported by many researchers, it was found that fluidized bed paddy drying using high drying air temperatures of over 100°C affected the head rice yield and whiteness of dried rice. However, only a few studies on fluidized bed paddy drying with drying air temperatures below 100°C were so far reported. The main objective of this work was therefore to study the effect of fluidized bed drying air temperature on various quality parameters of Suphanburi 1 and

*Correspondence: Supawan Tirawanichakul, School of Energy and Materials, King Mongkut's University of Technology, Thonburi, Bangkok 10140, Thailand; Fax: +662-470-8623; E-mail: supawanvachiramon@hotmail.com.

DOI: 10.1081/DRT-200025634
0737-3937 (Print); 1532-2300 (Online)

www.dekker.com

Pathumthani 1 *Indica* rice. Paddy was dried from the initial moisture contents of 25.0, 28.8, and 32.5% dry basis to 22.5 ± 1.2% dry basis using inlet drying air temperatures between 40 and 150°C at 10°C step. After fluidized bed drying, paddy was tempered and followed by ambient air aeration until its final moisture content was reduced to 16.3 ± 0.5% dry basis. The results showed that the head rice yield of Suphanburi 1 was significantly related to the inlet drying temperature and initial moisture content whilst there was no significant relationship between the head rice yield, drying temperature and initial moisture content for Pathumthani 1. The whiteness of the two rice varieties was slightly decreased with increase in drying air temperature and initial moisture content. It was also found that the hardness of both cooked rice varieties exhibited insignificant difference ($p < 0.05$) comparing to rewetted rice, which was gently dried by ambient air aeration in thin layer. The thermal analysis by DSC also showed that partial gelatinization occurred during drying at higher temperatures. Using inlet drying air temperatures in the range of 40–150°C therefore did not affected the quality of cooked rice and paddy. The milling quality of paddy was also well maintained.

Key Words: Amylose; High-temperature drying; Rice quality; Sensory evaluation.

INTRODUCTION

The management of highly moist paddy with moisture content of over 22% dry basis is an extremely serious problem in tropical countries since high humid air condition can accelerate an excessive mould growth, and yellowing of grains.[1–4] To prevent paddy deterioration, rapid reduction of moisture is essential and hot air drying seems to be the most appropriate drying technique under such weather condition. Some previous researches recommended that high moisture content of paddy should be first reduced to 22% dry basis within 24 h by hot air drying (using high temperature and short drying time) and then followed by natural air drying at lower temperature.[5,6] However, the use of heated air may damage some important grain qualities that are susceptible to thermal damage such as head rice yield, whiteness, physicochemical properties, and nutritional values.[7–9]

Hot air fluidized bed drying is one of the drying techniques that provides faster moisture reduction and uniformity of drying. The rapid drop in moisture content can, however, develop stresses inside the kernel, causing the reduction of head rice yield.[10] The head rice yield reduction decreases the value of rice since broken rice has lower commercial values than the complete one. To reduce the thermal stresses and maintain the full kernel, tempering stage is recommended after the first stage of drying.[11–14]

Although fluidized-bed dryer is well recognised in the grain industries, not much work is devoted to determining how this type dryer affects the quality of rice, especially in the low drying temperature range. Therefore, the main objective of this article was to investigate the effects of drying temperature and initial moisture content of paddy on various quality attributes of long grain rice varieties containing high and low amylose contents. The physical qualities tested were head rice yield, whiteness of rice, microstructure of rice kernel, and germination. The chemical properties of rice were determined in terms of amylose content and protein. The texture of cooked rice as well as the thermogram of rice determined using a differential scanning calorimetry (DSC) was investigated. Finally, overall acceptability of cooked rice by sensory evaluation was also determined.

EXPERIMENTAL SET-UP, MATERIALS, AND METHODS

1. Experimental Set-up

Figure 1 shows the schematic diagram of a batch fluidized bed dryer used in the present study. The dryer consists of a cylindrical shaped drying chamber, a 16 kW electric heating unit and a backward curved blade centrifugal fan driven by a 1.5 kW motor. The inlet drying air temperature was controlled by a PID controller with an accuracy of ±1°C. A mechanical variable speed unit was used for regulating air flow rate. A constant air velocity of 2.5 m/s was used for the bed of rice of 9.5 cm. The final moisture content required in the present study was approximately 22.5% dry basis as recommended by Poomsa-ad et al.[6]

2. Materials

Two varieties of long grain rough rice (Suphanburi 1 and Pathumthani 1) provided by the Rice Research Institute at Pathumthani province, Thailand, were rewetted, mixed, and kept in a cold storage at a temperature range of 4–6°C for one week prior to the

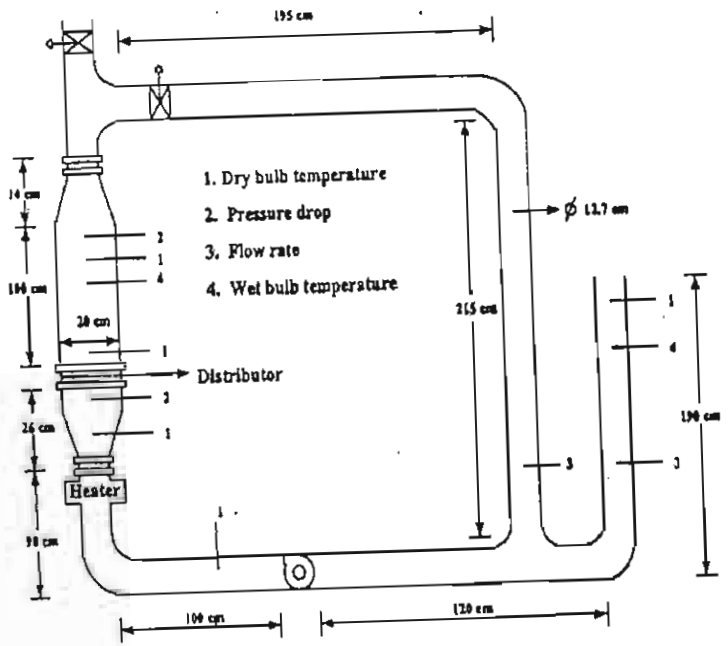

Figure 1. A schematic diagram of a batch fluidized bed dryer.

start of each experiment. The desired initial moisture content of rewetted paddy was about 25–33% dry basis. The local varieties of Suphanburi 1 and Pathumthani 1 contain amylose contents of 25–27% and 15–18%, respectively. Before starting the experiments, paddy was placed in an ambient environment until the thermal equilibrium was reached.

2. Methods

2.1. Paddy Drying Condition

Figure 2 illustrates a schematic diagram of the drying schedule used in this work. Wet paddy was first dried using a fluidized bed dryer by varying inlet air temperatures between 40 and 150°C with 10°C increment. It was subsequently tempered for 30 min.[15] During tempering, dried paddy was placed in a sealed glass bottle with an o-ring and kept in an oven at the same temperature as the grain

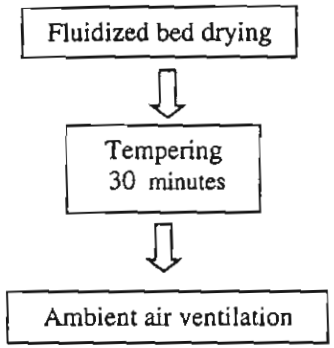

Figure 2. A schematic diagram of a fluidized bed drying system.

temperature. The tempering process was performed to relax some of thermal stresses developed during the first-stage drying.

To measure the grain temperature, paddy sample was taken out from the fluidized bed drying chamber at the end of drying time, corresponding to the final moisture content as aforementioned, and then measured when it was kept in the well-insulated vessel. This temperature was used for the tempering grain. By this measuring, it was concluded that at the inlet drying air temperature ranges of 40 to 90°C, the average grain temperature corresponded to the range of 38 to 75°C, respectively. For the inlet drying air temperature ranges of 100 to 150°C, the average grain temperature was in the range of 83 to 89°C, respectively.

After tempering paddy was taken out of the sealed bottle and ventilated immediately with a constant ambient airflow rate of 0.15 m/s until its moisture content reached 16.3 ± 0.5% dry basis as recommended by Soponronnarit.[16] A K-type thermocouple used for measuring the temperature of the bed was connected to a data logger with an accuracy of ±1°C. The determination of paddy moisture content was performed according to the AOAC method.[17] Air velocity was measured by a hot wire anemometer with a precision of ±0.1 m/s.

2.2. Quality of Rice

All qualities of rice samples after drying were determined comparing to the rewetted rice sample (so-called control rice), which was gently dried by ambient air ventilation in thin-layer. The various qualities of paddy

were analyzed as follows:

(a) Head Rice Yield

The determination of head rice yield was performed according to the USDA method.[18] Head rice yield was calculated by dividing the head rice weight by the initial rough rice weight. This value was determined in duplicate.

(b) Microstructure and Thermal Property of Rice

The microstructure of rice kernel was characterized by a scanning electron microscope (SEM) (JEOL, model LV5600, England) at 10–20 kV. The magnification range was 200–4000 times.

Thermal analysis of rice flour was determined by differential scanning calorimetry (DSC) (Perkin Elmer, model DSC-7, Norwalk, USA). The rice flour sample was heated from 40 to 95°C at a scanning rate of 10°C/min. From the DSC curve, the onset temperature, peak temperature, conclusion temperature, and transition enthalpy were recorded. The degree of gelatinization of hydrothermally-treated rice flour was calculated by the following equation[19]:

$$SG(\%) = \left(1 - \left[\frac{\Delta H}{\Delta H_c}\right]\right) \times 100 \quad (1)$$

where SG = degree of gelatinization (%)

ΔH = transition enthalpy of treated rice (J/g (dry weight basis))

ΔH_c = transition enthalpy of control rice (J/g (dry weight basis))

(c) Whiteness of Rice

The whiteness of milled rice was measured by a Satake milling meter model MM-113 (Japan). This value was determined in duplicate.

(d) Germination of Paddy

Before germination testing, dried mature paddy samples were kept at ambient air environment for 6 weeks. The mature paddy samples (200 seeds) were then used for each test. The germination test followed the guidelines given by the Rice Research Institute at Pathumthani province, Thailand. The experiments were performed in triplicate.

(e) Chemical Quality of Rice

Amylose was determined by simplified assay iodine colorimetric method of Juliano.[20] The content of protein was quantified as described by AOAC method.[17] These value was determined in duplicate.

(f) Textural Property of Cooked Rice

Hardness of cooked rice was determined by a bench-top texture analyzer model TA-XT2*i* (Stable Micro Systems Ltd., USA). A 30 g portion of each milled head rice sample was placed in an aluminum cylindrical cup (diameter of 7 cm and height of 7 cm). Before cooking, the rice sample was washed, rinsed, and then cooked with distilled water at rice-to-water weight ratios of 1:1.5 for Pathumthani 1 and 1:1.7 for Suphanburi 1.[21,22]

The initial height of the compression probe (Ottawa cell) was set at 120 mm and the pretest speed, test speed, and post speed of probe were 1.5, 0.5, and 10 mm/s, respectively. The maximum force required for compressing cooked rice to 90% of the initial height of 10 mm was indicated as the hardness of cooked rice. The hardness value was represented by the mean of 5 replications and the average value was expressed in kilogram unit.

(i) Sensory Evaluation of Cooked Rice

For determination of the cooking quality, 100 g of head rice was washed with tap water and cooked in an electric cooker at a rice-to-water ratio of 1:1.8 by weight.[22] The quality of cooked rice was evaluated on the basis of its palatability. Eight trained panelists from the Institute of Food Research and Product Development, Kasetsart University, Thailand were invited to evaluate the overall acceptability of cooked rice using hedonic scale of 1–9 with the following scales: 1 = extremely dislike, 2 = very much dislike, 3 = moderately dislike, 4 = slightly dislike, 5 = like nor dislike, 6 = slightly like, 7 = moderately like, 8 = very much like, and 9 = extremely like. Analysis of variance (ANOVA) and Duncan's new multiple range test (DMRT) were used to evaluate the effects of inlet drying air temperature on the quality of rice at 95% confidence limit ($p < 0.05$).

RESULTS AND DISCUSSION

1. Moisture Content and Drying Rate

For all experiments, the moisture content of paddy after the first stage drying was set at 22.5 ± 1.2% dry basis to avoid significant fissuring and subsequent breakage of rice. However, this moisture level is still not safe for long-term storage and hence paddy needs to be dried further. Reducing moisture content from this level to 16% dry basis can be

achieved by many means technique. In common practice paddy would be tempered at a suitable temperature[15,23] and dried by any low-temperature drying technique until the desired final moisture content of paddy of 14–16% dry basis is reached.[13,15]

Thus, in this work, the tempering process at grain temperature was performed and the tempered duration was fixed at 30 min. After tempering, paddy sample was thin-layer dried immediately by ambient air ventilation until the final moisture content was in range of 14–16% dry basis, resulting in minimal breakage and consequently a high head rice yield.[23]

Figures 3(a) shows the drying rates of paddy at three initial moisture levels of 25.0, 28.8, and 32.5% dry basis for Suphanburi 1 at inlet drying air temperatures of 40–150°C. It can be seen that the drying rates seem to be independent of an initial moisture content, indicating that the main part of moisture content, above 25.0% dry basis, existed only on the exterior surface, thus allowing easier water removal without any interference of disordered void spaces inside grain kernel during drying. As is seen in Fig. 3(b), the changes of drying rates for Pathumthani 1 with inlet air temperatures of 40–150°C and three initial moisture contents of 25.0, 28.8, and 32.5% dry basis show a similar trend to that found for Suphanburi 1.

2. Quality of Rice

(a) Head Rice Yield of Rice

Figure 4 shows the relationship between inlet drying air temperature and head rice yield. The head rice yield after rewetting reduces to lower level than that obtained before rewetting for both rice varieties. However, the amount of head rice yield reduction depends on the rice variety as observed from the experiments; Suphanburi 1 variety, which contains higher amylose content has larger amount of broken kernel although the head rice yield of both varieties before rewetting was nearly the same.

When paddy kernels were subjected to drying at different air temperatures, the changing of head rice yield was rather complicated. For Suphanburi 1 variety, as can be seen in Fig. 4(a), at air temperatures below 80°C or grain temperatures below 70°C, head rice yield of paddy samples at three different initial moisture contents of 25.0, 28.8, and 32.5% dry basis was insignificantly different, (when compared with the gently dried control sample) the values were between 43 and 45%. The maintained head rice yield could be explained by two possible reasons.

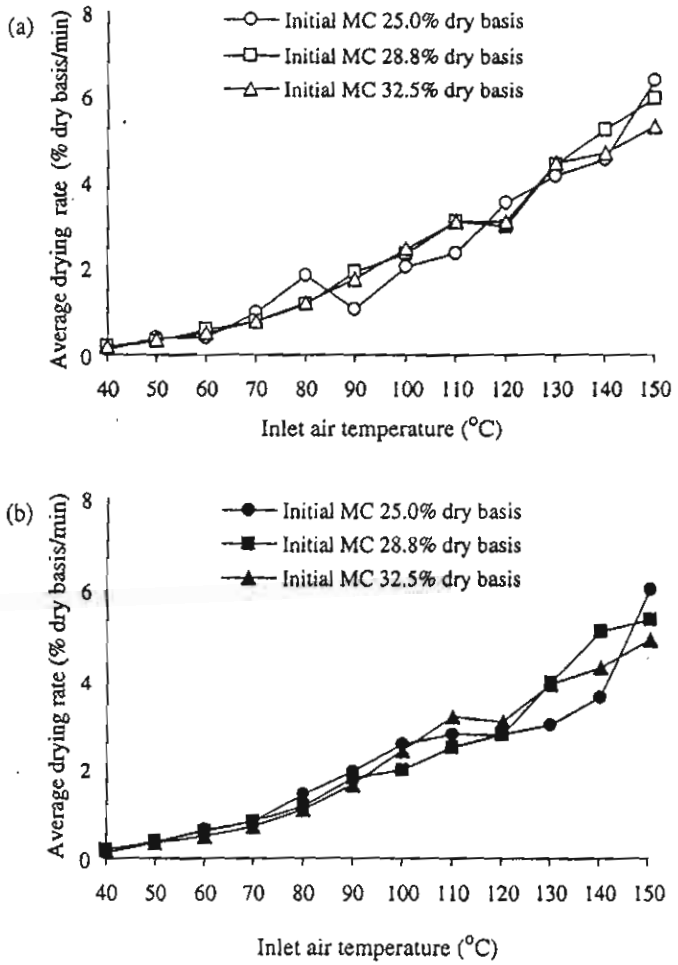

Figure 3. Effect of inlet air temperature on average drying rate of Suphanburi 1 and Pathumthani 1: initial moisture contents were in the range of 25.0–32.5% dry basis and final moisture content of 22.0 ± 1.2% dry basis (after fluidized bed drying). (a) Suphanburi 1, (b) Pathumthani 1.

Firstly, at low drying air temperatures of 40–50°C, which corresponded to the grain temperatures of 38–46°C, the moisture gradient developed inside a grain kernel during slow moisture reduction from any level to 22.5% dry basis was not sufficiently large to develop fissures. This is

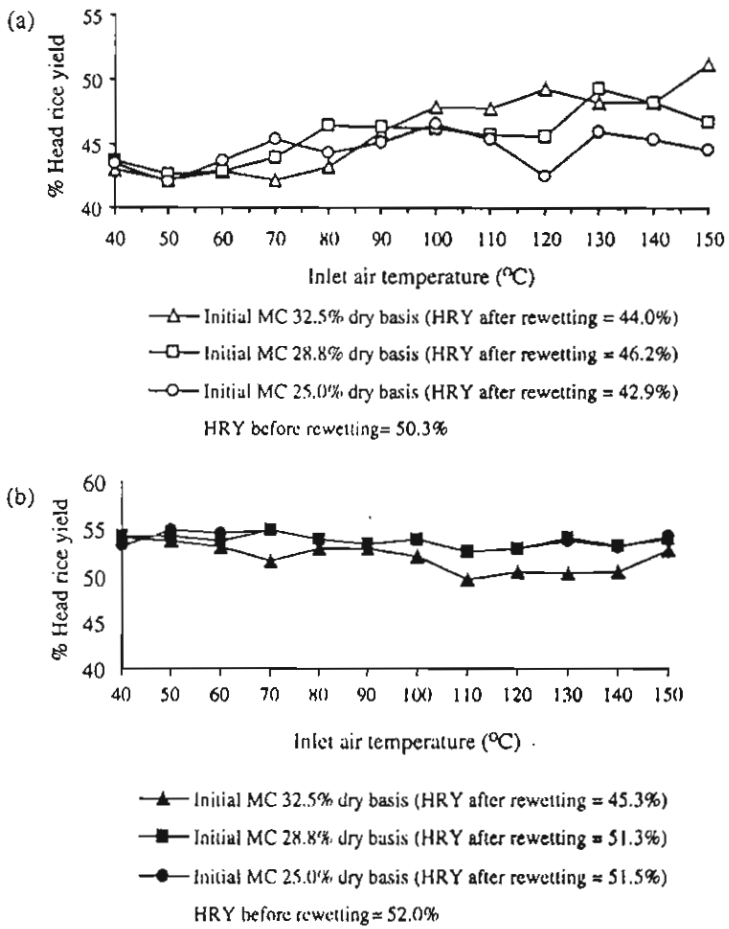

Figure 4. Effect of inlet air temperature on head rice yield of Suphanburi 1 and Pathumthani 1: initial moisture contents were in the range of 25.0–32.5% dry basis and final moisture contents of 22.0 ± 1.2% dry basis (after fluidized bed drying). (a) Suphanburi 1, (b) Pathumthani 1.

reason why drying and tempering at the drying air temperatures below the glass transition temperature did not cause significant fissuring and subsequent breakage of rice.[23,25]

For drying temperatures in the range of 60 to 70°C, even though the moisture gradient was sufficiently large and hence induced stresses inside

the kernel, tempering could still prevent the head rice yield reduction since paddy was tempered at temperatures above 50°C. Under this condition, paddy was in its rubbery state,[23] thus starch existed as a rubbery material with higher expansion coefficients.[26,27] Several researchers have reported that paddy drying at temperatures above 50°C could be detrimental to head rice yield if the moisture content drops larger than 3 percentages of moisture content in one drying pass and when tempering is not included between drying stages.[14,23,28,29] However, in this study, the moisture content of paddy sample was removed around 6.8–10.5% during for the first-stage drying and hence the head rice yield was not reduced when paddy was tempered at its own grain temperature after fluidized bed drying. Moreover, the tempering duration of 30 min used in this study was sufficient large to remove large portion of moisture content. Consequently, some of proteins or lipids might interact with amylose and carbonyl compounds presented in paddy,[30] resulting in subsequent improvement of milling resistance of paddy.[31,32]

The change of head rice yield of paddy dried at a higher temperature of 80°C was quite different to that dried at lower temperatures, however. At 80°C, the head rice yield was improved, particularly at an initial moisture content of 32.5% dry basis; even higher than 47% as can be seen in Fig. 4(a). This value was indeed higher than that of control sample. The larger percentage head rice yield for high temperature treated samples implies stronger intra-granular binding forces, which make the kernel more resistant to abrasive forces during milling. This improvement of binding forces amongst granules is caused by their swelling together with the leaching out of amylose molecule from starch granules into aqueous substrates.[33] The swollen granules were then gelatinized, but only partially, since the water content inside the kernel in the present study was not enough for a complete gelatinization.

It is interesting to note that, at each level of initial moisture content, the change of head rice yield with inlet drying air temperature for Pathumthani 1, which contains lower amylose content, was insignificantly different over the entire drying temperature range; the values laid between 53 and 55% for an initial moisture contents of 25.0 and 28.8% dry basis and between 52 and 54% for an initial moisture content of 32.5% dry basis. Such changes were not similar to those found for Suphanburi 1 variety, especially when drying at higher temperatures in which the head rice yield did not show an increasing trend although a high initial moisture content of 32.5% dry basis was employed. According to these results, it may be indicated that the amylose content significantly contributes to the improved intra-granular forces during

gelatinization; the lower the amount of amylose, the lower the binding forces are.

As shown in Fig. 4(b), the head rice yield for Pathumthani 1 sample with an initial moisture content of 32.5% dry basis and dried at a higher temperature of 80°C was lower than that of the other two initial moisture contents. The lower amount of full kernel was due to the dominant contribution of stresses, which consequently induced an irreversible structural damage although partial gelatinization occurred during drying. This change was not similar to Suphanburi 1 samples in which the head rice yield became higher with the initial moisture content.

(b) Microstructure and Thermal Analysis of Rice

To confirm the aforementioned occurrence of gelatinization, the microstructure of rice samples was examined by means of scanning electron microscopy (SEM). The gelatinization enthalpy was also determined by differential scanning calorimetry (DSC).

The results of SEM observation of the morphological changes of starch granules of Suphanburi 1 variety at various drying temperatures are shown in Figs. 5(a–d). As can be seen in Fig. 5(a), the starch granules in endosperms of control sample showed clearly the characteristically irregular polygons with diameters of 4–8 μm, while Figs. 5(b–d) show the morphology of starch granules of dried rice kernel at inlet drying air temperatures of 40, 120, and 150°C, respectively. Drying at low inlet air

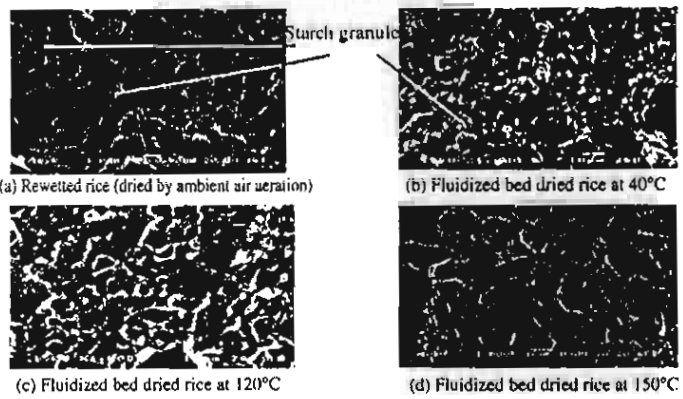

Figure 5. Scanning electron micrographs of Suphanburi 1 (initial MC = 32.5% dry basis) at various inlet air temperatures.

temperature of 40°C does not change the conformation of starch granules, as can be seen in Fig. 5(b), comparing to the morphology of starch granules of the control sample (Fig. 5(a)).

As can be observed in Figs. 5(c–d), during drying at high inlet drying air temperatures of 120 and 150°C (the average grain temperature was in range of 83 to 89°C), starch granules obviously exhibited swelling. This is due to the fact that the bonding between amylose and amylopectin molecules in starch granules was relaxed around their gelatinization temperatures of 68–78°C[34] and leaching of amylose from starch granules led to partial gelatinization.[7,35] These combined characteristics of the granule segments to form network-like structures contributed to the strong gel formation. The structure of starch granules eventually disintegrated and adjacent starch granules fused together to form the composite clusters with homogeneous interior and low well defined polygonal boundaries. The rice kernel appeared as dense and smooth layer throughout its cross-sectional area as shown in Fig. 5(d).

The above-mentioned partial gelatinization agreed well with the DSC results manifested by a certain degree of gelatinization as shown in Table 1, which shows the gelatinization and thermal properties of Suphanburi 1 and Pathumthani 1 rice varieties. The degree of gelatinization of both rice varieties after drying at 150°C was different from that of the reference sample. The higher degree of gelatinization was observed in rice that had higher initial moisture content and the longer drying time. The percentage degree of gelatinization for Suphanburi 1 and Pathumthani 1 calculated by Eq. (1) were in the range of 42–55% for the initial moisture content of 32.5% dry basis and less than 20% for the lower initial moisture content of 28.8% dry basis.

(c) Whiteness of Rice

Figure 6 shows the effects of drying air temperature and initial moisture content on the whiteness of rice for Suphanburi 1 and Pathumthani 1. After rewetting, the whiteness value of Pathumthani 1 rice sample remained the same as before rewetting whilst the color of Suphanburi 1 rice sample became less luminous, with the average whiteness value of 49.8. As paddy was subjected to drying at various drying air temperatures, the whiteness of Pathumthani 1 with initial moisture contents of 25.0, 28.8, and 32.5% dry basis showed an insignificant difference amongst each other at drying temperatures below 80°C and was equivalent to its original value of the control sample. On the other hand, the change in whiteness for Suphanburi 1 was

Table 1. Gelatinization properties of rice flour of Suphanburi 1 and Pathumthani 1 varieties.

Rice variety	Initial MC % dry basis	Inlet air temp. (°C)	Transition temp (°C) T_{onset}	T_{peak}	$T_{conclude}$	ΔH (J/g)[a]	% Degree of gelatinization
Suphanburi 1	32.5	Control	71.5	76.4	81.4	7.1	
		150	78.1	85.0	89.5	3.2	54.9
	28.8	Control	71.2	77.2	85.1	6.7	
		150	73.0	78.1	85.5	5.2	22.3
Pathumthani 1	32.5	Control	61.5	73.6	85.6	7.4	
		150	59.4	75.2	82.6	4.3	41.9
	28.8	Control	71.2	77.2	82.2	6.7	
		150	69.5	76.2	81.8	4.4	26.7

Note: control = Rewetted rice which was gently dried by ambient air ventilation in thin-layer.
[a]Based on dry starch weight.

Figure 6. Effect of inlet air temperature on whiteness of Suphanburi 1 and Pathumthani 1: initial moisture contents were in the range of 25.0–32.5% dry basis and final moisture content of 22.0 ± 1.2% dry basis (after fluidized bed drying). (a) Suphanburi 1, (b) Pathumthani 1. *(View image in color online.)*

rather sensitive to initial moisture content, with the lowest brightness being for the initial moisture content of 32.5% dry basis.

At a higher temperature of 80°C and at lower initial moisture content, changes in whiteness for both rice varieties were less pronounced. For paddy samples that had an initial moisture content of 25.0% dry basis, The value of whiteness varied between 49.8 and 51.3 for Suphanburi 1 and between 44.1 and 46.2 for Pathumthani 1. For paddy

samples with an initial moisture content of 28.8% dry basis, the values of whiteness varied between 50.3 and 52.1 for Suphanburi 1 and between 44.7 and 46.5 for Pathumthani 1 over the drying temperature range of 80 to 150°C. Most of these results indicated that the drying temperature range of 40–150°C along with the low initial moisture contents of rice samples of 25.0 and 28.8% dry basis for both rice varieties did not significantly affect the whiteness of rice ($p < 0.05$). However, a steep decrease in whiteness with increasing air temperature for the samples with a high initial moisture content of 32.5% dry basis for both rice varieties was evident. This can be explained by the effects of the longer drying time and the Maillard nonenzymatic browning reaction.[1,3,7] At this high initial moisture content, drying took longer time than that required by the sample that had lower initial moisture contents of 25.0 and 28.8% dry basis. In addition, the Maillard browning reaction rate was accelerated when the drying temperature increased. In contrast, their mobility and reactivity inside the paddy samples that had low initial moisture content were restricted, even though the temperature was risen. The resulting browning rate was thus retarded. In addition to the limitation of reactive biological components in seeds, the improved whiteness of rice samples was also due to the shorter drying time required for samples with lower initial moisture content. However, for all experiments, the whiteness values were within an acceptable range for the commercial purpose.[13]

(d) Germination of Paddy

Figures 7(a) and 7(b) show respectively the average percentage of germination for paddy with three initial moisture contents of 25.0, 28.8, and 32.5% dry basis for Suphanburi 1 and Pathumthani 1 rice varieties. The germination of both paddy varieties dried with hot air in the temperature range of 40–60°C was in range of 90–98%, with no significant difference between the dried paddy and the control paddy ($p < 0.05$). At the drying air temperature of 70°C the germination of paddy was only found in samples that had initial moisture contents of 25.0 and 28.8% dry basis, however.

When an inlet drying air temperature was higher than 80°C, the degradation of viability was high and the resulting germination of paddy samples of any initial moisture content did not occur. This is due to the fact that the gelatinization of starch granules was partially formed, thereby allowing the rice kernel to lose its biological activity in embryo. However, the germination of both paddy varieties dried using inlet drying

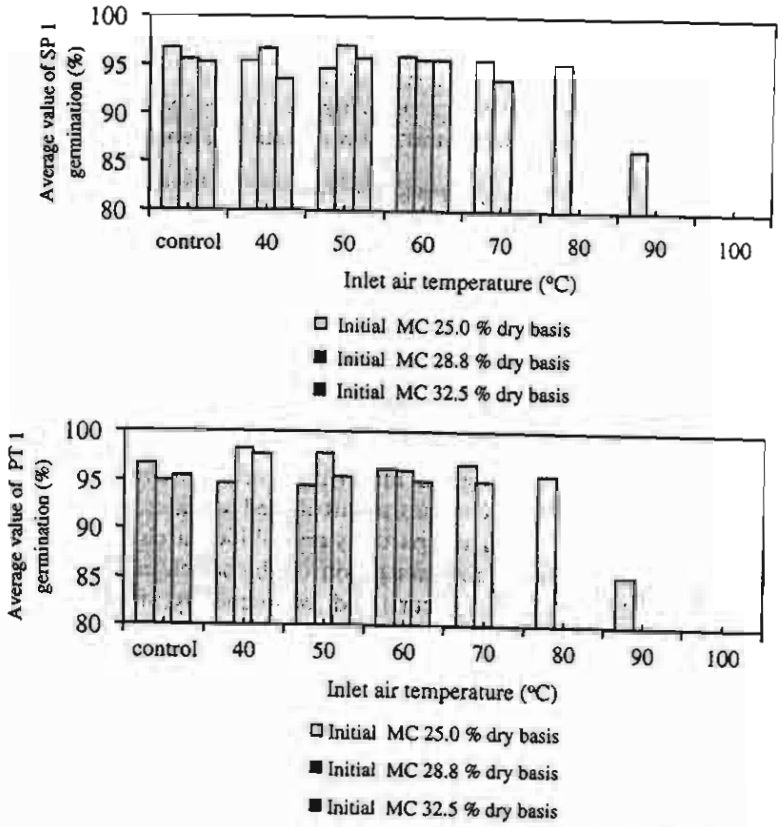

Figure 7. Effect of inlet air temperature on percent germination of Suphanburi 1 and Pathumthani 1: initial moisture contents were in the range of 25.0–32.5% dry basis and final moisture content of 22.0 ± 1.2% dry basis (after fluidized bed drying). (a) Suphanburi 1, (b) Pathumthani 1. *(View image in color online.)*

air temperatures below 60°C, was not significantly changed comparing to its control sample.

(e) Chemical Quality of Rice

Based on the determination of the chemical quality of the two rice varieties, it was found that the inlet drying air temperatures of 40–150°C had no significant effect on both amylose and protein contents of the

samples; the average amylose contents of rice before and after drying were in the range of 25.0 ± 2.8 and 14.5 ± 2.3% (dry weight basis) for Suphanburi 1 and Pathumthani 1, respectively. The average value of protein content was in the range of 7.50 ± 0.05 and 7.99 ± 0.05% (dry weight basis) for Suphanburi 1 and Pathumthani 1, respectively.

(f) Textural Property of Cooked Rice

Figures 8(a) and 8(b) show the hardness of cooked rice samples dried at different temperatures. The hardness of thermally untreated samples was 32.77 kg for Suphanburi 1 variety and 16.39 kg for Pathumthani 1. The difference in hardness is attributed to amylose content presented in paddy. When a certain amount of water was added to the sample and the rewetted sample was then gently dried, the hardness changed in a way that the samples with higher initial moisture contents had higher hardness, except for the range of initial moisture contents between 25 and 28.8% dry basis. These changes are attributed to water, which acts as plasticizer of the amorphous and partially crystalline starch systems. This subsequently facilitates the reorganization of the starch crystallites and amylose-lipid complexes to occur, and consequently, influences the textural properties of paddy.[36,37]

As can be seen in Fig. 8(a), the hardness of cooked Suphanburi 1 rice samples at each initial moisture content was insignificantly different from that of the control sample ($p < 0.05$). At an initial moisture content of 25.0% dry basis, the harness of cooked rice samples was between 34 and 37 kg, indicating the small variation with the drying air temperature while the trend of hardness was different for the samples that had initial moisture contents of 28.8% dry basis and 32.5% dry basis; the hardness values ranged between 31 and 40 kg when using drying air temperatures of 40–150°C.

Similarly, as can be seen in Fig. 8(b), the hardness of cooked Pathumthani 1 sample tended to be related to the initial moisture content whilst there was no significant difference among those samples dried at different drying air temperatures ($p < 0.05$). The hardness values of Pathumthani 1 rice sample at 32.5% dry basis, ranging between 19 and 24 kg, were above those of the samples that had initial moisture contents of 25.0 and 28.8% dry basis, which had the values of hardness vary in the range of 18–21 kg.

The results showed that the hardness of cooked rice increased with an increased initial moisture content. The reasons for these changes might be due to partial gelatinization of rice kernel and interaction between starch, lipid, and protein.[38]

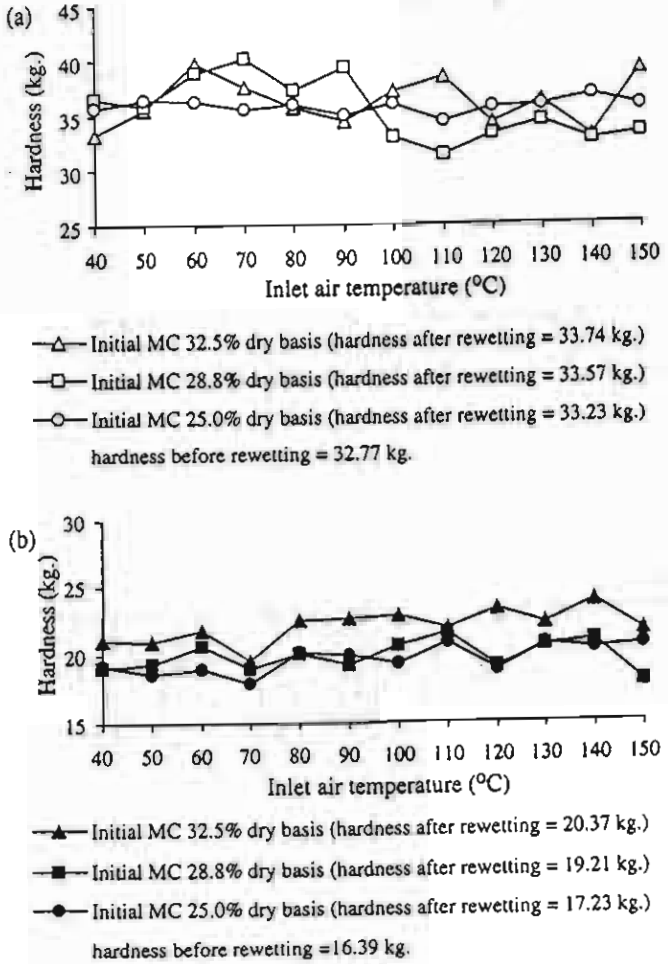

Figure 8. Effect of inlet air temperature on hardness of Suphanburi 1 and Pathumthani 1: initial moisture contents were in the range of 25.0–32.5% dry basis and final moisture content of 22.0 ± 1.2% dry basis (after fluidized bed drying). (a) Suphanburi 1, (b) Pathumthani 1.

(i) Sensory Evaluation

Table 2 shows the hedonic score of an overall acceptability of cooked Suphanburi 1 and Pathumthani 1 rice samples. The results show that for

Table 2. Effect of inlet drying air temperature on overall acceptability of cooked rice of Suphanburi 1 and Pathumthani 1 varieties.

	Overall acceptability of cooked rice					
Inlet air temp. (°C)	Initial MC: Pathumthani 1			Initial MC: Suphanburi 1		
	25.0% (dry basis)	28.8% (dry basis)	32.5% (dry basis)	25.0% (dry basis)	28.8% (dry basis)	32.5% (dry basis)
Control	6.94b	5.98a	4.96b	6.46a	4.53a	4.97a
40	7.54a	6.40a	8.38a	5.54a	4.57a	4.43b
60	7.21b	5.44b	7.92a	5.17b	4.55a	5.05a
80	7.18b	5.27b	7.83a	5.58a	4.46a	4.67a
100	7.37a	6.32a	4.96b	5.38b	4.05b	4.38b
120	7.52a	5.82b	6.63b	4.63b	4.05b	4.67a
140	7.52a	5.77b	4.92b	4.58b	4.51a	4.13b
150	7.37a	5.86a	7.08a	4.67b	4.86a	4.09b

Note: The same letter in the same column indicates no significant difference at $p < 0.05$.

Control = Rewetted rice which was gently dried by ambient air ventilation in thin-layer.

The meaning of hedonic score is as follows:

Hedonic scale from 1–9:

1 = Extremely dislike.
2 = Very much dislike.
3 = Moderately dislike.
4 = Slightly dislike.
5 = Like nor dislike
6 = Slightly like.
7 = Moderately like.
8 = Very much dislike.
9 = Extremely like.

all experiments except Pathumthani 1 with an initial moisture content of 25.0% dry basis, the overall acceptability was in preference scores, from 4.05 to 5.54, representing like nor dislike. The overall acceptability for Pathumthani 1 with an initial moisture content of 25.0% dry basis was in preference scores, from 4.92 to 8.38, which means like nor dislike to very much like. It can be concluded that the inlet drying air temperature and initial moisture content had an insignificantly change the overall acceptability of cooked rice comparing to the rewetted rice (control sample).

CONCLUSIONS

In this study the effect of inlet drying air temperature on various qualities of rice was experimentally investigated. It was found that paddy, either low- and high-amylose content varieties, which had initial moisture contents of 25.0–32.5% dry basis, and was subjected to fluidized bed drying at temperatures between 40–150°C could maintain high head rice yield comparing to the control rice samples.

The head rice yield of Suphanburi 1 samples, which have high amylose content, was significantly related to the inlet drying air temperature and initial moisture content whilst the head rice yield of Pathumthani 1 samples, which have lower amylose content, did not tend to be associated with the inlet drying air temperature as well as the initial moisture content. However, it was found that the whiteness of both rice varieties that had initial moisture contents of 25.0–32.5% dry basis slightly decreased with an increase in inlet drying air temperature; the effect was more pronounced at inlet drying air temperatures of over 80°C and the initial moisture content of 32.5% dry basis.

The germination of both paddy varieties dried at inlet drying air temperatures below 60°C was not significantly changed comparing to their control samples. When inlet drying air temperatures were higher than 80°C, however, germination of paddy samples of any initial moisture contents did not occur due to partial gelatinization of starch granules. This partial gelatinization at inlet drying air temperatures of over 90°C caused some effects on the morphology, endothermic energy of rice flour, hardness, and head rice yield of rice samples. Moreover, the overall acceptability of both cooked rice samples after drying had an insignificant correlation with inlet drying air temperature, initial moisture content, and rice variety comparing to those of control samples.

ACKNOWLDGMENTS

The authors wish to express their sincere thanks to the Thailand Research Fund (TRF) and the Japan International Research Center for Agricultural Sciences (JIRCAS) for their financial support and to the Institute of Food Research and Product Development (IFRPD) of Kasetsart University, Thailand for testing rice qualities and to the Institute of Technology Rajchamongkrala, Headquarter, Pathumthani, Thailand for rice whiteness testing.

REFERENCES

1. Gras, P.W.; Banks, H.J.; Bason, M.L.; Arriola, L.P. A qualitative study of the influences of temperature, water activity and storage atmosphere on the yellowing of milled rice. J. Cereal Science **1989**, *9*, 77–89.
2. Bason, M.L.; Gras, P.W.; Banks, H.J.; Esteves, L.A. A qualitative study of the influences of temperature, water activity and storage atmosphere on the yellowing of paddy endosperm. J. Cereal Science **1990**, *12*, 193–201.
3. Soponronnarit, S.; Srisubati, N.; Yoovidhya, T. Effect of temperature and relative humidity on yellowing rate of paddy. J. Stored Prod. Res. **1998**, *34* (4), 323–330.
4. Yap, A.B.; Juiliano, B.O.; Perez, C.M. Artificial yellowing of rice at 60°C. Proceedings Group, The Source of Yellow Grains in Rice, Myc. Centralbl **1988**, *3*, 153–157.
5. Driscoll, R.H.; Adamczak, T. Drying systems for the humid tropics. In bulk handling and storage of grain in the humid tropics. ACIAR Proceedings **1988**, *22*, 58–68.
6. Poomsa-ad, N.; Soponronnarit, S.; Terdyothin, A.; Prachayawarakorn, S. *Head Rice Yield after Drying by Fluidization Technique and Tempering*, Proceedings of the 2nd Asian-Oceania Drying Conference, Batu-Feringhai, Penang, Malaysia, Aug 20–22, 2001.
7. Inprasit, C.; Noomhorm, N. Effect of drying air temperature and grain temperature of different types of dryer and operation on rice quality. Drying Technology **2001**, *19* (2), 389–404.
8. Bonazzi, C.; du Peuty, M.A.; Themelin, A. Influence of drying conditions on the processing quality of rough rice. Drying Technology **1997**, *15* (3&4), 1141–1157.
9. Daniel, M.J.; Marks, B.P.; Siebenmorgen, T.J.; Mcnew, R.W.; Meullenet, J.F. Effects of long-grain rough rice storage history on end-use quality. J. Food Sci. **1998**, *63* (5), 832–835.
10. Soponronnarit, S.; Prachayawarakorn, S. Optimum strategy for fluidized bed paddy drying. Drying Technology **1994**, *12* (7), 1667–1686.
11. Steffe, J.F.; Singh, R.P.; Bakshi, A.S. Influence of tempering time and cooling on rice milling yields and moisture removal. Trans. of the ASAE **1979**, *22*, 1214–1218, 1224.
12. Zhang, Q.; Litchfield, J.B. An optimization of intermittent corn drying in a laboratory scale thin layer dryer. Drying Technology **1991**, *9* (1), 233–244.

13. Soponronnarit, S.; Wetchama, S.; Swasdisevi, T.; Poomsa-ad, N. Managing moist paddy by drying, tempering and ambient air ventilation. Drying Technology **1999**, *17* (1&2), 335–344.
14. Cnossen, A.G.; Jimenez, M.J.; Siebenmorgen, T.J. Rice fissuring response to high drying and tempering temperatures. J. Food Eng. **2003**, *59*, 61–69.
15. Poomsa-ad, N.; Soponronnarit, S.; Prachayawarakorn, S.; Terdyotin, A. Effect of tempering on subsequent drying of paddy using fluidisation technique. Drying Technology **2002**, *20* (1), 195–210.
16. Soponronnarit, S. *Drying in Bulk Storage of High Moisture Grains in the Kingdom of Thailand*, Final report submitted to Australian Centre for International Agricultural Research, Canberra, 1987.
17. AOAC. *Official Methods of Analysis, Association of Official Analytical Chemists*, 15th Ed; Washington, D.C., USA, 1995.
18. USDA. *Grain Grade Procedure*; Federal Grain Inspection Service: Washington, DC, USA, 1988.
19. Marshall, W.E.; Wadsworth, J.I.; Verma, L.R.; Velupillai, L. Determination the degree of gelatinization in parboiled rice: comparison of a subjective and an objective methods. Cereal Chem. **1993**, *70*, 226–230.
20. Juliano, B.O. A simplified assay for mill-rice amylose. Cereal Sci. Today **1971**, *16*, 334–338.
21. Kongseree, N. *Training Course in Standardization and Quality of HoomDokMali Rice*; Rice Research Station: Pathumthani, Thailand, 22–24 Dec. 1995.
22. Tungtrakul, P. *Quality and Physicochemical Properties of Rice Related to Rice Noodle*, United Nations University Research Fellowship Report; Tsukuba, Japan, 1997.
23. Cnossen, A.G.; Siebenmorgen, T.J. The glass transition temperature concept in rice drying and tempering: effect on milling quality. Trans. of the ASAE **2000**, *23* (6), 1661–1667.
24. Perdon, A.A. Amorphous State Transition in Rice during the Drying Process, Ph.D. diss., Fayetteville, Ark, Department of Food Science, University of Arkansas, USA, 1999.
25. Siebenmorgen, T.J.; Perdon, A.A. *Applying Glass Transition Principle to Explain Fissure Formation during Drying Process*, Presented in the 1999 Int. Starch Tech. Conf., Urbana, June 7–9, 1999; Volume III.
26. Slade, L.; Levine, H. A polymer science approach to structure/property relationships in aqueous food systems: non-equilibrium

behavior of carbohydrate-water systems. In *Water Relationships in Foods*; Levine, H., Slade, L., Eds.; Plenum Press: New York, USA, 1991; 29–101.
27. Slade, L.; Levine, H. Glass transitions and water-food structure interactions. Adv. Food Nutrit. Res. **1995**, *38*, 103–269.
28. Kunze, O.R. Fissuring of the rice grain after heated air drying. Trans. of the ASAE **1979**, *22* (5), 1197–1202, 1207.
29. Aquerre, R.; Suarez, C.; Viollaz, P.E. Effect of drying on the quality of milled rice. J. of Food Tech. **1986**, *21*, 75–80.
30. Eliasson, A.C. Interactions between starch and lipids studied by DSC. Thermochimica Acta **1994**, *246*, 343–356.
31. Moritaka, S.; Yasumatsu, K. Studies on cereals X. The effect of sulfhydryl groups on storage deterioration of milled rice. Eiyo To Shokuryo **1972**, *25*, 59–62.
32. Teo, C.H.; Abd. Karim, A.; Cheah, P.B.; Norziah, M.H.; Seow, C.C. On the roles of protein and starch in the aging of non-waxy rice flour. Food Chem. **2000**, *69*, 229–236.
33. Swinkels, J.J.M. Starch, source, chemistry and physics. In *Starch Conversion Technology*; van Beynum, G.M.A., Roels, J.A., Eds.; Marcel Dekker, Inc.: New York, USA, 1985; 31–35.
34. Sander, J.P.M. Starch manufacturing in the world. In *Advanced Post Academic Course on Tapioca Starch Technology*; AIT Center: Bangkok, Thailand; 22–26 Jan & 19–23 Feb 1996.
35. Miah, K.M.A.; Haque, A.; Douglass, M.P.; Clarke, B. Parboiling of rice part I: effect of hot soaking time on quality of milled rice. Int. J. of Food Sci. and Tech. **2002**, *37*, 527–537.
36. Juliano, B.O. *Rice: Chemistry and Technology*, 2nd Ed.; American Association of Cereal Chemists, Inc., St. Paul: Minnesota, USA, 1985; 774.
37. Beynum, G.M.A.; Roels, J.A. *Starch Conversion Technology*; Marcel Dekker, Inc.: USA, 1985; 40–41.
38. Parnsakhorn, S. *The Effect of Steaming Treatment on Accelerated Aging of Rough Rice*. M.E. thesis, School of Environment, Resource and Development, Asian Institute of Technology, Bangkok, Thailand, 2001.

DRYING TECHNOLOGY
Vol. 22, No. 8, pp. 1845–1867, 2004

A Comparative Study of Low-Pressure Superheated Steam and Vacuum Drying of a Heat-Sensitive Material

S. Devahastin,[1,*] P. Suvarnakuta,[1] S. Soponronnarit,[2] and A. S. Mujumdar[3]

[1]Department of Food Engineering and
[2]School of Energy and Materials, King Mongkut's,
University of Technology Thonburi, Bangkok, Thailand
[3]Department of Mechanical Engineering,
National University of Singapore, Singapore

ABSTRACT

Using carrot cubes as a model heat-sensitive material, experimental investigations were conducted to examine the drying kinetics and various quality parameters of the dried product undergoing both low-pressure superheated steam and vacuum drying. Effects of operating parameters such as pressure and temperature on the drying characteristics as well as quality attributes, i.e., volume, shrinkage,

*Correspondence: S. Devahastin, Department of Food Engineering, King Mongkut's University of Technology Thonburi, 91 Pracha u-tid Road, Bangkok 10140, Thailand; Fax: 662 470 9240; E-mail: sakamon.dev@kmutt.ac.th.

DOI: 10.1081/LDRT-200032818

0737-3937 (Print); 1532-2300 (Online)
www.dekker.com

apparent density, color, and rehydration behavior, of the dried product underwent the two drying processes were also evaluated and compared. Although low-pressure steam drying required longer dwell time to achieve the same final moisture content than vacuum drying, some of the quality attributes were superior to those obtained in vacuum drying.

Key Words: Apparent density; Carrot; Color; Rehydration behavior; Shrinkage; Volume.

INTRODUCTION

During the past decade the idea of using superheated steam to dry food has been derived from other drying applications, e.g., paper drying,[1–3] coal drying,[4] wood particles drying,[5] sludge,[6] and beat pulp drying.[7,8] The notable advantages of superheated steam drying (SSD) that are of interest to food industry include the absence of oxidative reactions (e.g., enzymatic browning, lipid oxidation) due to lack of oxygen, high drying rates in both constant and falling rate periods, depending on steam temperature and pressure, and its ability to yield a higher porosity dried product due to an evolution of steam within the product. Moreover, SSD strips more of the acids that contribute to an undesirable taste or aroma of the products.[9]

Despite the many advantages of SSD as mentioned earlier, several limitations, especially when applying it to drying heat-sensitive materials like foods and bioproducts, are still present. Since most foods or other heat-sensitive products melt, undergo glass transition or are damaged at the saturation temperature of superheated steam corresponding to the atmospheric or higher pressures, one possible way to prevent the products from being damaged in a high-temperature environment of SSD is to operate a dryer at reduced pressure.[9–11] Lowering the dryer operating pressure is a feasible option that not only preserves the quality of the dried product, but may also enhance the drying rate as well.[9,12–15] However, very little is reported on low-pressure (or sub-atmospheric) superheated steam drying of foodstuffs both from drying kinetics and dried product quality points of view.

Chen *et al.*[16] performed a laboratory-scale testing of a sub-atmospheric pressure superheated steam drying of silk cocoons (at temperature around 45°C) and found that this drying technique helped improving the quality of silk produced in terms of the brightness and strength of fiber. The increased cost of steam drying was therefore

justified by the additional credit received for the enhanced quality of the silk.

Pang and Dakin[17] studied the drying rates and temperature profiles of stacks of softwood lumber undergoing vacuum SSD in a Moldrup kiln. The superheated steam temperature used was 90°C and had a circulating velocity of 10 m/s. Vacuum SSD was found to yield lower drying rates of whole lumber stack than those obtained using hot moist air. This is due to the fact that the wood temperatures in a vacuum SSD were lower than those used in hot air drying. However, the defects of the dried product such as kiln brown stain and drying stresses were lower. To reduce the drying time in a vacuum SSD, it was recommended that a higher steam circulating velocity (more than 10 m/s) be used.

Elustondo et al.[11] studied sub-atmospheric pressure superheated steam drying of foodstuffs both experimentally and theoretically. Wood slab, shrimp, banana, apple, potato and cassava slices were dried using the steam pressures of 10,000–20,000 Pa, the steam temperatures of 60–90°C and the steam circulating velocities of 2–6 m/s. A semi-empirical mathematical model was also developed based on a theoretical drying mechanism, which assumed that the water removal was carried out by evaporation in a moving boundary allowing the vapor to flow through the dry layer built as drying proceeded to predict the drying characteristics of foodstuffs undergoing this drying operation. A simplified expression, which has two experimentally determined parameters, was derived and used to predict the drying rate of the tested samples. A model proposed was found to predict the drying kinetics reasonably well. No mention about the dried product quality is given, however.

The present work was therefore aimed at the design, fabrication and testing of a cabinet-type low-pressure superheated steam dryer and to investigate the influence of various operating parameters on the drying and heat transfer characteristics as well as various quality attributes of a heat-sensitive food product (carrot) undergoing this drying operation. Comparison was also made with the similar sets of information obtained from vacuum drying experiments conducted in the same drying chamber.

EXPERIMENTAL SET-UP, MATERIALS AND METHODS

Experimental Set-up

A schematic diagram of the low-pressure superheated steam dryer and its accessories is shown in Fig. 1. The dryer consists of a stainless

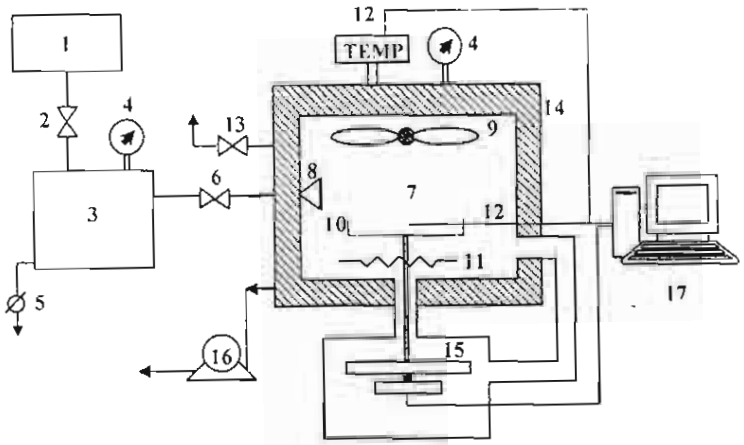

Figure 1. A schematic diagram of the overall experimental set-up. 1, boiler; 2, steam valve; 3, steam reservoir; 4, pressure gauge; 5, steam trap; 6, steam regulator; 7, drying chamber; 8, steam inlet and distributor; 9, electric fan; 10, sample holder; 11, electric heater; 12, on-line temperature sensor and logger; 13, vacuum break-up valve; 14, insulator; 15, on-line weight indicator and logger; 16, vacuum pump; 17, PC with installed data acquisition card.

steel drying chamber, insulated carefully with rock wool, with an inner dimension of $45 \times 45 \times 45\,cm^3$; a steam reservoir, which received the steam from the boiler and maintained its pressure at around 200 kPa (gage); and a liquid ring vacuum pump (Nash, model ET32030, Germany), which was used to maintain the vacuum in the drying chamber. Steam trap was installed to reduce the excess steam condensation in the reservoir. An electric heater, rated at 1.5 kW, which was controlled by a PID controller (Omron, model E5CN, Japan) was installed in the drying chamber to control the steam temperature and to minimize the condensation of steam in the drying chamber during the start-up period; with the use of a heater the initial steam condensation during the start-up period was reduced considerably. A variable-speed electric fan was used to disperse steam throughout the drying chamber. The steam inlet was made into a cone shape and was covered with a screen to also help distribution of the steam in the chamber. The sample holder was made of a stainless steel screen with a dimensions of $12 \times 12\,cm^2$. The change of the weight of the sample was detected

continuously (at 30 s intervals) using a load cell (Minebea, model Ucg-3 kg, Japan), which was installed in a smaller chamber connected to the drying chamber by a flexible hose (in order to maintain the same vacuum pressure as that in the drying chamber), and also to an indicator and recorder (AND A&D Co., model AD 4329, Japan). The temperatures of the steam and of the drying sample were also measured continuously using type K thermocouples, which were connected to an expansion board (Omega Engineering, model no. EXP-32, USA). Thermocouple signals were then multiplexed to a data acquisition card (Omega Engineering, model no. CIO-DAS16Jr., USA) installed in a PC. LABTECH NOTEBOOK software (version 12.1, Laboratory Technologies Corp., USA) was then used to read and record the temperature data.

Materials and Methods

Fresh carrot was obtained from a local supermarket and stored at 4°C. Prior to the start of each experiment carrot was peeled and diced into $1\,cm^3$ cubes. To perform a drying experiment approximately 35 cubes of carrot (about 40 g) were placed on the sample holder. The drying chamber was then sealed tightly. Valve 2 was opened to allow the steam from the boiler to flow into the reservoir; the steam pressure was maintained at about 200 kPa (gage) in the reservoir. A vacuum pump was then switched on to evacuate the drying chamber to the desired operating pressure and the steam regulator was opened to slowly flash the steam into the drying chamber. Due to the low-pressure environment of the chamber the steam became superheated. An electric heater was used to maintain the steam temperature at a desired drying temperature. At the end of the drying process the break-up valve was opened to allow the air into the drying chamber (to regain an atmospheric condition) before opening up the chamber door and loading off the dried product.

For vacuum drying experiments the same experimental set-up was used but without the application of steam to the drying chamber. The same operating conditions were therefore achievable. The experiments were performed at the following conditions: steam absolute pressures of 7, 10, and 13 kPa; steam temperatures of 60, 70, and 80°C. The flow rate of steam into the drying chamber (in the case of SSD) was maintained at about 26 kg/h and the speed of the fan was fixed at 2100 rpm.

Volume and Apparent Density Measurements

The measurement of the sample volume (V) was performed using a liquid pycnometer with n-heptane as the working liquid. The apparent density (ρ_{app}) of the sample was also readily obtained using this technique. The volume and apparent density of the sample were calculated according to the following equations:

$$V = \frac{[m_{Ph} - m_P] - [m_{Phs} - m_P - m_s]}{\rho_h} \quad (1)$$

$$\rho_{app} = \frac{\text{weight of sample in air}}{V} \quad (2)$$

where m_{Ph}, m_P, m_{Phs}, and m_s are respectively masses of a pycnometer filled with n-heptane, empty pycnometer, pycnometer with sample and n-heptane, and mass of the sample. ρ_h is the density of n-heptane. The average values of five samples were reported. All measurements were performed in duplicate.

Shrinkage Measurement

Five samples were used for a shrinkage measurement of each experimental condition. Shrinkage was expressed in terms of the percentage change of the volume of the original sample volume.

$$\%\text{shrinkage} = \frac{V_i - V}{V_i} \times 100 \quad (3)$$

where V_i and V are respectively the volumes of carrot at the beginning and at the end of each drying experiment. The average values of five samples were reported. All measurements were performed in duplicate.

Rehydration Ability

The rehydration ratio (R) of the dried sample was determined by immersing dried carrot sample in hot water at 100°C for 10 min. The sample was then drained and its volumes, both before and after immersion, were measured by a pycnometer. The rehydration ratio of the dried carrot was calculated by:

$$R = \frac{V_{after}}{V} \quad (4)$$

where V_{after} and V are respectively the volumes of dried carrot after and before immersion in hot water, respectively. The average valves of five samples were reported and all measurements were performed in duplicate.

Color Measurement

Colors of the samples were measured in a Hunter Lab color system using a colorimeter (Juki, model JP 7100, Japan). For each drying experiment the color measurement was performed on five dried samples and the color values were compared with those of fresh samples. All experiments were performed in duplicate and the average values were then reported. The color changes (L and a values only) were calculated by:

$$\Delta L = \frac{L - L_i}{L_i} \quad \text{and} \quad \Delta a = \frac{a - a_i}{a_i} \quad (5)$$

where L and a represent the lightness and redness of the dried sample, respectively. L_i and a_i are respectively the lightness and redness of the fresh carrot sample.

All experimental data were analyzed using an analysis of variance (ANOVA). Tukey's test was employed to establish the multiple comparisons of mean values. Mean values were considered significantly different when $p < 0.05$. From reproducibility tests the reproducibility values of the volume, density, percentage of shrinkage, rehydration ratio, Δa, and ΔL were within ± 1.8, 2.5, 4.2, 12.8, 6.1, and 5.5%, respectively.

RESULTS AND DISCUSSION

Drying and Heat Transfer Characteristics of Carrot

After the low-pressure superheated steam dryer was fabricated it was tested to ensure that the distribution of the steam temperature within the drying chamber was uniform. It was found from this study that the maximum difference of the steam temperature within the drying chamber was within ± 3 C. The dryer was then used to conduct both low-pressure

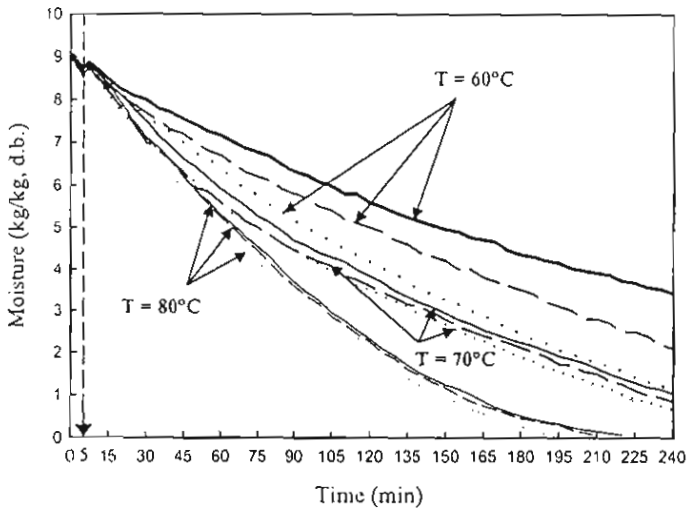

Figure 2. Drying curves of carrot undergoing LPSSD during the first 4 h of experiments (Legends used are the same as in Fig. 3).

superheated steam drying (LPSSD) and conventional vacuum drying experiments.

Carrot that had an initial moisture content of about 9 kg/kg (d.b.) (or about 90% w.b.) was dried to a final moisture content of about 0.07 kg/kg (d.b.) (or about 6.5% w.b.) in the dryer using both low-pressure superheated steam and conventional vacuum drying. The drying curves of carrot undergoing LPSSD are shown in Fig. 2; a slight decrease in the moisture content during the first 5 min of the process was due to the initialization of the chamber pressure and of the load cell. Drying indeed started at about 5 min after the weight was initially recorded. It can be seen in this figure that all samples gained a small amount of moisture during the first few minutes of drying (after the above-mentioned 5 min) for all drying conditions due to steam condensation. This phenomenon is indeed typical of superheated steam drying[8,9] although, in this study, the drying chamber was preheated at 50°C during the first 5 min of the process. Nevertheless, the condensation of steam was rather negligible if the operating pressure was low; for example, the samples gained moisture of about 1.4, 1.3, and 1% when drying at 60, 70, and 80°C at 7 kPa, respectively. Accordingly, the restoration time, which

Table 1. Average drying times of LPSSD and vacuum drying of carrot at various operating conditions.

	Temperature (°C)		
Pressure (kPa)	60	70	80
Drying time of LPSSD (min)			
7	389	280	198
10	N/A	290	210
13	N/A	317	230
Drying time of vacuum drying (min)			
7	235	205	159
10	241	223	175
13	255	265	206

N/A implies that, at this condition, the final carrot moisture content of 0.07 kg/kg (d.b.) was not achievable.

is the time by which the original mass has returned to its original value[18] was 5, 4 and 4 min for drying at 60, 70, and 80°C at 7 kPa, respectively.

Table 1 lists the drying times of all LPSSD and vacuum drying experiments. It can be seen from this table and also from Fig. 2 that the effect of temperature on the drying rates was greater than the effect of pressure in the case of LPSSD, especially at higher drying temperatures. The effect of operating pressure was less clear even at lower temperature (60°C) for the case of vacuum drying, as can be seen in Fig. 3, however. This may probably due to the fact that the steam thermal properties were affected by temperature to a larger extent than those of air, especially at lower drying temperatures. No initial condensation was also observed, as expected, in the case of vacuum drying. It can also be seen that the moisture decreased faster at a higher temperature than at a lower temperature because the temperature difference between the sample and the medium at a higher drying temperature was greater than that at a lower temperature. For example, an increase of the drying temperature from 60 to 80°C led to a reduction in the drying time of about 49 and 32% in the case of LPSSD and vacuum drying at an operating pressure of 7 kPa, respectively. In addition, it was observed that the moisture content decreased faster, especially in the case of LPSSD at lower drying temperatures, at lower pressures since water in carrot boiled and evaporated at lower temperatures; a decrease of the pressure from 13 to 7 kPa, for example, led to a reduction of the drying time by 14 and

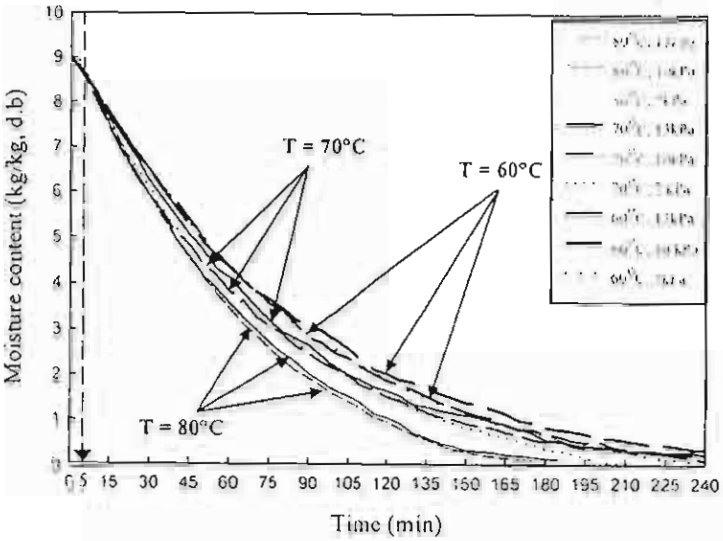

Figure 3. Drying curves of carrot undergoing vacuum drying during the first 4 h of experiments.

23% in the case of LPSSD and vacuum drying at a temperature of 80°C, respectively. Performing LPSSD experiments at higher pressures and lower temperatures also led to another problem, i.e., it was not able to dry carrot to the required moisture content of 0.07 kg/kg (d.b.) because there was an excessive amount of steam condensation in the drying chamber.

It was found that the drying times of vacuum drying were shorter than those of LPSSD (at the same pressure) for all conditions tested. This is probably due to the fact that the electric heater was used more often during vacuum drying since it was the only source of energy for drying. This might increase the amount of radiation absorbed by the carrot surfaces, thus explaining the higher drying rate during vacuum drying. The initial steam condensation on the product surface might also contribute to the longer drying times for the case of LPSSD. The differences between the two sets of drying times, however, were smaller at higher drying temperatures. Raising the drying temperature further would eventually lead to equal rates of drying at an inversion temperature (due to increased temperature difference between the

steam and the product as well as a reduction of the initial steam condensation). This could not be done in this case, however, as it would adversely affect the quality of the dried carrot.

Figure 4 illustrates changes of moisture content and temperature of carrot undergoing LPSSD at some selected conditions. It can be seen in this figure that the shapes of the drying and temperature curves were affected by both the drying temperature and pressure. At lower drying temperatures (say, at 60 and 70°C) the temperature of carrot changed suddenly from its initial value (after initial adjustment) and remained rather constant at the boiling temperature of water corresponding to the operating pressure until the first falling rate period drying ended (drying rate data are not shown here for the sake of brevity). Beyond this point, the carrot temperature rose again and finally approached the temperature of the drying medium. As the medium temperature increased (at the same operating pressure) it can be seen (for example, from Fig. 4c) that the period of constant product temperature was shorter; the product temperature rose almost steadily from its initial value to the medium temperature. At the same drying temperature, however, increasing of the operating pressure led to a lower rate of drying but a longer period of constant product temperature (as can be seen from Figs. 4c and d). It may depend both on the characteristics of the drying product and on these effects to determine the optimum operating conditions of an LPSSD.

Figure 5 shows the evolutions of moisture content and temperature of carrot undergoing vacuum drying at the same operating conditions as those used for LPSSD shown in Fig. 4. It can be seen from this figure that the drying and heat transfer behavior of carrot undergoing vacuum drying was quite different from that of LPSSD; the product temperature, in this case, rose almost steadily from its initial value to the medium temperature. However, the rates of moisture reduction in the case of vacuum drying were higher than those belonged to LPSSD, especially at lower drying temperatures as mentioned earlier.

Attempts were also made to compare the present data with a similar set of data available in the literature, i.e., the processes of freeze drying, air drying and microwave vacuum drying of carrot, in terms of the average drying rates over the whole period of drying.[19] It was found that the lowest drying rates obtained in the present study (which corresponded to using LPSSD at 60°C and 7 kPa) of 1.38 kg water kg^{-1} dry matter h^{-1} was, as expected, lower than that achievable by microwave vacuum drying (19.1 kg water kg^{-1} dry matter h^{-1}) but was still higher than those obtained by air drying and freeze drying of blanched carrot slices (1.31 and 0.013 kg water kg^{-1} dry matter h^{-1}, respectively). It should be

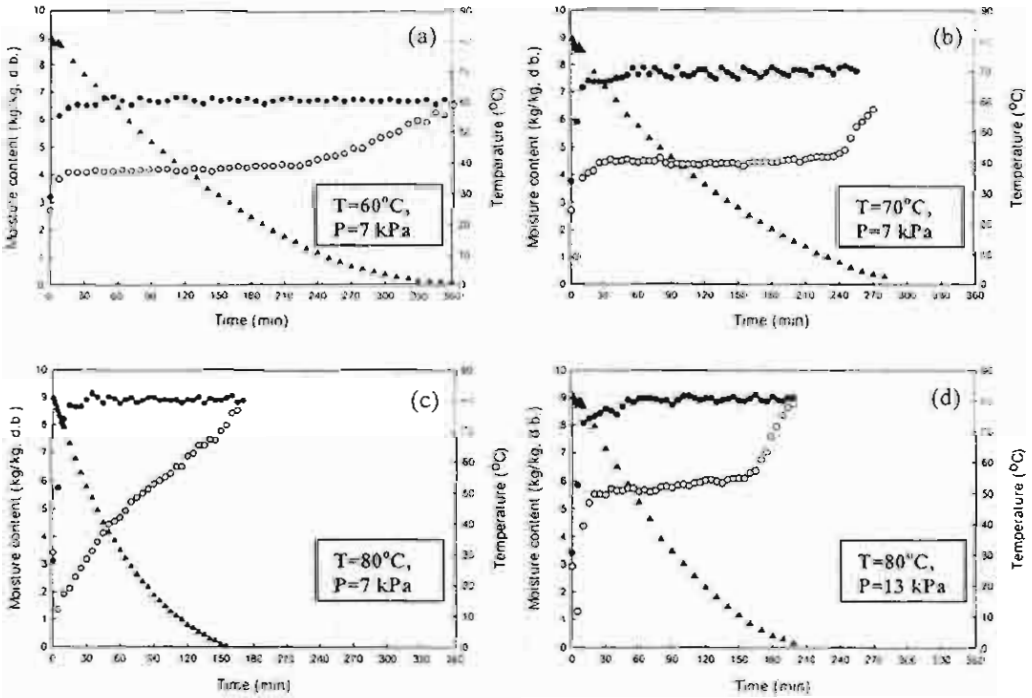

Figure 4. Changes in moisture content and temperature of carrot undergoing LPSSD at different operating conditions. ▲ moisture content; ● steam temperature; O sample temperature.

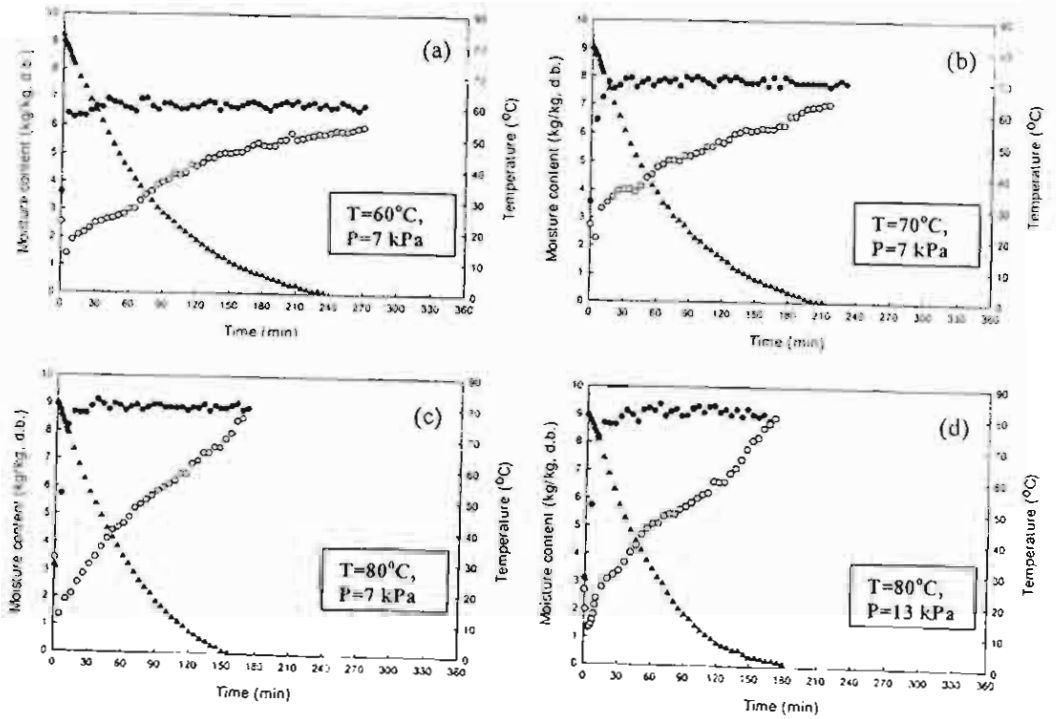

Figure 5. Changes in moisture content and temperature of carrot undergoing vacuum drying at different operating conditions. ▲ moisture content; ● steam temperature; O sample temperature.

noted that it is easier to dry blanched carrot than fresh carrot used in the present study. The carrot slices used by Lin et al.[19] also had less thickness (4 mm) than that used in our study as well.

. Volume, Apparent Density, Shrinkage, and Rehydration Behavior of Carrot

Table 2 illustrates the effects of the drying temperature and pressure of both LPSSD and vacuum drying on various physical properties of carrot, i.e., volume, density, shrinkage, and rehydration behavior. It was found that the volume of dried carrot was inversely proportional to its apparent density; carrot that had lower apparent density has larger volume, as expected. It can be seen also that the volume and apparent density of dried carrot undergoing both drying techniques slightly decreased and increased, respectively, as the operating pressure increased. This is due to the fact that pressure affects the percentage of air pores developed in the final dried products[20]; both properties changed only slightly in this case, however, because of the narrow range of operating pressures tested. Different drying techniques as well as the drying temperature also did not have much effect on the volume and density of the final dried products in this case. This is in accordance with the results reported by Krokida et al.[21] who compared the apparent density of dried carrot and other dried food products undergoing convective hot-air, microwave, freeze, and osmotic drying; it was found in their work that the operating pressure significantly affected the apparent density of the dried products than did the other operating parameters. Lowering the pressure during subatmospheric drying (both LPSSD and vacuum drying) also helped preventing the structural collapse of foods, especially in the case of carrot.

Table 2 also shows the results of shrinkage of carrot undergoing different drying techniques and operating conditions. Like the apparent density, shrinkage values correlated directly with the volume of dried carrot. It can be seen from Table 2 that the percentage of shrinkage of LPSSD and vacuum dried carrot was similar although superheated steam drying is known to have a potential to reduce the degree of shrinkage of the drying product due to an evolution of vapor inside the product that expands into cells, leading to a normally porous dried product.[15,22,23] This improvement in terms of shrinkage may only be seen clearly when comparing the dried product obtained with that dried by a conventional atmospheric hot air drying.

Table 2. Physical properties of carrot undergoing LPSSD and vacuum drying at different drying conditions.

Drying process	Temperature (°C)	Pressure (kPa)	Volume (cm^3)	Density (g/cm^3)	Shrinkage (%)	Rehydration ratio
LPSSD	$T = 60$ °C	7	0.092 ± 0.002^{d}	1.43 ± 0.03^{a}	90.80 ± 0.09^{ab}	5.19 ± 0.08^{f}
		10	N/A	N/A	N/A	N/A
		13	N/A	N/A	N/A	N/A
	$T = 70$ °C	7	0.092 ± 0.008^{d}	1.42 ± 0.02^{a}	90.77 ± 0.09^{a}	5.21 ± 0.09^{fg}
		10	0.087 ± 0.01^{a}	1.50 ± 0.04^{d}	91.21 ± 0.07^{de}	5.10 ± 0.14^{de}
		13	0.086 ± 0.004^{a}	1.51 ± 0.06^{de}	91.23 ± 0.10^{eh}	4.94 ± 0.04^{d}
	$T = 80$ °C	7	0.093 ± 0.009^{c}	1.43 ± 0.11^{ab}	90.8 ± 0.09^{ab}	5.23 ± 0.15^{h}
		10	0.09 ± 0.006^{b}	1.44 ± 0.01^{b}	90.82 ± 0.06^{b}	5.19 ± 0.05^{f}
		13	0.088 ± 0.008^{ab}	1.45 ± 0.08^{c}	91.09 ± 0.02^{f}	5.15 ± 0.07^{e}
Vacuum drying	$T = 60$ °C	7	0.092 ± 0.009^{c}	1.42 ± 0.1^{ab}	90.85 ± 0.11^{cd}	4.39 ± 0.18^{b}
		10	0.09 ± 0.012^{b}	1.43 ± 0.04^{ab}	90.97 ± 0.14^{d}	4.17 ± 0.16^{a}
		13	0.09 ± 0.007^{b}	1.43 ± 0.03^{ab}	90.99 ± 0.08^{d}	4.10 ± 0.04^{a}
	$T = 70$ °C	7	0.092 ± 0.003^{c}	1.43 ± 0.07^{ab}	90.82 ± 0.04^{b}	4.51 ± 0.03^{bc}
		10	0.091 ± 0.004^{bc}	1.40 ± 0.09^{a}	91.08 ± 0.04^{cf}	4.47 ± 0.09^{c}
		13	0.091 ± 0.01^{bc}	1.43 ± 0.02^{ab}	90.93 ± 0.05^{d}	4.13 ± 0.07^{b}
	$T = 80$ °C	7	0.092 ± 0.002^{c}	1.42 ± 0.04^{ab}	90.79 ± 0.04^{a}	4.82 ± 0.04^{de}
		10	0.092 ± 0.009^{c}	1.42 ± 0.12^{ab}	90.82 ± 0.11^{b}	4.56 ± 0.15^{c}
		13	0.09 ± 0.009^{b}	1.42 ± 0.07^{ab}	90.95 ± 0.09^{d}	4.51 ± 0.13^{c}

[a,b,c,d,e,f,g]In the same column with different superscripts means that the values are significantly different ($p < 0.05$).
N/A implies that, at this condition, the final carrot moisture content of 0.07 kg/kg (d.b.) was not achievable.

As mentioned earlier, carrot that was dried at various temperatures but at the same pressure in LPSSD and vacuum dryer had similar values of the final volume and apparent density and similar degrees of shrinkage. Although it is known that the temperature directly affects the shrinkage property of the dried product because high temperature drying results in a higher moisture gradient within the material and so higher internal stresses, which leads to a larger degree of shrinkage, the effect of temperature on shrinkage was not indeed much significant in this case, both for the cases of LPSSD and vacuum drying. This is probably due to the fact that the differences in drying temperature used might not be large enough to cause significant differences in shrinkage. This is in accordance with the results of Ratti[24] who also found that the shrinkage characteristics were independent of drying conditions over a limited range of drying temperature.

It should be noted, however, that although the values of shrinkage of carrot that underwent LPSSD and vacuum drying were similar, the shrinkage patterns resulted from the two different drying processes were quite different. Carrot that underwent vacuum drying tended to shrink nonuniformly. This characteristic is indeed rather typical of most food products.[25] In a more rapid drying (as in the case of vacuum drying when compared with LPSSD) the surface of the drying product became dry and rigid long before the center had dried out; the center dried and shrank much later than the outer surface did and pulled away from the rigid surface layers and caused a nonuniform shrinkage. Drying carrot in LPSSD, however, led to a more uniform shrinkage; in this case shrinkage seemed to occur because the carrot structure could not support its own weight and hence collapsed under gravitational force in the absence of moisture.[26] This is because LPSSD offered a milder drying condition (since the drying chamber was moister than in the case of vacuum drying). Dense or rigid large formation might not as much be formed in the case of LPSSD as in the case of vacuum drying. The photographs of carrot cubes both after drying and after rehydration are shown in Fig. 6

Regarding the rehydration ability of carrot undergoing both drying processes it can be seen in Table 2 that carrot that underwent LPSSD had much better rehydration capability than that vacuum dried. This is also due to the formation of dense layers in the case of vacuum drying, which led to nonuniform shrinkage mentioned earlier; the rather dense and rigid layers prevented the re-adsorption of water and hence led to lower degrees of rehydration. This can also be seen from SEM photographs of Figs. 7a and b, which show the microstructure of LPSSD and vacuum dried carrot, respectively. It is seen from these figures that carrot that underwent vacuum drying developed a rather dense layer and its pore

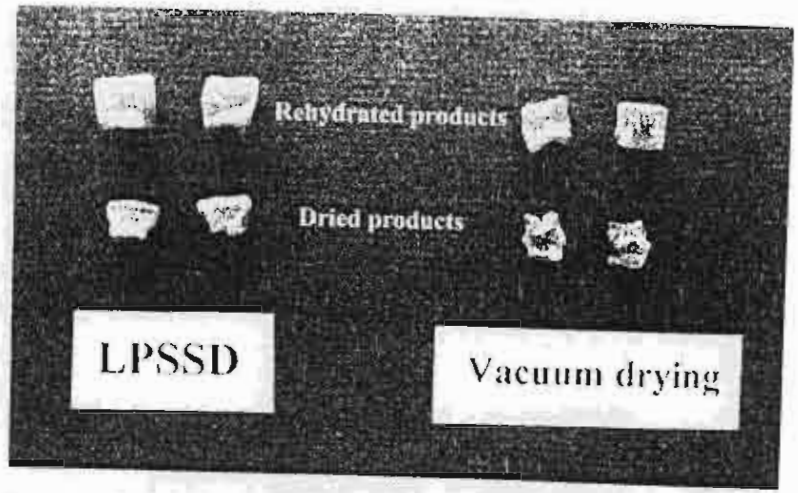

Figure 6. Photographs of carrot cubes both after drying and after rehydration.

distribution was rather nonuniform comparing with carrot that underwent LPSSD (see Figs. 8a and b), which also did not have dense layer that prevented re-adsorption of water. It was also found that, in general, there existed an adverse relationship between the degree of rehydration and that of shrinkage.

Color Parameters

The changes of color parameters (Δa and ΔL) of carrot undergoing LPSSD and vacuum drying are listed in Table 3. It was observed that all dried carrot was redder than fresh carrot as can be seen from the positive Δa values. This is probably due to the concentration of color pigments in carrot when moisture is removed. On the other hand, it was observed that almost all drying conditions (for both LPSSD and vacuum drying) yielded dried carrot with negative ΔL values, which implied that the dried carrot was slightly darker than the fresh one.

It can be observed from Table 3 that, when comparing the effects of different drying methods, LPSSD yielded carrot of redder and lighter colors than those obtained by vacuum drying. These results were similar to those reported by Caixeta et al.[27] who compared the color values of potato chips undergoing impingement superheated steam drying and hot air drying. It was also found that lower drying temperatures gave redder

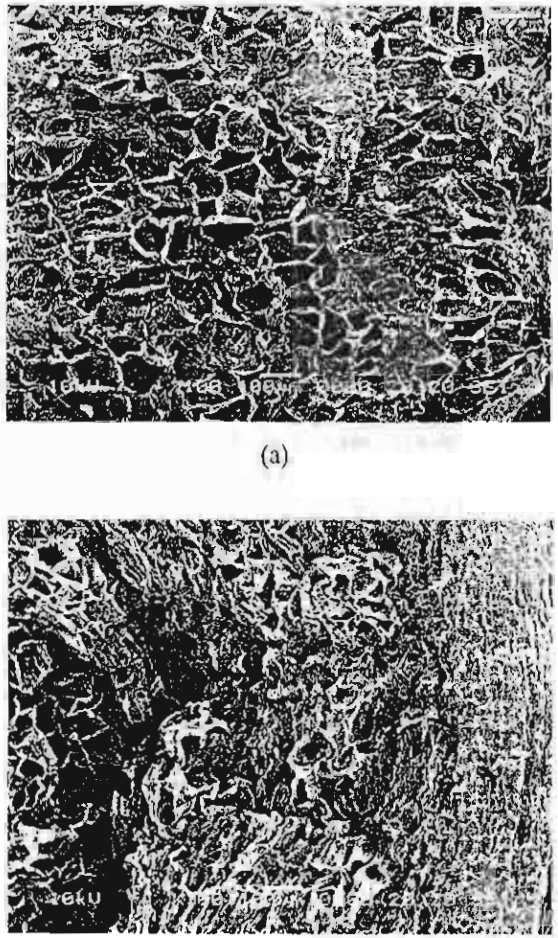

(a)

(b)

Figure 7. SEM photographs of carrot undergoing (a) LPSSD, (b) vacuum drying.

and lighter dried carrot. This may be due to the fact that red color is attributed to the presence of β carotenes[19] and the degradation of β carotene in carrot is inversely proportional to the drying temperature.[28] Operating pressure seems to have only a small effect on the colors of the dried carrot, however.

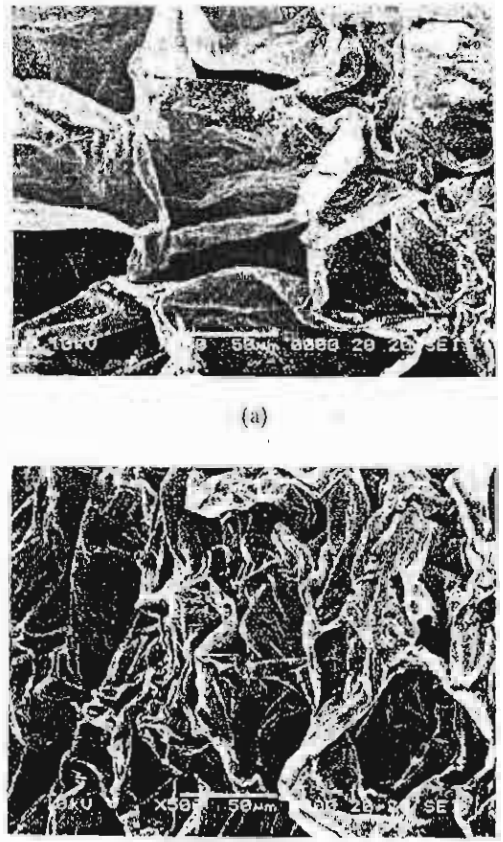

(a)

(b)

Figure 8. SEM photographs showing pore distribution of carrot undergoing (a) LPSSD, (b) vacuum drying.

CONCLUSIONS

Detailed experimental evaluation of low-pressure superheated steam drying showed that, despite lower drying rates due to poorer convective heat transfer under reduced pressures, the process gave superior quality dried product compared to that obtained using conventional vacuum drying. It was observed that the effect of operating pressure was less significant than that of steam temperature. It is interesting to note that

Table 3. Average values of Δa and ΔL of carrot undergoing LPSSD and vacuum drying at different operating conditions.

Drying process	Temperature (°C)	Pressure (kPa)	Δa	ΔL
LPSSD	$T=60$°C	7	0.2 ± 0.04^{e}	0.01 ± 0.02^{f}
		10	N/A	N/A
		13	N/A	N/A
	$T=70$°C	7	0.17 ± 0.02^{d}	-0.04 ± 0.03^{e}
		10	0.16 ± 0.06^{d}	-0.04 ± 0.02^{e}
		13	0.16 ± 0.04^{d}	-0.04 ± 0.04^{e}
	$T=80$°C	7	0.15 ± 0.01^{c}	-0.06 ± 0.08^{d}
		10	0.15 ± 0.01^{c}	-0.09 ± 0.17^{abc}
		13	0.15 ± 0.06^{c}	-0.08 ± 0.11^{cd}
Vaccum drying	$T=60$°C	7	0.10 ± 0.02^{ab}	-0.05 ± 0.03^{de}
		10	0.10 ± 0.02^{ab}	-0.06 ± 0.03^{d}
		13	0.09 ± 0.02^{ab}	-0.1 ± 0.08^{ab}
	$T=70$°C	7	0.07 ± 0.06^{a}	-0.09 ± 0.02^{a}
		10	0.07 ± 0.05^{a}	-0.1 ± 0.04^{ab}
		13	0.07 ± 0.1^{a}	-0.1 ± 0.03^{ab}
	$T=80$°C	7	0.07 ± 0.01^{a}	-0.1 ± 0.06^{ab}
		10	0.07 ± 0.04^{a}	-0.1 ± 0.03^{ab}
		13	0.07 ± 0.07^{a}	-0.1 ± 0.02^{ab}

[a,b,c,d,e,f]In the same column with different superscripts means that the values are significantly different ($p<0.05$).
N/A implies that, at this condition, the final carrot moisture content of 0.07 kg/kg (d.b.) was not achievable.

the operating pressure and temperature affected the shapes of the drying rate and temperature curves differently in steam drying and vacuum drying. The two drying techniques yielded differing structural and optical properties of the dried product. Steam drying provided better rehydration and a redder dried carrot than that obtained in vacuum drying over the operating parameter ranges studied.

NOMENCLATURE

m_p	Mass of an empty pycnometer (g)
m_{Ph}	Mass of a pycnometer filled with *n*-heptane (g)
m_{Phs}	Mass of a pycnometer with sample and *n*-heptane (g)
m_s	Masses of the sample (g)
R	Rehydration ratio (–)
V	Volume (cm^3)
V_i	Volume of fresh carrot (cm^3)

Greek Letters

ρ_{app}	Apparent density (g/cm^3)
ρ_h	Density of *n*-heptane (g/cm^3)

ACKNOWLEDGMENTS

The authors would like to express their sincere appreciation to the Thailand Research Fund (TRF) and the International Foundation for Science (Sweden) for supporting this study financially.

REFERENCES

1. Mujumdar, A.S. *Recent Developments in Drying*, Annual Conference of the Indian Institute of Chemical Engineering, Madras, India, 1981.
2. Cui, W.K.; Mujumdar, A.S. Paper drying—an overview of developments. In *Drying of Solids*; Mujumdar, A.S., Ed.; Wiley Eastern: New Delhi, 1986; 142–156.
3. Douglas, W.J.M. Drying paper in superheated steam. Drying Technology **1994**, *12* (6), 1341–1355.
4. Potter, O.E.; Beeby, C. Modelling tube to bed heat transfer in fluidized bed steam drying. In *Drying '86*; Mujumdar, A.S., Ed.; Hemisphere: Washington, 1986; Vol. 2, 595–603.
5. Salin, J.G. Steam drying of wood particles for particleboard. In *Drying'86*; Mujumdar, A.S., Ed.; Hemisphere: Washington, 1986; Vol. 2, 572–574.
6. Mujumdar, A.S. Superheated steam drying. In *Handbook of Industrial Drying*; Mujumdar, A.S., Ed.; Marcel Dekker, Inc.: New York, 1995; 1071–1086.
7. Urbaniec, K.; Malczewski, J. Experimental investigations of beet pulp drying in superheated steam under pressure. Drying Technology **1997**, *15* (6–8), 2005–2011.

8. Tang, Z.; Cenkowski, S.; Muir, W.E. Dehydration of sugar-beet pulp in superheated steam and hot air. Transactions of the ASAE **2000**, *43* (3), 685–689.
9. Mujumdar, A.S. Superheated steam drying—technology of the future. In *Mujumdar's Practical Guide to Industrial Drying*; Devahastin, S., Ed.; Exergex: Brossard, Canada, 2000; 115–138.
10. Kumar, P.; Mujumdar, A.S. Superheated-steam drying: a bibliography. Drying Technology **1990**, *8* (1), 195–205.
11. Elustondo, D.; Elustondo, M.P.; Urbicain, M.J. Mathematical modeling of moisture evaporation from foodstuffs exposed to subatmospheric pressure superheated steam. Journal of Food Engineering **2001**, *49* (1), 15–24.
12. Shibata, H.; Mada, J.; Shinohara, H. Drying mechanism of sintered spheres of glass beads in superheated steam. Industrial & Engineering Chemistry Research **1988**, *27* (12), 2353–2362.
13. Shibata, H.; Mada, J.; Funatsu, K. Prediction of drying curves on sintered spheres of glass beads in superheated steam under vacuum. Industrial & Engineering Chemistry Research **1990**, *29* (4), 614–617.
14. Senda, Y.; Bando, Y.; Yasuda, K.; Nakamura, M.; Sugimura, Y.; Shibata, M. *Development of Superheated Steam Dryer at Reduced Pressure*, Proceedings of the 1st Asia-Pacific Drying Conference, Bali, Indonesia, 2001; 247–256.
15. Elustondo, D.M.; Mujumdar, A.S.; Urbicain, M.J. Optimum operating conditions in drying foodstuffs with superheated steam. Drying Technology **2002**, *20* (2), 381–402.
16. Chen, S.R.; Chen, J.Y.; Mujumdar, A.S. Preliminary study of steam drying of silkworm cocoons. Drying Technology **1992**, *10* (1), 251–260.
17. Pang, S.; Dakin, M. Drying rate and temperature profile for superheated steam vacuum drying and moist air drying of softwood lumber. Drying Technology **1999**, *17* (6), 1135–1147.
18. Iyota, H.; Nishimura, N.; Yoshida, M.; Nomura, T. Simulation of superheated steam drying considering initial steam condensation. Drying Technology **2001**, *19* (7), 1425–1440.
19. Lin, T.M.; Durance, T.D.; Scaman, C.H. Characterization of vacuum microwave, air and freeze dried carrot slices. Food Research International **1998**, *31* (2), 111–117.
20. Krokida, M.K.; Maroulis, Z. Quality changes during drying of food materials. In *Drying Technology in Agriculture and Food Science*; Mujumdar, A.S., Ed.; Science Publishers, Inc.: Enfield, 2000; 61–106.

21. Krokida, M.K.; Oreopoulou, V.; Maroulis, Z.B. Modeling shrinkage and porosity during vacuum dehydration. International Journal of Food Science and Technology **1997**, *32* (6), 445–458.
22. Seyed-Yagoobi, J.; Li, Y.B.; Moreira, R.G.; Yamsaengsang, R. Superheated steam impingement drying of tortilla chips. Drying Technology **1999**, *17* (1&2), 191–213.
23. Moreira, R.G. Impingement drying of foods using hot air and superheated steam. Journal of Food Engineering **2001**, *49* (4), 291–295.
24. Ratti, C. Shrinkage during drying of foodstuffs. Journal of Food Engineering **1994**, *23* (1), 91–95.
25. Potter, N.N.; Hotchkiss, J.H. *Food science*, 5th Ed.; An Aspen Publication: Gaithersburg, 1998.
26. Achanta, S.; Okos, M.R. Quality changes during drying of food polymers. In *Drying Technology in Agriculture and Food Science*; Mujumdar, A.S., Ed.; Science Publishers, Inc.: Enfield, 2000; 133–147.
27. Caixeta, A.T.; Moreira, R.; Castell-Perez, M.E. Impingement drying of potato chips. Journal of Food Process Engineering **2002**, *25* (1), 63–90.
28. Pan, Y.K.; Zhao, L.J.; Dong, Z.X.; Mujumdar, A.S.; Kudra, T. Intermittent drying of carrot in a vibrated fluid bed: effect on product quality. Drying Technology **1999**, *17* (10), 2323–2340.

DRYING TECHNOLOGY
Vol. 22, No. 9, pp. 2095–2118, 2004

Effective Diffusivity and Kinetics of Urease Inactivation and Color Change During Processing of Soybeans with Superheated-Steam Fluidized Bed

Somkiat Prachayawarakorn,[1,*] Paveena Prachayawasin,[1] and Somchart Soponronnarit[2]

[1]Department of Chemical Engineering, [2]School of Energy and Materials, King Mongkut's University of Technology, Thonburi, Bangkok, Thailand

ABSTRACT

Influences of temperature and moisture content on diffusional transport property and kinetics of both urease inactivation and color change during soybean treatment with superheated steam in the temperatures of 120–150°C were investigated. The experimental results have shown that the effective diffusivity and apparent rates of such reactions are related to temperature in a way that the rates of

*Correspondence: Somkiat Prachayawarakorn, Department of Chemical Engineering, King Mongkut's University of Technology, Thonburi, Suksawat 48 Road, Bangkok 10140, Thailand; E-mail: somkiat.pra@kmutt.ac.th.

DOI: 10.1081/LDRT-200034265 0737-3937 (Print); 1532-2300 (Online)

water transport, urease inactivation, and brown pigment formation are higher with higher temperature. In addition, these rates are also enhanced by increasing moisture content, except for the browning reaction that is inhibited by this factor due to the dilution effect. The reduction in urease activity is reasonably described by modified first-order reaction and the color change of soybeans is characterized by three Hunter parameters in which the changes of *L*-, *a*- and *b*-values are followed according to zero-order, modified Monod and first-order reactions, respectively. The kinetics of inactivation and color change, along with the experimental data of protein solubility and lysine content, have been suggested that the soybean should be treated with superheated steam at the temperature ranging from 120 to 135°C. The superheated-steam fluidized-bed technique can simultaneously be applied for both drying and inactivating such components in soybeans by a single operation when the initial moisture content falls within a suitable range, approximately lower than 20%d.b. At elevated initial moisture contents, two-stage drying technique is recommended in order to avoid excessive cooked soybeans.

Key Words: Color; Legume; Superheated steam; Trypsin; Urease.

INTRODUCTION

Legumes are valuable potential source of good-quality protein that is used as a main ingredient of animal feed and are increasingly important in human nutrition. Soybean is the most important legumes in relation to total world legume production because of its relative cheapness and high protein content. However, the utilization of nutritional value of soybean is limited due to the presence of certain antinutritional factors, such as trypsin inhibitor, hemagglutinins, saponins, and urease. Trypsin inhibitor inhibits the growth rate by 30–50% and causes the pancreatic hypertrophic response in animals when raw soybean meal is fed.[1] Urease enzyme, which catalyzes the urea converted into ammonia and carbon dioxide, does not affect on the physiological functions in humans, but is toxic to animals when fed with raw soybean meal. These antinutritional factors are destroyed by thermal processing methods such as roasting, cooking/autoclaving, micronization, and extrusion.[2–5] In addition to elimination of such factors, the thermal treatments improve nutritional value through conversion of native protein into more digestible denaturated forms.[6]

Roasting, one of the most frequently used techniques, involves cooking of soybeans using heated air with temperature above the normal boiling point of water. There are several roasting methods, ranging from salt bed roasting, rotary dryer similar to a common grain dryer. These methods provide nonuniform degree of cooking since the poor contact between grains and medium is encountered. The nonuniform cooking can be diminished by using fluidized-bed technique by which the hot-air stream with a sufficiently high velocity is forced through grain bed and consequently, the particles are suspended in hot air and move randomly within the bed. Besides the improvement of cooking, this technique gives rise to inactivation of the trypsin inhibitors and urease enzyme without losses of nutritional values in particular lysine.[7,8] In the present work, however, superheated-steam is chosen as heating media, in stead of hot air, to eliminate the antinutritional factors. Use of superheated steam is an attractive technology that offers improved thermal efficiency, thereby gaining improvements in economy and minimising environmental impact.[9,10] In addition to these advantages, the waste heat and water vapor evaporated from product can be recovered and used in other processes. The idea of using superheated steam to destroy the antinutrients originates from its unique characteristic, that is, the superheated steam is condensed when it is contacted with cold surface of material, thus releasing latent heat along with a rapid increase in particle temperature. With such peculiar phenomenon, it motivates us to quantify the effect of superheated steam in destroying antinutritive substances and simultaneously maintaining the high protein solubility.

Although treatment by thermal processes is able to reduce the levels of antinutritional factors satisfactorily, color deterioration of the product is unavoidable since temperature is an important factor in accelerating the formation of brown pigment, thus resulting in poor product quality. In general, the soybean color after processing should be yellow or light brown. The kinetics of color change is therefore a subject to be considered in the present investigation, in addition to the kinetics of urease inactivation.

MATERIALS AND METHODS

Samples

Dry soybeans, with moisture content of 13.5% d.b., were purchased from the local market and then adjusted to initial moisture contents of 19.5% and 36% by adding the required calculated amount of water.

The rewetted samples were kept in the cold storage room at 8-10°C for a week in order to allow water to penetrate uniformly into every part of the kernel.

Equipments

Figure 1 shows a schematic diagram of a superheated-steam fluidized-bed system. A fluidized-bed dryer has a cylindrical shape with a dimension of 15 cm diameter and 100 cm height. The saturated steam generated from a small boiler, with a capacity of 31 kg/h at the condition of 100°C and 106 kPa absolute pressure, flows through the dryer forced

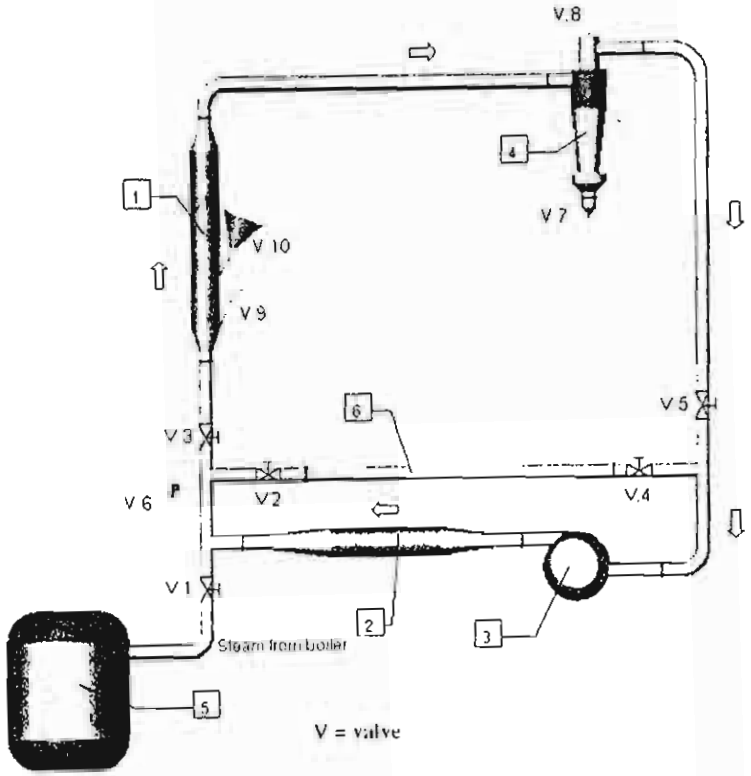

Figure 1. Schematic diagram of superheated-steam fluidized-bed system. (1) fluidized-bed dryer, (2) heater unit, (3) fan, (4) cyclone, (5) boiler (6) bypass line.

by a backward-curved blade centrifugal fan driven by a 2.2 kW motor. Before reaching the dryer, the saturated steam was passed through 13.5 kW electrical heaters to rise its temperature up to the desired level. This accordingly changed the saturated vapor into the superheated steam. The steam flow rate required for fluidizing the solid particles was precisely controlled by a frequency inverter and the desired superficial velocity at the drying chamber inlet was fixed at 3.2 m/s, which is 1.7 times higher than the minimum fluidizing velocity for soybean particle.[7] The steam velocity was measured by a pitot static tube.

The designed system can be used either for hot air or steam. In the superheated steam operation, the hot air is initially used for warming up the equipments and steam ducts of the system in order to prevent water condensation. The warming up period was stopped when the temperature in every part of the system reached the desired level and the steam was replaced accordingly by opening a valve V.1. At the same time, the air was delivered to atmosphere via a valve V.8 and this valve was closed again when the experiment was started. During the drying period, the steam flowing out of the dryer is directed to a reverse flow cyclone to collect the small particles being suspended in the fluid stream. The cleaned steam was reused again.

Before starting the experiments, samples were taken out from the storage room and left in the ambient condition until the grain temperature approached the ambient temperature. Amount 1 kg of soybeans, corresponding to a bed depth of 10 cm, was then dried at temperatures of 120, 135, and 150°C. A PID controller, with an accuracy of ±1°C, was used to maintain the steam temperature at the drying chamber inlet. Temperature at different positions within the drying chamber was monitored by a data logger with an accuracy of ±1°C. The sample was taken from the dryer at valve V.9 to examine the moisture content, urease activity, and quality. The moisture content of soybean was determined by drying in an electrical oven at 103°C for 72 h.[11]

Urease Activity Measurement

Urease test measures the activity of urease after processing. This test is an indirect method to indicate the level of trypsin inhibitor since rate of its inactivation becomes almost identical to that of trypsin inactivation.[8,12] It measures the change of pH which results from the urease enzyme converting the urea to ammonia. The determination of urease activity was followed by the direction of AACC method 22-90.[13] The pH difference of raw soybeans throughout the experiments was

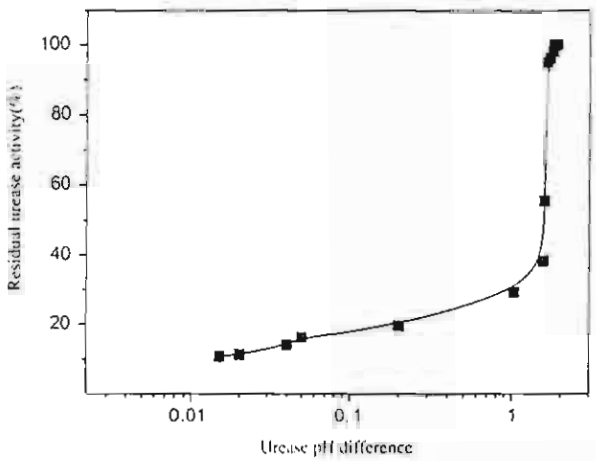

Figure 2. Relationship between pH difference and residual urease activity.

approximately 1.9. The relationship between pH difference and percent residual urease activity is given in Fig. 2. This figure was achieved by taking the samples dried at various drying times to measure the pH difference and the residual urease activity. The residual urease activity determination was followed with Rasmussen's method.[14] The reaction time for urease enzyme to develop ammonia was 60 min. The residual urease activity is expressed as the ratio of milliequivalents of ammonia produced from urea per gram of thermally treated soybeans to that obtained from raw soybeans. In uncooked soybean, ammonia was produced with an approximate value of 5 milliequivalents/g.

As shown in Fig. 2, the change in pH difference is not proportional to that of percent residual urease activity, with a steep rise in the residual urease activity at the pH difference higher than unity. From ASA standard, the adequately cooked soybeans possess the urease values in the range of 0.02 to 0.3 pH difference[11] and the corresponding percent residual urease activity is between 10 and 20%.

Colour Measurement

A Minolta CR-300 tristumulus colorimeter was used to determine the L, a, b values of samples. In Hunter Lab Color Space, the L-value presents the degree of lightness or darkness. The chromatic proportion of

the color space is based on rectangular Cartesian coordinates (a, b), with red represented by $+a$, green represented $-a$, yellow by b and blue by $-b$. The L-value gives a spectrum in the range from 0 to 100, with the highest value showing whiteness whereas the lowest value indicates the blackness. The a- and b-values represent the same spectrum range from -60 to 60. Before the color measurements, the colorimeter was standardized each time with a black and a white ceramic plates. The color was measured for soybeans thermally treated at various drying times, temperatures and initial moisture contents. Before measuring, the dried soybeans in each set were finely grounded using a mixer and then spread on a plate.

Protein Solubility Measurement

Protein solubility was determined according to the AOCS method BA 10-63.[15] This method involves the dispersion of proteins in 0.2% KOH solution. The protein solubility is defined as the ratio between nitrogen content in the supernatant after extraction with 0.2% KOH and total nitrogen content of material. The total nitrogen content and the nitrogen content in the supernatant were performed by Kjeldahl method.

Lysine Measurement

Lysine content in soybean was analyzed by AccQ-Tag method.[16] The grounded soybean was hydrolyzed with HCl solution at 110°C for 22 h and was then derivatized with 6-aminoquinolyl-N-hydroxysuccinimidyl carbamate (AccQ-Flour reagent). The lysine content was eventually determined by a high performance liquid chromatography.

Moisture Diffusion

In the present study, a method of slopes was applied to study the effect of moisture content on the effect diffusivity, D_{eff}.[17,18] Determination of effective diffusivity was written based on the Fick's second law equation, under the initial and boundary conditions that the moisture distribution inside a soybean kernel was specially uniform at the beginning; and the moisture at the exterior surface, after drying has started, rapidly vaporized reaching almost zero value since the temperature used

for drying was above the normal boiling point. The solution of Fick's equation for sphere-shaped soybean is given by[19]

$$\frac{M(t)}{M_{in}} = \frac{6}{\pi^2}\sum_{n=1}^{\infty}\frac{1}{n^2}\exp\left(-\frac{n^2\pi^2 D_{eff}t}{r^2}\right) \quad (1)$$

where, $M(t)$ is the moisture content at time t (dry basis, kg H_2O/kg dry matter), and M_{in} is the initial moisture content, D_{eff} is the effective diffusivity (m^2/s), t is the drying time (s) and r is the sphere radius (m). To determine the effective diffusivity along the change in moisture content with drying time, it can be accomplished by differentiating Eq. (1) with respect to t, yielding

$$\frac{d(M(t)/M_{in})}{dt} = -\frac{6D_{eff}}{r^2}\sum_{n=1}^{\infty}\exp\left(-\frac{n^2\pi^2 D_{eff}t}{r^2}\right) \quad (2)$$

The slope of experimental drying curve was known at every time and used as input parameter on the left hand side of Eq. (2) and the effective diffusivity was then estimated. The main assumptions of Eq. (2) were that the moisture transport occurred only in the radial direction and the sample was homogeneous, without shrinkage during drying.

Kinetics of Urease Inactivation

Inactivation of urease enzyme during thermal treatment by superheated steam was assumed to follow the modified first-order kinetics expressed as

$$C = (C_o - C_{eq})\exp(-kt) + C_{eq} \quad (3)$$

where, C_o is the activity of urease enzyme at the beginning (dimensionless), k is the apparent rate constant (min^{-1}). C_{eq} is the equilibrium activity and can be determined by a linear regression.

Kinetics of Color Change

The color change of thermally treated soybean is caused by the non-enzymatic browning reaction, where the interaction between carbonyl compounds (sugars and carbohydrates) and amine compounds (amino acids and proteins) has occurred. In addition, it is possibly produced by the structural deformation of pigments. There have been numerous

research studies on the kinetics of color changes during storage and processing.[20-22] Generally, the apparent rate change of color is presented by the zero- or first-order kinetics. As observed from the experiments, the change of individual color parameters, representing by L-, a- and b-values, with time appears to be clearly different and hence, different kinetic models are used to describe their changes. A zero-order reaction is chosen to describe the change of L-value and it is expressed by

$$L = L_o + (-k_L t) \quad (4)$$

where, k_L is the rate constant for the L-value, min^{-1}, L is the L-value at time t and L_o is the initial L-value. For the b-value, a first-order reaction is adopted and it is given by

$$b = b_o\exp(-k_b t) \quad (5)$$

where, k_b is the rate constant for the b-value, min^{-1}, b is the b-value at time t and b_o is the initial b-value. A modified Monod equation is accounted for the change of a-value and it is written as

$$a = \frac{a_o c\exp(k_a t)}{c + a_o\exp(k_a t)} \quad (6)$$

where, k_a is the rate constant for the a-value, a_o is the initial a-value and c is the constant value related to the equilibrium a-value. If $c \gg a_o\exp(k_a t)$, Eq. (6) then approaches Eq. (5).

Adequacy of Model

Several criteria for adequacy of fit such as coefficient of determination (r^2) and residual sum of squares (RSS) were used to choose the appropriate models for the effective diffusivity, urease enzyme, and color changes. The RSS can be calculated by the following equation:

$$RSS = \sum_{i=1}^{n}(Z_{exp,i} - Z_{cal,i})^2 \quad (7)$$

where, Z_{exp} is the experimental value of the dependent variable, Z_{cal} is the calculated value from the model and n is the total number of experimental data. The best model describing the transport property and quality change was selected as the one with the highest coefficient of correlation and the least value of RSS.

RESULTS AND DISCUSSION

Change of Moisture Content

Figure 3 shows the change of moisture content at three initial moisture contents of 13.5, 19.5, and 36% d.b., all of which were dried at a temperature of 120°C. The characteristic curve of moisture content during superheated steam drying is different to that found with the conventional hot air drying. Two phenomena are observed in the superheated steam drying, which are the moisture uptake period followed by the evaporation period whereas only latter period is found with the hot air.

In the first period, the steam is in close contact with the bed of particles having a lower temperature which causes the steam to be condensed. The amount of moisture uptake is related to the initial moisture content and superheated steam temperature. The first period can be seen in Fig. 3, which shows the condensation period in the first 2 min of drying time and the amount of moisture content increased from the beginning to the highest point is approximately 4% d.b. for an initial moisture content of 14% d.b. and less than 3% d.b. for the higher initial moisture contents. The lowering of moisture uptake at higher moisture content is probably due to the higher occupancy of water in the

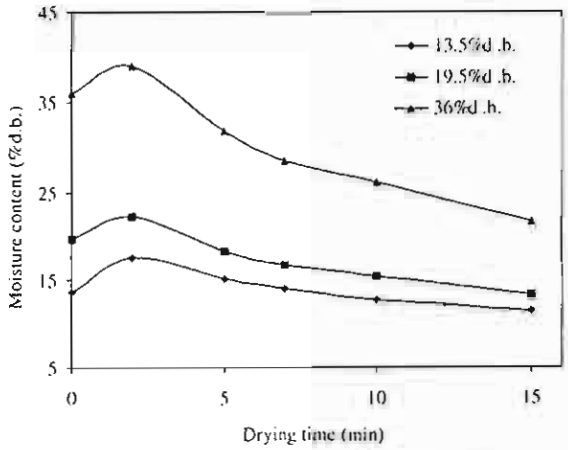

Figure 3. Change of moisture content at three different initial moisture contents (inlet superheated steam temperature of 120°C).

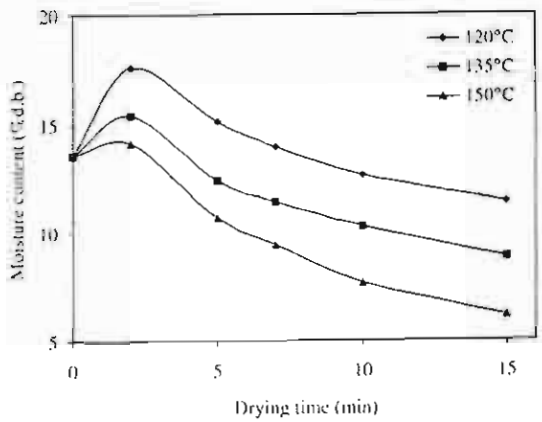

Figure 4. Change of moisture content at three different inlet steam temperatures (initial moisture content of 13.5% d.b.).

void spaces of the kernel, so that the less condensed water can penetrate into the kernel. In addition to this effect of high moisture content, the lower quantity of moisture uptake is obvious with higher inlet superheated steam as shown in Fig. 4: the moisture uptake into the samples in the superheated steam temperatures at 120, 135, and 150°C are 4.0, 1.8, and 0.6% d.b., respectively. The possible explanation of these results is due to the higher degree of superheat, resulting in a smaller amount of condensed steam.

When the evaporation period starts, transport of moisture is in the diffusion controlled region, as indicated by the exponential decay of moisture characteristic curve. The drying rate in this region is dependent on moisture content and temperature. An increase in initial moisture content or inlet steam temperature increases the soybean drying rate, as shown by the slopes of the characteristic curves in Figs. 3 and 4, respectively.

Change of Bed Temperature

Figure 5 illustrates the change in bed temperature for the samples at different initial moisture contents using the inlet steam temperature of 120°C. The bed temperature is strikingly increased for a short period and then rises gradually for the remaining drying time, corresponding to the

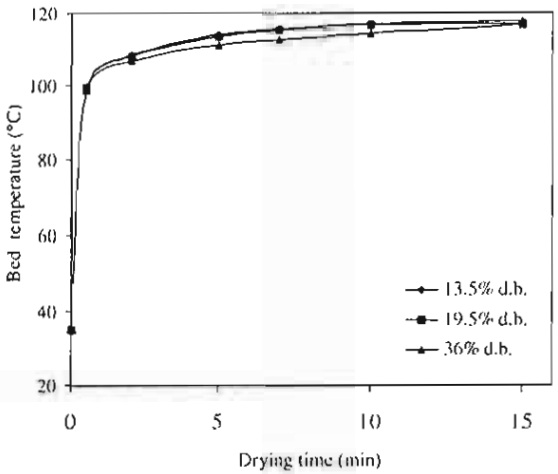

Figure 5. Change of bed temperature at different initial moisture contents (inlet superheated steam temperature of 120°C).

evaporation period. The rapid rise in temperature is attributed to the release of latent heat from the condensing steam, thus fast heating the kernels. As illustrated in Fig. 5, the bed temperatures during condensation period are in the range of 98 and 100°C, the lowest temperature corresponding to the initial moisture content of 36% d.b. The condensed steam did not take seriously the operational problem in this case but it produced the desirable result of soybean product quality, with the rapid inactivation of urease enzyme. For a few minutes of drying, the residual urease activity fell off by 100% to the range of 10 to 96%, depending upon the inlet temperature and initial moisture content. The details will be given in the section of urease inactivation.

Moisture Diffusivity

Data from a particular evaporation period of the drying experiment were analysed for calculating the effective diffusion coefficient. Figure 6 shows the relationship between the effective diffusion coefficient and moisture content at various temperatures. Values vary considerably from 1.8×10^{-11} to 1.5×10^{-8} m^2/s. D_{eff} have high values in the early stages of evaporation period, where the moisture content is high, and then

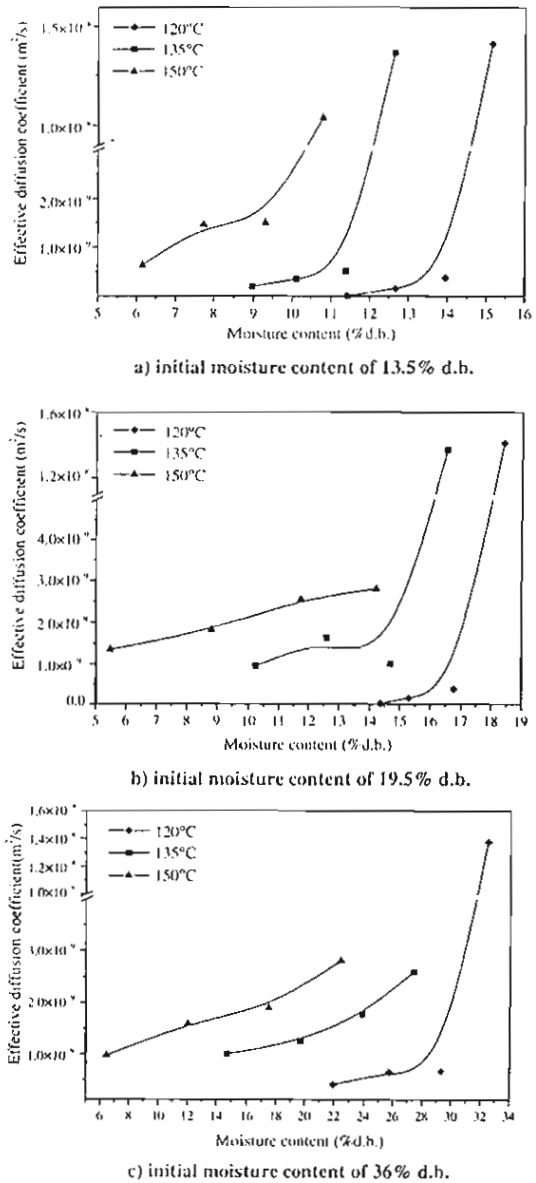

Figure 6. Relationships between effective diffusion coefficient and moisture content at different steam temperatures.

becomes monotonically decreasing in the later stages, where the moisture content appears to be lower. The decrease of D_{eff} at lower moisture content may be due to the complex structure of the kernel restricting the transport of water from the interiors to the exteriors. In addition to moisture effect, the effective diffusion coefficient also varies with temperature by a way that the diffusivity increases with increase in temperature.

It is noted that for some dying conditions, viz., at temperatures of 120 or 135°C and initial moisture content of 13.5 or 19.5% d.b., the effective diffusion coefficient is very high particularly at the beginning of evaporation period. This high value corresponds to the reduction in moisture content from the peak to the next data point, suggesting that the condensed steam only penetrates into the kernel around the outer layer during this short period of condensation. Accordingly, when the evaporation period starts, the moisture is removed easily without the interference of soybean structure and leads to extremely high drying rates.

In order to obtain the representative model for the effective diffusivity, the values of D_{eff} were fitted with an empirical equation treating D_{eff} as the dependent variable with temperature and moisture content as the independent variables. The analysis of the data using a non-linear regression technique suggests the following form:

$$D_{eff} = \left[5.4364 \times 10^{-20} + 5.111 \times 10^{-18} M^2\right] \exp(0.057318T) \qquad (8)$$

where, D_{eff} is the effective diffusion coefficient, m^2/s, T is the bed temperature, K. The values of R^2 and RSS for Eq. (3) are 0.8 and 1×10^{-18}, respectively.

Urease Activity

Figure 7 depicts some illustrative residual urease activity curves of soybeans at initial moisture content of 19.5% d.b. and inlet steam temperatures of 120–150°C. This enzyme is progressively destroyed by heat, whereby a sharp decline in urease activity occurs at the early period of drying, except for the conditions where the samples at initial moisture contents of 13.5 and 19.5 % d.b. are dried at lower temperature of 135°C, and a slow reduction is a consequence. This figure also shows the faster rate of inactivation at the higher temperature, as would be expected because more thermal energy is being transferred when drying temperature is increased. The inactivation results for the samples at the initial moisture contents of 13.5 and 36% d.b. showed the same fashion as in Fig. 7, but the rate of inactivation amongst their initial moisture

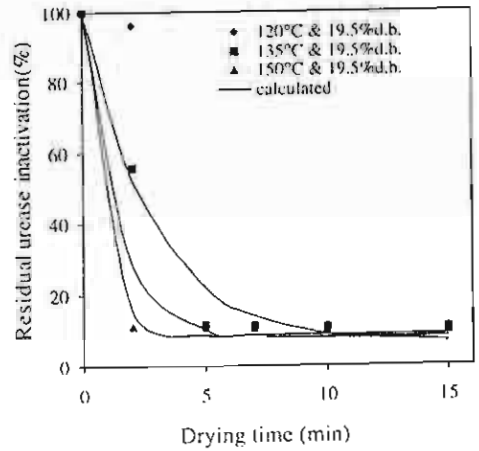

Figure 7. Change in residual urease activity versus time at different inlet steam temperatures.

contents was not identical even though the inlet steam temperature was the same, a relatively faster rate of inactivation for the samples at higher moisture content. These results can clearly be seen in Fig. 8, presenting the apparent reaction rate constant for the inactivation versus bed temperature. These reaction constants were obtained from statistical fitting of Eq. (3) to the residual urease activity data.

To reduce the residual urease activity to an acceptable range, it required 7–8 min at a temperature of 120°C and became shorter at the higher temperature for the initial moisture content of 13.5% d.b. The treatment time was decreased as the initial moisture content increased, with the treatment time of 5 min at temperatures of 120–135°C and 2 min at the temperature of 150°C for the moisture content of 19.5% d.b. In addition, for the initial moisture content of 36% d.b., the treatment time was only about 2 min, which is long enough for inactivating the urease enzyme under the above-mentioned temperature range.

Figure 8 demonstrates how the temperature and initial moisture content can cause a rapid inactivation of urease through the thermal treatment with fluidized bed. Large differences in the patterns of inactivation are observed between such operating parameters. The influence of temperature plays an important role in accelerating the urease inactivation for soybean containing low to moderate moisture contents, in particular at the initial moisture content of 19.5% d.b. showing a large